THE UNIVERSITY
of EDINBURGH

The Cellular and Molecular Mechanisms underpinning Microglial Activation during Remyelination

Amy Frances Lloyd

Doctor of Philosophy

The University of Edinburgh

2018

Thesis Abstract

Failed regeneration of myelin in the central nervous system (CNS) contributes to axon loss/ dysfunction in prevalent neurodegenerative disorders, for which there is an unmet need for effective therapies. Previous work from this lab has demonstrated that remyelination requires a transition in microglia activation from pro-inflammatory (inducible nitric oxide synthase (iNOS)+) to pro-regenerative (arginase-1 (Arg-1+). However, the mechanisms underpinning microglia activation remain unknown, and the assumption that *in situ* tissue macrophages can transition in activation state has never been substantiated. Here, unexpectedly it is revealed that microglia activation during remyelination is driven by their death and subsequent repopulation. More specifically, pro-inflammatory microglia undergo controlled necrosis (necroptosis), followed by repopulation via residual microglia and CNS-resident Nestin+ cell differentiation into microglia. Blocking necroptosis prevented microglial death and maintained their pro-inflammatory (iNOS+) activation, which consequently hindered remyelination. In human brain tissue, necroptosing and repopulating microglia were only significantly increased in white matter lesions with a high potential for remyelination. These results overturn current assumptions that following injury, microglia simply switch their activation from an initial pro-inflammatory phenotype to become pro-regenerative. Impairment in microglia death and/or repopulation may thus underpin the chronic pro-inflammatory microglia activation associated with failed remyelination in human pathology,

highlighting a novel therapeutic strategy in the treatment of chronic inflammatory and neurodegenerative diseases.

Lay Summary

Multiple Sclerosis (MS) is an autoimmune disease of the central nervous system (CNS) where the electrical insulation covering nerves (myelin) is destroyed in a process termed demyelination. Although in the early stages of MS, myelin can be repaired (remyelination), this eventually fails, leading to a progressive worsening of symptoms and an increase in disability. Currently there are no approved therapies aimed at promoting remyelination in MS, therefore greater knowledge of how remyelination takes place is needed in order to develop such therapies.

Previous work from our lab has shown that the microglia, the immune cells of the brain, are important in driving remyelination; microglia respond initially to damage by becoming inflammatory, and later change to become anti-inflammatory and promote repair of the myelin. In progressive MS, it has been suggested that this switch in microglia behaviour doesn't take place, which results in failed remyelination. Therefore, uncovering how microglia change their behaviour to promote remyelination may represent a new therapeutic target for MS.

Work from this thesis has shown that inflammatory microglia undergo cell death by a process called necroptosis. Blocking inflammatory microglia from dying resulted in inflammatory microglia persisting, and this lead to a reduction in remyelination, suggesting that inflammatory microglia need to die for remyelination to take place.

Death of the inflammatory microglia leads to new microglia being generated from two sources; expansion of microglia that did not die, and stem cell-like cells becoming new microglia.

Lastly, by looking at post-mortem brain tissue from MS patients, microglia undergoing necroptosis and repopulation are increased in areas of damage that have high potential for remyelination (active lesions), but not in lesions that have poor remyelination potential (inactive lesions). This would suggest that for remyelination to take place, inflammatory microglia must die in order for the activation of anti-inflammatory microglia to occur, which can help repair areas of damage. Furthermore, inflammatory microglia being resistant to dying may contribute to remyelination failure in progressive MS. Therefore, promoting inflammatory microglial death may be a novel way to promote remyelination in MS.

Declaration of Original Work

I am the sole author of this thesis, and the work within it is entirely my own unless otherwise indicated. This work has not been submitted for any other degree or professional qualification.

Amy Frances Lloyd

Acknowledgements

There are so many people to acknowledge and give special thanks to that without their help these last four years would have not been possible. Firstly, I would like to thank staff in LF2 for help with colony management and training, and the Flow Cytometry staff for help with all things Flow and FACS related.

Thank you to Professor Anna Williams and Professor Jeff Pollard for their supervision with my project, and invaluable input and guidance. To that end, I would also like to thank the staff and students in the Pollard, Williams and ffrench-Constant lab for feedback and support with the project (even if it meant facing my fears and having to present in front of you guys). I would also like to particularly thank the Williams lab for sharing precious human MS tissue and mouse LPC tissue with me that allowed me to discover so many cool things about microglia.

Thank you to Jill Richardson and Andrew Brown at GSK for supporting my project as well as providing lots of useful feedback for my project and the paper.

I would like to give a special thanks to Yasmine Labrak, Dario Carradori and Dr Anne des Rieux at UCL Belgium for making the LNCs for one of the most important parts of my project. Thank you to Yasmine in particular for being ready to make the LNCs and ship them to me with such short notice, despite having such a busy project going on yourself!

I would also like to thank Professor Josef Priller for the amazing feedback, guidance and support with the project and the paper, and for the chance to work in your Berlin lab for a month which I enjoyed immensely. Furthermore, I

would like to thank Chotima and Jasmin as well as the rest of the Priller lab for all of their help and hospitality during my time there.

To everyone in the Miron lab, thank you for being such an amazing and talented group of people that not only have been fantastic supports throughout, but have pushed me academically. I have had the opportunity to work with some wonderful people over the last four years that I can truly call some of my best friends. To Rebecca, Ally and Irene, I have needed you guys more than you can imagine. Thank you for all of the laughs, hugs, shoulders to cry on, and emergency chocolate mousses during particularly severe crisis moments.

To Veronica, I don't think that I can begin to thank you enough for everything over these last four years. I definitely didn't make it easy for you in the beginning but your patience, perseverance and faith in me is the reason that I am able to write this! I am eternally grateful to have such an amazing role model as my supervisor; I have learned so much from you during my PhD that I am certain I will carry throughout my career and cannot believe how much I have developed as a scientist owing to your mentoring. Thank you for being such an inspiration.

Lastly, to my family, particularly my mom and dad, who told me to do whatever makes me happy. Thank you for the unconditional love and (financial) support over the years. Unfortunately I picked the wrong career to ever be able to repay you fully, but at least I am doing something that makes me happy (most of the time).

Contents

Chapter 1. Introduction

1.1. Overview

Microglia are the resident immune cells of the central nervous system (CNS). As part of the innate immune system, and accounting for as much as 12% and 16% of the total neural cells in the mouse and human brain, respectively (*1, 2*), microglia belong to a family of mononuclear phagocytes, which encompasses other tissue-resident macrophages, all CNS resident macrophages and monocyte derived cells (*3*). Microglia are the first line of defence for the CNS, constantly surveying the environment for signs of trauma or infection. Microglia are particularly sensitive to such changes, in part due to their ability to rapidly respond to ATP (released by dying cells) through their P2RY12 receptor (*4*), changes in extracellular potassium (indicating changes in neural activity) through their expression of sensitive potassium channels (*5*), and the detection of infection or injury by their expression of toll-like receptors (TLRs) (*6*). Although traditionally perceived as purely inflammatory cells, research from the last decade has uncovered previously underappreciated roles of microglia in inflammation resolution and tissue repair. In particular, microglia have been shown to promote remyelination (*7, 8*), the restoration of myelin around axons, which restores neural health and prevents neurodegeneration. Damage to myelin (demyelination) is a hallmark of multiple sclerosis (MS). Although remyelination can take place in early phases of MS, it is in the progressive phase of the disease where this process often fails, leading to neurodegeneration for which there is an unmet need for therapeutics. Furthermore, microglia show a

high degree of diversity and plasticity in their phenotype and function, and manipulation to promote a pro-repair phenotype may represent a novel therapeutic target for inflammatory and neurodegenerative diseases like MS. It is therefore important to uncover how microglia activation is orchestrated in order to harness their regenerative properties.

1.2. Myelin in the CNS

1.2.1. Myelin Properties and Function

Myelin is a lipid-rich sheath that wraps around axons in the peripheral (PNS) and central nervous systems (CNS). In the PNS, Schwann cells are the source of myelin, and each cell can myelinate one peripheral axon. In the CNS, oligodendrocytes are able to myelinate up to 50 axons each (*9*), therefore it is conceivable that damage to a single oligodendrocyte can have greater consequences than that of a single Schwann cell. Furthermore, repairing damage to myelin in the PNS is more rapid and efficient (*10*), as Schwann cells can remove myelin debris and dead cells before remyelinating the same axon (*11*), which oligodendrocytes do not have the capacity to do (*9*).

The formation of myelin (myelination) in humans begins around gestational week (g.w.) 27 and continues well into early adulthood. Myelin was first discovered to provide electrical insulation to axons, enabling signals to be communicated faster by increasing the conduction velocity of the impulse. For example, unmyelinated axons have conduction velocities that may reach 10 meters per second (m/s), whereas myelinated axons can conduct at velocities up to 150 m/s (*12*). Each myelin sheath is separated by a small gap along the axon called a Node of Ranvier, a voltage-dependent sodium channel-dense area where action potentials are propagated, enabling the electrical signal to travel rapidly between each sheath for faster (saltatory) conduction. Myelin has also been shown to provide trophic and metabolic support to the axon, including

lactate transfer from oligodendrocytes to the axon, essential for axonal Krebs cycle- dependent generation of ATP (*13, 14*).

Myelin is comprised of approximately 80% lipid and 20% protein (*9*). The myelin proteins are comprised mainly of proteolipid protein (PLP), myelin basic protein (MBP), myelin oligodendrocyte glycoprotein (MOG) and myelin associated glycoprotein (MAG), each playing important roles in adhesion, structural support and wrap formation (*15*).

Proper myelination is essential for nervous system development and function. Human diseases where myelin fails to develop properly including Pelizaeus-Merzbacher disease (PMD) (and animal models of dysregulated myelin) have allowed for greater insight into the consequences of improper myelination on neural function and health. PMD is characterised by poor motor development and severe learning difficulties that begins in childhood, attributed to the failure of myelination and consequent axonal degeneration, often leading to death in late childhood (*13*). Therefore, myelin is vital for generation of rapid electrical signals through the axon and the maintenance of neural health and function.

1.2.2. Demyelination

Given the importance of myelin in neural function and health, it is therefore not surprising that damage to myelin can be detrimental to the axon in a multitude of ways, leading to a range of pathological consequences. Demyelination is the loss of compact myelin, which can be caused by direct damage to the sheaths

themselves or by death of the oligodendrocyte, causing loss of saltatory conduction and therefore slower transmission of electrical signals, as well as loss of trophic and metabolic support to the axon (*13*). Furthermore, demyelination causes a rapid redistribution of ion channels across the axon spreading out from the Nodes of Ranvier, leading eventually to Ca^{2+} influx, excitotoxicity, impairment of mitochondrial function and axon degeneration (*13, 16*).

Demyelination can be caused by many factors including exposure to environmental toxins like pesticides, genetic disorders, trauma and inflammation. Demyelination can have inflammatory and non-inflammatory causes and can be categorized as myelinoclastic where myelin is damaged by external factors, such as by exposure to toxins or inflammation, or leukodystrophic where inherited or spontaneous mutation leads to abnormal myelin development that degenerates. Clinically, demyelination is often detected by magnetic resonance imaging (MRI), a medical imaging technique where grey matter (cell bodies) and white matter (myelin) of the brain and spinal cord can be distinguished based on differences of high water (grey matter) and high fat content (myelin). This principle therefore also allows for the detection of demyelinated areas in the white matter that appear as bright spots or 'plaques' in the white matter.

1.2.3. Remyelination

Remyelination is the reinstatement of myelin around a demyelinated axon. Efficient remyelination prevents axonal damage and loss, shown experimentally where remyelinated areas are associated with a lower incidence of axonal loss than areas of demyelination without repair (*17-19*). Remyelination can also restore conduction velocity, shown by electrophysiological studies on remyelinated axons in the rat spinal cord and brainstem (*20*), and restore axonal function, as demyelination-induced paraplegia and blindness were reversed in cats that were allowed to recover from irradiation-induced demyelination (*21*).

The development of models to study remyelination has improved our knowledge on the cellular and molecular mechanisms involved, as well as the potential to improve remyelination in diseases where it fails. Simplistic models involve inducing a focal demyelinating lesion in the CNS white matter, usually the corpus callosum or spinal cord, or globally to brain explant cultures, by using toxins that target myelin or the oligodendrocyte. The most widely used compounds are lysolecithin (LPC), to induce a focal demyelination of the mouse corpus callosum or spinal cord, and ethidium bromide to induce demyelination in the rat cerebellar peduncles. An advantage of focal lesioning is that a single demyelinating insult with these toxins produces a well-defined temporal response of remyelination that can be studied without ongoing (and confounding) demyelination. However, a major disadvantage of using these models is that they do not model the complexity of demyelinating diseases where there is ongoing demyelination and remyelination, nor do they model the

chronic inflammation that may also play a role in such diseases; therefore, they are not suitable as disease models, but nevertheless provide a great deal of insight into the mechanisms underpinning efficient remyelination. More complex models of demyelination and remyelination include the cuprizone model, where oral treatment with the copper chelator causes a more global CNS demyelination in mice and rats (*22*). Similar to the other models, cuprizone produces a predictable time course of remyelination allowing for detailed study of molecular and cellular events during remyelination but differs slightly in that there is a phase of ongoing demyelination and remyelination that must be taken into account. Moreover, as cuprizone is supplemented into the chow of these animals, variabilities in the extent of demyelination between animals can occur depending on their food intake. Finally, experimental autoimmune encephalomyelitis, or EAE, is a model of CNS autoimmune-mediated inflammation and demyelination. This is achieved by injecting myelin proteins with an adjuvant to drive an autoimmune response, which leads to demyelination in the CNS. Although often mistaken for a model of MS, EAE does not recapitulate the full complexity of the disease, such as the heterogeneity presented in the human disease between patients and even between lesions. Furthermore, induction of disease in EAE is artificial, and most likely does not represent the initiation of disease in MS; indeed, clinical onset of symptoms in EAE is rapid, manifesting in days to weeks, yet it is thought that physiological processes that underlie MS go undetected for years before symptoms manifest (*23*). Nevertheless, EAE has been useful to understand some aspects of pathology such as acute and chronic lesion formation (*19*).

The stages of remyelination are now well characterised. In response to a demyelinating insult, oligodendrocyte progenitor cells (OPCs) need to migrate to the demyelinated lesion, proliferate to populate the lesion area, and finally differentiate into oligodendrocytes capable of producing new myelin sheaths (*24*). It has been shown that even if the oligodendrocyte survives, it does not have the ability to remyelinate the axon, as shown by transplantation of mature oligodendrocytes to demyelinated lesions (*25*), and therefore the recruitment of new OPCs to the lesion area is needed for remyelination to take place. Indeed, transplantation of progenitor cells into cuprizone-induced demyelinated brains irradiated of resident progenitor cells results in remyelination and a reduction of axonal damage compared to those without progenitor transplantation (*17*).

Efficient remyelination relies on the presence of initial pro-proliferation cues, followed by distinct survival and differentiation cues. For example, tumour-necrosis factor alpha (TNF-α), an inflammatory mediator released by immune cells like microglia, can promote OPC proliferation (*26*) but inhibits their differentiation (*8*), and is indeed secreted by microglia in the first few days following LPC-mediated demyelination of the corpus callosum corresponding with the peak in OPC proliferation (*8*). OPC differentiation firstly involves maturation into pre-oligodendrocytes that contact the demyelinated axon, and then differentiation into oligodendrocytes that produce compact myelin around axons (*24*). It is during this time that the OPCs are particularly susceptible to death, and survival and differentiation cues such as insulin-like growth factor (IGF-1) (*27*), transforming growth factor beta (TGF-β) (*28*) and microglial secreted activin-A (*8*), are needed to maintain OPC survival, promote cell cycle

exit and differentiation. More recently, the growth regulatory protein CCN3 which is secreted from regulatory T-cells has been shown to also promote oligodendrocyte differentiation and myelination *in vitro (29)*. Therefore, efficient remyelination requires precise timing and coordination of OPC activation that is reliant on other neural cell responses, and disruption at any stage can inhibit remyelination.

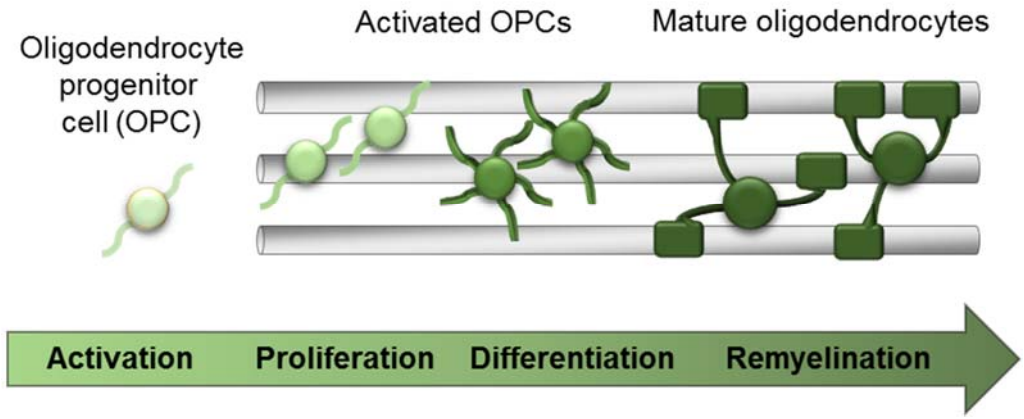

Diagram 1. Remyelination requires activation of OPCs. OPCs must become activated, migrate to the area of demyelination, proliferate, differentiate and mature into myelinating oligodendrocytes.

1.3. Multiple Sclerosis

1.3.1. Overview of Multiple Sclerosis

Multiple Sclerosis (MS) is an autoimmune disease characterised by chronic inflammation, demyelination and spontaneous remyelination that becomes less efficient over time (*24*). In the UK alone, around 100,000 people have MS, which affects women nearly 3 times more than men, and is usually diagnosed in young adulthood. Symptoms include visual, motor, sensory, and cognitive impairments. Although not fully understood, the causes of MS are attributed to a combination of environmental factors and genetic susceptibility. Such environmental factors include smoking (*30*), vitamin D deficiency (*31*) and previous viral infections, particularly infections with the Epstein-Barr virus (*32*). The genetic susceptibility of MS has been associated with allelic variations of the Major Histocompatibility Complex class II (MHC-II), molecules found on antigen-presenting cells of the immune system which are important for communicating with and initiating T-cell responses (*33*).

There are three subtypes of MS: relapse-remitting (RRMS), secondary progressive (SPMS) and primary progressive (PPMS). 85% of patients have RRMS, which involves distinct attacks of symptoms (relapses) followed by complete or partial remission of symptoms that can repeat many times over decades. In roughly 70% of RRMS cases, recovery of symptoms does not take place, leading to a continuous worsening of symptoms and an increase in disability, progressing to secondary progressive (SPMS). In rare cases (10-20%), patients will have a progressive disability from diagnosis, known as a

primary progressive form of the disease (PPMS). Although there are many drugs available to dampen inflammation and prevent relapses in RRMS, there has been less success in finding effective drugs to treat the progressive forms of MS, with Ocrelizumab being the only currently approved therapy PPMS.

1.3.2. Inflammation and demyelination in MS

Along with the subtypes, MS can be split into two pathological phases; the first is associated with chronic inflammation, where ongoing demyelination and spontaneous remyelination occurs. Both primary and secondary progressive MS are less associated with inflammation but more with an increased and continuous loss of neurological function that is linked to failed remyelination and neurodegeneration. The initial causes of MS are unknown however two hypotheses have been proposed. Firstly the 'outside-in' hypothesis that suggests dysregulated peripheral immune activation, particularly T-cell driven responses lead to their migration into the CNS via disruptions in the blood brain barrier and their attack on myelin. Secondly, the 'inside-out' hypothesis suggests that degeneration to myelin occurs first, leading to an immune response that results in further degeneration and inflammation (*34*).

As remyelination can take place in the early stages of MS, it is still not well understood why it inevitably fails as the disease progresses. Potential reasons have been proposed, including a failure of OPCs to be recruited (*35*), a depleted source of OPCs and a block in OPC differentiation; causes of which may be due to repeated bouts of demyelination depleting the progenitor pool (*36*) and the

chronic inflammatory environment preventing OPC differentiation (*22*). Indeed, tissue samples from some MS patients have shown by immunohistochemistry that there may be a lack of OPCs around demyelinated lesions (*36*). However, this is not always the case, as other studies have shown that demyelinated lesions in some patients are not associated with a lack of OPCs, but rather a failure of OPC differentiation (*37, 38*). Some patient lesions contain PLP+ pre-myelinating oligodendrocytes that have undergone some degree of differentiation from OPCs, but a lack of MBP+ cells suggests that they but cannot fully differentiate into myelinating oligodendrocytes (*39*). The differences in patient findings highlight the heterogeneity and complexity of lesion formation in MS.

1.4. Microglia: Innate Immune Cells of the CNS

Microglia were first identified in the 1880s by Franz Nissl, when the Nissl staining technique was developed, which lead to the conclusion that microglia were related to peripheral macrophages (*40*). Indeed, activated microglia were later observed by Victor Babes in 1897 after finding clusters of these cells in virally infected brain sections (*40*). It wasn't until 1920 however, that Pio del Rio Hortega called these cells microglia. Rio Hortega went on to pioneer early microglia research, phenotypically characterising microglia in white matter during homeostasis and in response to lesion formation (*40*). A century of research later, great advances in our knowledge of microglia ontogeny and function has highlighted the importance of microglia in CNS development, homeostasis and disease. Shown to be similar to peripheral macrophages, it was thought for decades that microglia shared a similar blood monocytic origin (*41*), however in recent years, lineage tracing studies have revealed microglia arise from precursor cells in the embryonic yolk sac (*42*). Microglia have since been shown to have distinct transcriptional profiles in homeostasis and disease compared to their peripheral counterparts (*43, 44*), although they share functional similarities including antigen presentation, immune surveillance and phagocytosis (*3*). For a long time the brain was thought to be an 'immune privileged' site, with microglia erroneously considered to be relatively quiescent, however recent live imaging techniques have uncovered that on the contrary, microglia are highly active during homeostasis, constantly surveying their local microenvironment by extending and contracting their processes (*45, 46*). Furthermore, microglia are now appreciated to communicate with other

neural cell types, and are vital for efficient neurodevelopment and homeostasis (*46-48*) as well as in response to injury or infection.

1.5. Microglia Origins in the Central Nervous System

1.5.1. Microglia Origins during Embryogenesis

Microglia appear in the blood islands of the mouse yolk sac at embryonic day (E) 9.0 and have been shown to populate the neuroepithelium by E9.5, prior to definitive haematopoiesis in the foetal liver and bone marrow (*42, 49*). Following the formation of the blood brain barrier (BBB) by E13.5, the migrated microglia become isolated from the periphery, yet they continue to populate the entire CNS via rapid proliferation from E10.5 up until birth, maturing into ramified microglia (*50, 51*). Early colonisation of microglia to the CNS is well conserved across vertebrates (*52*). In humans, IBA-1$^+$ CD68$^+$ CD45$^+$ MHCII$^+$ amoeboid microglia invade the cerebral cortex by g.w 4.5 (*53, 54*) and migrate to the immature white matter via the ventricular lumen and leptomeninges (*53*). A second wave of microglial infiltration at g.w 12-13 then seeds the embryonic brain via the vasculature (*54*). By g.w 22 microglia take on a ramified morphology and become fully mature by g.w 35.

Microglia, unlike other tissue-resident macrophages, originate from erythromyeloid progenitors (EMPs) in the yolk sac (*42*) during primitive haematopoiesis. This was shown by fate mapping using a transgenic line where progenitor cells that express runt-related transcription factor 1 (RUNX1) express YFP after tamoxifen-induced Cre recombination (*42*). Injection of 4-hydroxytamoxifen (4-OHT) into pregnant females prior to definitive haematopoiesis (at E7.5) allowed for specific labelling of yolk sac derived EMPs that were traced to the developing brain (*42*). This migratory process is

circulation-dependant, as sodium-calcium exchanger knockout mice (*Ncx-1*$^{-/-}$) that develop without a functioning blood circulation lack CNS microglia (*55*) despite undergoing normal haematopoiesis (*42*). EMPs commit to a microglia fate by massive changes in gene and protein expression, firstly by differentiating into CD45^{+}c-Kit^{lo}CX3CR1^{-} precursors and then maturing into CD45^{+}c-Kit^{-} CX3CR1^{+} yolk sac macrophages (*51*). Once in the CNS, these cells downregulate *Timd4* and *Cd206* and upregulate microglial signature genes *Sall1* and *Sall3 (56)*. Microglia specification is also dependent upon interferon regulatory factor 8 (IRF-8), working in a heterodimeric partnership with transcription factor PU.1 (*51*). Furthermore, RNA-seq analysis revealed precise coordination of gene expression that directs differentiation of early progenitors (expressing *Mcm5*, *Dab2*, *Lyz2* and *Pf4*) into post-natal microglia (upregulating *Csf1R* and *Cxcr2*) and then finally into mature microglia (expressing *Cd14* and *Mafb*) (*57*). Furthermore, microglial maturation in the CNS is dependent on factors produced by other CNS-resident cell types. For example, an *in vitro* co-culture study of astrocytes with microglia show that after one week microglia elongate and become ramified, suggestive of maturation, and astrocyte conditioned media alone can also induce this (58.59). Moreover, *ex vivo* experiments have shown that astrocyte-derived factors including TGF-B2, CSF1 and cholesterol can also promote the ramification and survival of microglia (60). Co-culture studies of induced pluripotent stem cell (iPSC) derived neurons and primitive macrophages lead to dramatic morphological changes in the macrophages similar to ramified microglia (*58*), although this did not take place with

neuronal conditioned media alone, suggesting direct contact between neurons and primitive macrophages may be needed to induce maturation.

Yolk sac-derived microglia can persist throughout adulthood (*42, 59, 60*), although there is a possibility that some microglia may be replaced by haematopoietic stem cells (HSCs). This is because adult microglia in the zebrafish originate from the ventral wall of the dorsal aorta (VDA), a source of definitive haematopoiesis (*59*), although it is unclear whether this reflects differences in developmental pathways between species. However, recent experimental evidence using a Vav-1+Cre:Dicer mouse model, in which definitive haematopoiesis is prevented, showed a 40% reduction in IBA-1+ cells in the CNS compared to WT littermates, suggesting a second wave of microglial infiltration to the developing CNS originating HSCs (*61*). However, in light of recent evidence demonstrating a transient population of monocyte-derived macrophages entering the CNS during development (*62*) and a lack of microglial-specific markers used in the Vav-1Cre:Dicer experiments, it cannot be ruled out that this model is only preventing the migration of a transient macrophage population. Rapid and dramatic increases in microglia numbers are observed in the CNS shortly after birth in the mouse (*50, 61*), although whether this a second wave of microglia or a peripheral cell contribution is debated. Indeed, in a PU.1 knockout mouse model (lacking embryonic microglia), bone-marrow transplants from wild type mice can lead to a fully populated microglial presence in the CNS (*63*) however it is unclear the extent to which blood-derived monocytes contribute to the stable microglial population in the CNS under normal conditions.

1.5.2. Microglia in Adulthood

In the first two weeks of life after birth, microglial numbers increase, which is then followed by a decrease to a steady homeostatic level via apoptosis and reduced proliferation (*50, 64, 65*). Under homeostatic conditions, yolk-sac derived microglia were historically considered to be long-lived cells with low turnover, however it has recently been shown that microglia numbers in the mouse brain are dynamically regulated by apoptosis and proliferation, with around 1.38% of microglia estimated to be proliferating (as shown by BrdU incorporation) and 1.23% of microglia dying every 24 hours (*66*). Therefore, it is estimated that an entire microglial population in the mouse CNS can turn over in 96 days. In the human brain, slightly higher rates of proliferation were observed ($Ki67^+$ $IBA\text{-}1^+$ cells), but rates of death are unknown. Dynamic regulation of the microglia population in the adult mouse brain has also been observed by repopulation from CNS-resident cells following global depletion of microglia (*66-69*). As these studies involved adult mice rather than neonates, this reveals that repopulation of microglia differs from the original seeding taking place during development. There are currently 2 proposed models to explain how microglia repopulation in the adult CNS takes place. The first study using a *Cx3cr1*-CreERT2;iDTR mouse model ablated a minimum of 80% of microglia in the cortex, cerebellum, and spinal cord by 3 days post-diphtheria toxin (DT) administration (*68*). A rapid microglial repopulation event was observed at 7 days post-DT, mediated by self-renewing proliferating microglia (expressing Nestin), with numbers returning to control levels 1 week later (*68*). The second model, where >99% of microglia were depleted using a CSF1R

inhibitor, observed repopulation from a CX3CR1 negative CNS-resident cell (*69*). Furthermore, BrdU labelling showed that 70% of labelled cells were Nestin+ but negative for microglia markers such as IBA-1. When repopulation was complete, almost all BrdU labelled cells were positive for microglial markers, leading to the conclusion that the Nestin+ cells differentiated into microglia (*69*). These repopulating cells heterogeneously expressed a range of markers for hematopoietic and neural stem cells including Nestin, c-kit, and CD34, as well as lectin-IB4, CD45, and Ki67 (*69*). The repopulated microglia also have similar inflammatory gene expression and functional responses to lipopolysaccharide compared to pre-depletion microglia (*69*). However, the identity and origin of these progenitor cells remains unclear. Definitive lineage tracing and RNA-sequencing of these Nestin+ cells in all depletion studies would be beneficial in uncovering their identity and role in the CNS. Indeed, lineage tracing of repopulating microglia in two depletion/repopulation studies have both concluded that residual microglia are the sole source of repopulation after depletion, with no evidence for a Nestin+ cell origin (*68, 70*), however whether this is the case for all depletion studies remains to be determined. Differences in repopulation outcomes in all depletion studies may reflect how different depletion methods and the extent of depletion (>99% (*69*) compared to 80% (*68*) for example), impact other neural cell types, as only the DTR-driven depletion lead to a robust pro-CNS inflammatory response and astrogliosis (*68*) which may also impact how repopulation takes place. Although there is uncertainty as to the role of Nestin in microglia repopulation, be it re-expression by residual microglia (*68, 70*) or progenitor cells capable of differentiating into

microglia (*69*), cells expressing Nestin are nonetheless integral to the rapid repopulation of microglia following depletion, and need to be investigated further.

1.6. Microglia Activation and Function

1.6.1. Microglial Activation and Function in vitro

Microglia can respond to a multitude of factors in their microenvironment, interacting with other cell types and responding to secreted products (such as cytokines). They also survey their environment for signs of injury by the detection of damage-associated molecular patterns (DAMPS) released by damaged and dying cells and by identifying signs of infection by the detection of pathogen-associated molecular patterns (PAMPS) (*71*). As a result, microglia can adopt differential functional responses associated with changes in particular marker expression, known to indicate different 'activation' phenotypes. Furthermore, their phenotype can also reflect different functions, particularly relevant in models of CNS injury and regeneration. Insight into how their phenotypes and functions are regulated may provide greater insight into the possibility of targeting microglia therapeutically in order to promote CNS repair.

Historically, microglia were characterised broadly into two polarising categories, with 'M1' classifying microglia activated to a pro-inflammatory state, and 'M2' describing anti-inflammatory/ tissue reparative microglia. However, this terminology originated from activating peripherally derived macrophages *in vitro* with either interferon gamma (IFN-γ; M1) or interleukin 4 (IL-4; M2), and later, by treatment with granulocyte macrophage colony stimulating factor (GM-CSF; M1) or macrophage colony stimulating factor (M-CSF; M2) (*72*). It was then recognised that macrophages responded differently to other stimuli, and

so additional categories including M2a, M2b and M2c were devised. The 'M1'-'M2' paradigm was further scrutinised following profiling of 299 human-derived macrophage transcriptomes subjected to 29 different stimuli *in vitro*, showing by co-regulation and Pearson correlation analysis that there were large diversities in transcript expression profiles that did not fit into the classic 'M1' or 'M2' profiles (*73*). Additionally, genome-wide expression profiling of microglia from different mouse models of CNS disease including amyotrophic lateral sclerosis (ALS) (*74*), EAE (*75*) and traumatic brain injury (TBI) (*76*) failed to show evidence that microglia fall simply into an M1 or M2 category. Therefore there is substantial evidence for this paradigm oversimplifying and underestimating the activation potential of microglia, and in order to avoid assumptions of gene expression or function that may impede experimental reproducibility, Murray at al., (*77*) proposed to define macrophage activation by stimuli used, experimental conditions and a combination of markers.

Although *in vitro* stimulation of macrophages may not recapitulate the full complexity of the *in vivo* environment, it has still given researchers useful insight into gene expression profiles and biochemical/functional responses associated with different microglial activation states (*78*). For example, *in vitro* activation using combinations of potent inflammatory mediators including interferon gamma (IFN-γ) and bacterial peptide lipopolysaccharide (LPS), IFN-γ and Fc receptor (FcγR) stimulation, or IL-4 treatment alone produce unique gene, transcript and protein expression patterns, such that only macrophages exposed to IFN-γ express pro-inflammatory associated enzyme inducible nitric oxide synthase (iNOS), whilst only IL-4-treated macrophages express anti-

inflammatory marker arginase-1 (Arg-1) (*78*). It is important to note that exposure of macrophages to different inflammatory environments not only induces differential marker expression, but also distinct functions and behaviours. This was first shown by identifying that microglia exposed to different inflammatory mediators *in vitro* could influence distinct neural progenitor responses (*79*). Co-culturing LPS-treated microglia with neural progenitor cells (NPCs) or OPCs blocked progenitor cell differentiation via microglial secretion of pro inflammatory TNF-α (*79*). Although both IFN-γ and IL-4 co-cultures promoted NPC differentiation into oligodendrocytes, the effects of IL-4 on oligodendrogenesis were much more pronounced, through secretion of high levels of IGF-1 (*79*). Previous studies from our lab have found that microglia treated with IFN-γ and LPS express iNOS, co-stimulation molecule CD86, and Fc receptor CD16/32, associated with *in vitro* induction of OPC proliferation and migration (*8*). Conversely, only treatment with IL-13 or IL-10 increased expression of Arg-1, mannose receptor and IL1Ra, and conditioned media from these cultures enhances OPC survival under death-inducing conditions and OPC differentiation into mature oligodendrocytes (*8*). Although these experiments were carried out under artificial environments, they have helped to reveal the importance of microglia-derived factors in regulating progenitor responses which are critical for remyelination.

1.6.2. Microglial Activation and Function in vivo

The diversity in microglial activation can significantly impact regeneration in the CNS. For example, in a spinal cord injury model using electromechanical displacement where axon regeneration is poor, gene expression profiles previously associated with macrophage activation changed dynamically over time after injury (*80*). Early time points were associated with increased expression of pro-inflammatory mediators iNOS, CD16/32, CD86, IFN-γ, as well as mannose receptor and Arg-1, whereas expression of mannose receptor and Arg-1 decreased at later time points, pro-inflammatory mRNA levels persisted. This suggested that an unresolved, chronic pro-inflammatory microglial phenotype in CNS lesions may be associated with poor axonal regeneration. Injection of IL-4 treated macrophages did not rescue this effect, as once injected these cells changed their phenotype to mirror the inflammatory environment in the lesion. However, direct delivery of IL-4 into the CNS was able to overcome this, and induce a pro-regenerative Arg-1+ macrophage phenotype (*81, 82*), as well as markedly improving functional outcome and reducing tissue damage compared to non-IL-4 treated lesions with chronic pro-inflammatory microglia (*82*). IL-4 injection also had a pro-regenerative effect in the EAE model, where it increased oligodendrogenesis in the spinal cord, suggesting a role for microglia/macrophages in remyelination. The first evidence of microglial/ macrophage involvement in remyelination came from using LPC to induce a focal demyelinating lesion in the mouse spinal cord, and showing that depletion of macrophages early after injury using clodronate liposomes results in a significant delay in remyelination (*83*). This study therefore showed the

importance of microglia in promoting remyelination after injury. The pro-regenerative role of microglia was later associated with many functions including phagocytosis of myelin debris, clearance of which is vital for remyelination to take place (*84, 85*) and recruitment of OPCs to lesions (*86*). Previous work from our lab subsequently showed that dynamic temporal regulation of microglia/macrophage activation controls OPC responses during remyelination (*8*). Using LPC to induce a focal demyelinating lesion in the mouse corpus callosum, microglia/macrophage activation was investigated over time during remyelination using markers associated with macrophages in regeneration of other tissues (*80, 87-89*). Immunostaining revealed that a iNOS+CD16/32+TNF-α+ microglia/macrophage population was present at 3 days post lesion, which by 10 days post lesion switched to an Arg-1+IGF-1+mannose receptor+ population. Depletion of the pro-inflammatory iNOS+ population using gadolinium chloride ($GdCl_3$) (inhibitor of calcium signalling, previously used to deplete pro-inflammatory macrophages *in vivo*; (*90*)) reduced OPC proliferation, whereas specific depletion of the mannose receptor+/Arg-1+ population using mannosylated-clodronate liposomes reduced OPC differentiation into mature oligodendrocytes and impaired remyelination (*8*). Additionally parabiotic studies where the circulation of a young mouse was connected to an old lesioned mouse caused enhanced remyelination in the latter (*91*). Recruitment of young macrophages to the lesion was associated with an increase in Arg-1+ and mannose-receptor+ cells, but not iNOS+ or CD16/32+ microglia/macrophages, therefore associating the increased Arg-1+ population with improved remyelination (*8, 91*). Interestingly,

lineage tracing demonstrated that only a small proportion of the Arg-1+ macrophages were derived from the young mouse, showing that old microglia/ macrophages have the capacity to adopt the regenerative phenotype when exposed to the young macrophages (*8*). Furthermore, another study blocking secreted TNF-α in the cuprizone model improved phagocytosis of myelin debris, promoted early remyelination, and prevented the disease-associated decline in motor function (*92*). Altogether, these studies have demonstrated how dynamic regulation of microglia/macrophages can be dependent on the CNS microenvironment, resulting in adoption of activation phenotypes that either impede or promote regeneration. A key commonality between these studies is that the temporal regulation of microglia/macrophage activation, i.e., a turning off of "pro-inflammatory" responses and switch to "pro-regenerative" function, is an essential aspect of efficient regeneration (see *Diagram 2*).

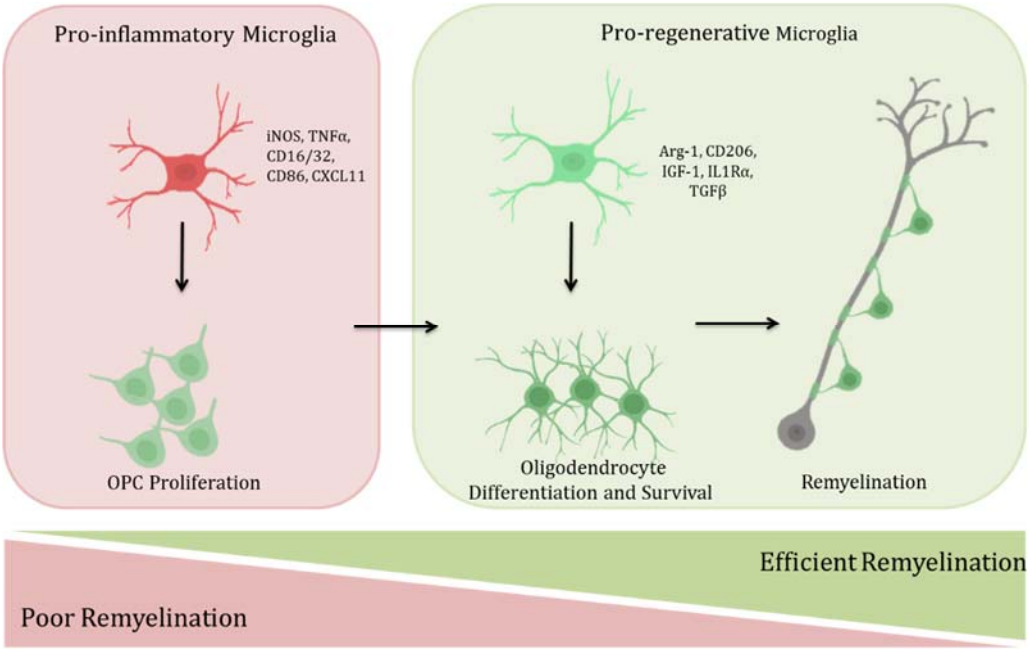

Diagram 2. Microglial activation regulates OPC responses and remyelination. Pro-inflammatory microglia, identified by their expression of pro-inflammatory markers such as iNOS and TNF-α, drive the proliferation of OPCs, but for efficient remyelination to take place, microglia must transition to an anti-inflammatory/ pro-reparative phenotype that express Arg-1/ mannose receptor (CD206) and secrete IGF-1 and TGF-β, for OPCs to differentiate and remyelinate.

1.7. Microglia in Multiple Sclerosis

1.7.1. Microglia Activation in MS

Destruction of myelin in MS is associated with microglia and macrophages (*93, 94*), both of which are thought to be important in the pathogenesis of the disease. Interestingly, increased densities of microglia and macrophages have also been associated with remyelination of MS lesions in some studies (*8, 95*), demonstrating their regenerative potential in the CNS, and highlighting their dual roles in degeneration and regeneration. Microglia play important roles in inflammation and immune responses, expressing major histocompatibility complexes (MHC) I and II, and complement receptors CR1, 2 and 4 to potentiate immune responses, and secreting potent inflammatory factors including TNF-α, interleukin (IL)-1 and IL-10 (*96*). Microglial activation in MS is complex; experimentally, microglia can drive inflammation and damage oligodendrocytes and myelin sheaths (*97*), yet can also resolve inflammation and promote tissue repair by their secretion of anti-inflammatory and tissue reparative factors (*7, 8*). Activated microglia and macrophages in active MS lesions have been shown to be a major source of oxidative species release that most likely contributes to myelin pathology (*98*) and have also been shown to localise near damaged axons, suggesting a role in neurodegeneration (*99*). Lesions that fail to remyelinate in MS are associated with an abundance of iNOS+ pro-inflammatory microglia, and "active" lesions with high remyelination potential are associated with mannose receptor+ pro-regenerative microglia (*8*). Furthermore, it is thought that chronic pro-inflammatory activation of microglia may be at least part responsible for driving the pathogenesis of MS. Microglia therefore may

hold important insight into how to not only resolve inflammation, but also promote remyelination in diseases like MS.

Microglia and macrophages represent the majority of immune cells in active MS lesions (*100*). Recent advances have allowed for the differentiation of microglia and monocyte derived macrophages (MDMs) by the identification of microglial-specific markers including TMEM119 and P2RY12 (*101-103*). Distinguishing between these two macrophage populations enables greater insight into the differing roles both populations play in diseases like MS. Strong evidence for the distinct roles of microglia and MDMs in such diseases came from experiments using the EAE model. Using $Cx3cr1^{GFP/+}$ and $Ccr2^{RFP/+}$ mice to distinguish microglia (GFP+) from MDMs (RFP+), the authors were able to show that MDMs were closely associated with demyelinating axons, and may initiate demyelination (*75*). Conversely, microglia were associated with the clearance of debris, and displayed much less of an activated morphology. Furthermore, *Ccr2* knockout mice (which inhibits MDM migration and therefore infiltration of the CNS) displayed a significant reduction in demyelinated white matter areas compared to controls, supporting the role of MDMs in driving demyelination. Gene expression profiling of microglia and MDMs revealed distinct inflammatory signatures in both populations, such that MDMs displayed a much more dramatic increase in inflammation and phagocytosis associated gene expression at the onset of EAE, whereas microglia downregulated many genes including those associated with cellular metabolism (*75*), highlighting the pathogenic role of MDMs in EAE. It is important to note that not all MDMs express CCR2 (*104*) and therefore other MDMs may have underappreciated

roles in this study. Furthermore, the early response of MDMs compared to microglia may reflect the peripheral route of adjuvant/myelin protein administration. Indeed, human TMEM119+ IBA-1+ microglia rather than MDMs (TMEM119-IBA-1+) have been shown to be present early during lesion formation in MS, dominating new active lesions and the site of expansion in chronic lesions (*105-107*), and therefore may play a more active role in MS compared to what is observed in experimental models.

Antigen presentation from microglia and perivascular macrophages enables communication with the adaptive immune system, particularly T-cells. Although perivascular macrophages constitutively express MHC Class II proteins (*108*), expression is further upregulated in these cells in MS lesions. Human microglia within the CNS parenchyma express much lower levels of MHC class II (*109*), although they can upregulate this expression after damage or infection (*110*). Although this suggested that both microglia and macrophages are capable of antigen presentation to T-cells to drive autoimmunity, recent evidence using microglial-specific (*Cx3cr1* promotor-driven Cre) knockout of MHCII proteins (which did not affect peripheral myeloid cells) showed that disease progression and severity of EAE was unaltered (*111*), suggesting antigen presentation is peripheral myeloid cell-driven. This was further supported by monocyte ablation which significantly ablated disease progression, although monocyte-specific MHCII knockout studies were not carried out. Susceptibility to MS has been linked with particular MHC class II protein variants, e.g. HLA-DRB1 (*112-114*). It is unclear however if microglial activation, or adaptive immune system dysregulation drives the initial pathology in MS. Experimental evidence in EAE

has shown that microglia become activated before the onset of lesion formation, and depletion of microglia in EAE attenuates disease progression (*115, 116*), which would therefore suggest that microglia can indeed promote disease progression. However, there was no discrimination between microglia and MDMs in these studies, so it is unclear to the extent that microglia and MDMs play in the pathogenesis of the disease.

1.7.2. Microglial Phenotypes in MS and disease models of MS

Given the importance of microglial activation states in remyelination, it has been postulated that dysregulation of microglial/ macrophage activation may contribute to the failure of remyelination in MS. Microglia and macrophages in early active lesions are associated with a pro-inflammatory phenotype, particularly associated with phagocytosis (CD68), antigen presentation (MHC I and II, CD86) and reactive oxygen species production (p22phox), but later active lesions are associated with anti-inflammatory and tissue reparative markers like CD206 and CD163 (*106*), which may be a sign of lesion repair. Indeed, chronic inactive lesions associated with poor remyelination potential are associated an abundance of iNOS+ macrophages whereas mannose receptor+ macrophages are associated with acute lesions with high remyelination potential (*8, 117*), suggesting that a phenotypic switch in microglial activation may be necessary for lesion repair. Furthermore, oxidative burst from pro-inflammatory microglia and macrophages are thought to be the major source of reactive oxygen species in MS (*118*). Lipid and DNA oxidation

levels correlate with increases in oxidative injury to oligodendrocytes and neurons, associated with active demyelination and neurodegeneration (*119*), indicating how pro-inflammatory microglia and macrophages can cause significant damage during chronic inflammation. Interestingly, a population of macrophages with an "intermediate" phenotype, characterized by expression of CD86, CCL22 and costimulatory molecule CD40, and negative for mannose receptor, are present in "pre-active" normal appearing white matter (NAWM) and remyelinating lesions, suggestive of a population of macrophages caught mid-switch (*120*). However, another intermediate macrophage population, this time identified by the expression of CD40 and mannose receptor, is associated with chronic inactive lesions that fail to remyelinate (*117*) suggestive in this case of a pathological block in macrophage phenotypic switching. The balance between macrophage activation states is predictive of disease severity in EAE. An abundance of iNOS+ macrophages is associated with a significantly higher risk of relapsing EAE, and equal numbers of iNOS+ and Arg-1+ macrophage populations predicts a milder disease outcome (*121*). Additionally, high numbers of Arg-1+ microglia/ macrophages are associated with attenuation of inflammation and decreased disease severity (*122*). Work from Mikita et al., (*121*)) demonstrated the importance of Arg-1+ macrophages in the recovery of EAE suggesting that promoting their activation may represent a novel therapeutic target for MS. Whereas increased iNOS expression in circulating monocytes and suppression of Arg-1+ macrophages and microglia predicted increased relapse occurrences, milder pathologies were characterized by low numbers of activated iNOS+ monocytes in the brain stem. Furthermore,

administration of IL-13- and IL-4-treated monocytes decreased disease severity significantly, accompanied by increased Arg-1 expression in the brain stem. These studies suggested that promoting activation of macrophages associated with Arg-1 expression may not only resolve inflammation, but also promote CNS regeneration.

1.8. Microglial Plasticity

1.8.1. Overview of Microglial Plasticity

Macrophages are able to rapidly and dynamically respond to stimuli in their microenvironment, and as such are known for their plasticity in responses and functions. The concept of "macrophage plasticity" suggests that they are able to adjust their activation and function, or even revert to a homeostatic 'surveying' state in response to changes in their microenvironment. This is an important concept as it suggests that it may be possible to therapeutically target the ability of microglia/ macrophages to switch from pro-inflammatory (and damaging if chronically active) to pro-regenerative activation states. However, it remains to be determined if macrophages have the potential to undergo an *in situ* switch, changing their genetic, metabolic and functional states in response to different stimuli.

There are many *in vitro* studies aimed at reversing or switching microglial phenotypes once polarised, identified by observing changes in gene and protein expression. However, LPS treatment of microglia followed by treatment with IL-4 could not reverse the production of TNF-α or promote the production of IGF-1 (*79*). Whether this shows that pro-inflammatory activation commits the cells to an irreversible fate or reflects the potency of LPS as an irreversible inflammatory stimuli remains uncertain. However, other similar experiments treating microglia with LPS followed by IL-4 have shown a significant decrease in the mRNA expression of pro-inflammatory genes iNOS, Cox-2 and CD86, with increased expression of mannose receptor and Arg-1 surpassing expression

levels that were observed with IL-4 treatment alone (*123*). Contradictions in experimental outcomes in these studies may be due to differences in culture conditions, treatment exposure times and experimental end points. Polarising anti-inflammatory microglia to a pro-inflammatory phenotype seems to be easier to achieve, as although IL-4 treated microglia do not produce IL-10, addition of LPS induces a modest production of microglial IL-10, suggesting that plasticity of polarised microglia is possible (*78*). Furthermore, IL-4-induced IGF-1 production was blocked by LPS co-treatment (*79*). However, it is unclear how biologically relevant *in vitro* microglia and macrophage studies are, and therefore suitable *ex vivo* and *in vivo* models are warranted.

Indeed, there is *in vivo* evidence for changes in macrophage activation following CNS injury. In a model of rodent contusion-induced spinal cord injury, distinct populations of macrophages are recruited to the lesion site through different routes such that $Ly6C^{hi}CX3CR1^{lo}$ macrophages associated with expression of IL-1β, TNF-α, and IL-12 are recruited through the leptomeninges, and $Ly6C^{lo}CX3CR1\text{-}GFP^{hi}$ macrophages expressing mannose receptor, IL-10 and TGF-β are recruited via the choroid plexus (*80, 124*). This research gave a new perspective on microglial/ macrophage plasticity by showing how the choroid plexus may prime macrophages to become pro-regenerative prior to exposure of damage at the lesion site, a previously unidentified mechanism regulating macrophage diversity.

Cross-talk between macrophage signal transduction pathways involved in both the initiation and resolution of inflammation during remyelination results in

tightly regulated responses. For example, msh homeobox 3 (MSX3) promotes pro-regenerative responses in microglia that lead to oligodendrocyte survival *in vitro* and suppression of EAE *in vivo*, potentially through its ability to suppress pro-inflammatory pathway activation (*125*). MSX3 leads to activation of PPARγ and STAT6, both of which are able to inhibit pro-inflammatory pathways including NFκB (*126, 127*). Transcriptional profiling of LPS-treated microglia *in vitro* showed that 72 out of 465 NFκB target genes analysed were significantly repressed or induced (*128*). Moreover, expression of CD40, a costimulatory molecule associated with autoimmunity and implicated in MS, is upregulated in microglia and macrophages following LPS treatment via activation of NFκB (*129*). Its tight autoregulation ensures rapid activation that is controlled and resolved efficiently; however dysregulation can lead to a prolonged inflammatory response and neurodegeneration. Mutations in genes associated with inhibition (*130*) or constitutive activation of NFκB (*131*) have been found in peripheral blood mononuclear cells (PBMCs) of patients with MS (*132*). Furthermore, another study showed by immunostaining post mortem tissue from MS patients that strong NFκB activity was localized to microglia and macrophages near lesions (*133*), suggesting that a lack of regulation of NFκB may contribute to the inflammation and pathology of the disease. Therefore, a switch in macrophage phenotype and functions may be achieved by blocking the activation of inflammatory pathways such as those mediated by NFκB, leading to the resolution of inflammation and promotion of remyelination.

1.8.2. Endogenous drivers of microglial plasticity

Endogenous regulators of inflammation may also provide clues as to how microglia and macrophage activation are regulated during CNS injury and repair. One example is of PPARγ; when activated, it translocates to the nucleus and is able to bind to NFκB-specific binding sites, preventing NFκB activation and the transcription of pro-inflammatory mediators in a process called trans-repression (*134, 135*). As such, it has long represented a promising experimental candidate to suppress inflammation and promote repair. Administration of a PPARγ agonist *in vivo* has previously been shown to promote functional recovery in a rodent spinal cord injury (SCI) model (*136*) and neuroprotection when administered before EAE induction (*137*), although it is uncertain whether PPARγ agonists can promote recovery in these models through other cell types, as PPARγ receptors are ubiquitously expressed. However, PPARγ expression is upregulated in IL-4 treated microglia *in vitro* (*135*), and is associated with anti-inflammatory/ pro-regenerative microglia. Indeed, *In vitro* activation with specific PPARγ agonists can decrease pro-inflammatory and increase anti-inflammatory marker expression in macrophages infected with the parasite *t.Cruz*i, a parasitic protozoan that causes a potent pro-inflammatory response in macrophages (*138*). PPARγ activation also promotes the transcription of anti-inflammatory molecules such as IL-10 (*134*) and has therefore been suggested to be a potential activation switch regulator for microglia and macrophages.

Another example is the neuropeptide Substance P, a member of the tachykinin family most characterised in the perception of pain and release from sensory

neurons. Substance P has also been shown to promote activation or infiltration of tissue-reparative macrophages *in vivo*, and its receptor Neurokinin 1 is upregulated in IL-4-treated macrophages *in vitro* (*139*). In a model of spinal cord contusion, Substance P administration at the time of injury induction significantly decreased iNOS, IL-6, and TNF-α mRNA expression whilst increasing IL-10 and Arg-1 expression, as well as being associated with increased mannose receptor+ macrophages, conserved myelin sheaths and functional recovery (*140*).

17β-Estradiol, the main estrogen produce by the pre-menopausal ovary can prevent NFκB activation in macrophages by directly disrupting the microtubules important for the translocation of NFκB to the nucleus, thereby preventing transcription of NFκB-dependant pro-inflammatory mediators (*141*), and can additionally promote PPARγ activation (*142*). Administration of 17β-Estradiol in EAE decreases inflammatory cell infiltration, delays the onset of symptoms and prevents deterioration of neurological function (*143*). This is associated with decreased protein levels of pro-inflammatory mediators including IL-1β, TNF- α, IL-17, Rho kinase II, and increased IL-4 (*143*). Furthermore, *in vitro* treatment of macrophages with 17β-Estradiol significantly decreases LPS-induced IL-1α, IL-6, and TNF- α protein expression (*144*).

Lastly, inhibition of an upstream activator of the NFκB pathway, Rho kinase, with the Rho kinase inhibitor Fasudil modulates microglial activation, reduces microglial infiltration to the spinal cord and improves functional outcome in the SOD1 mutant mouse model of ALS (*145*). *In vitro* treatment of microglial

cultures with Fasudil also decreases LPS-induced protein expression of TNF-α, IL-6, and inflammatory chemokines CCL3, CCL5 and CXCL1.

Although our own lab demonstrated changes in the activation and function of microglia/ macrophages during efficient remyelination, a direct *in situ* switch in the same cells remains unproven. Evidence suggests that either microglia can adopt polarising phenotypes, or distinct populations are regulated in response to the environment. Uncovering how microglial phenotypes are regulated during remyelination will be important in order to understand how to prevent chronic inflammatory microglial activation. Furthermore, this knowledge will give a greater insight into finding ways to specifically promote a microglial pro-regenerative phenotype that may represent a novel therapeutic method in promoting remyelination.

1.8.3. Microglia Heterogeneity

Not only can microglia adopt different genetic and functional identities in response to differing stimuli, it has been shown in recent years that CNS regional heterogeneity exists in homeostatic conditions. The first evidence for this was almost 30 years ago by immunohistochemical staining of microglia in different CNS regions (*146*). Immunostaining of microglia marker F4/80 revealed significant differences in microglia density throughout the brain; grey matter areas in particular had greater overall densities of microglia compared to white matter areas. Furthermore, microglia represented 5% of all cells in the cortex compared to representing 12% of the total cell population in the

Substantia Nigra (SN). Regional differences in microglial density did not necessarily correlate with levels of developmental cell death in each region, and therefore regional differences in microglial densities is not as a result of microglial activity during development. Additionally, morphological heterogeneity was also observed between CNS regions, ranging from round and compact to highly branched. Taken together, this was the first evidence to suggest that microglial heterogeneity may be a result of microenvironmental heterogeneity.

Since then, other studies have aimed to uncover factors that underpin microglial heterogeneity. Transcriptional profiling of adult microglia from distinct brain regions (cerebellum, hippocampus, striatum and cerebral cortex) revealed interesting regional differences in gene expression profiles (*147*). Principle component analysis showed particular differences in pathways involved in respiration and metabolism including glycolysis, TCA cycle and ATP synthesis, with cerebellar and hippocampal microglia being the most energy-demanding (*147, 148*). Furthermore, comparison of each regional microglial group with LPS-induced activated microglia gene expression data uncovered similar upregulation of genes associated with microglial activation in cerebellar microglia, suggesting an increased state of 'alertness' in these cells. Interestingly, transcriptomic analysis of microglia from adulthood to early and late ageing showed regional-dependant changes in gene expression profiles in response to ageing. In particular, cerebellar microglia showed increases in genes associated with activation (*Sirpb1a, Trem3, Trem1, Cd300*), as well as showing greater transcriptomic diversity from other regional microglia over

time. Conversely, hippocampal microglia displayed a decrease in distinction from other microglial groups with ageing, demonstrating how ageing impacts microglia differently in a region-dependant manner. Loss of microglial homeostatic identity has been previously associated with activation in MS (*106*), and ageing revealed a loss of homeostatic gene expression (*Tmem119, P2ry12, Fcrls*) in microglia from all regions, but particularly in cerebellar microglia (*147*). This may help to understand why microglia in ageing and in diseases like MS are associated with dysregulated pro-inflammatory activation that fails to resolve.

Regional heterogeneity of microglia occurs even in structures with close proximity. For example, analysis of microglia from 4 regions of the basal ganglia revealed marked differences in density, morphology, activity and transcriptomics (*149*). Interestingly, the Substantia Nigra reticulata (SNr) had the greatest density of microglia (723/mm^2), up to 3 times the density of other areas such as the Ventral Tegmental Area (VTA; 262/mm^2), as well as having the most metabolically active microglia (indicated by numbers of lysosomes per microglia). Conversely, despite having the lowest microglia density, the VTA microglia had the highest transcriptomic diversity compared the other nuclei, although microglia-specific genes (*Tmem119, Csf1r, Fcrls, P2ry12* etc) were highly conserved throughout all microglia populations. Depletion of microglia using a CSF1R inhibitor or via genetic ablation with *Cx3cr1*-DTR mice revealed that repopulation lead to the same regional differences in density, morphology and activity, indicating that the local environment shapes microglial phenotypes.

Important questions have arisen from these important studies. A previous study showed that taking microglia out of the brain into an *in vitro* environment lead to vast changes in gene expression, and therefore environmental factors shape microglia identity (*150*). However, it is still unclear if established microglia transplanted to a distinct brain region change in response to their new environment. Furthermore, although comparisons of brain and spinal cord microglia after LPS-induced inflammation revealed differences in magnitude of microglial responses (*151*), a closer examination of regional differences in microglial responses to inflammatory stimuli may help to understand why pathological responses and ageing of microglia occur in a region-dependant manner.

Taken together, there is vast evidence for the involvement of microglia not only in the initiation and progression of CNS damage and disease, but also in the resolution of inflammation and promotion of tissue repair, and the regional heterogeneity of microglial activation in these processes. Understanding how microglia become activated during efficient remyelination will uncover ways to harness their regenerative properties in chronic inflammatory and demyelinating diseases like MS.

1.9. Hypothesis and Aims of Thesis

Given that a transition in microglia activation from a pro-inflammatory to pro-regenerative phenotype is critical for efficient remyelination, and that persistent pro-inflammatory microglial activation is associated with remyelination in diseases like MS, it is imperative to understand the mechanisms that underpin microglial activation and phenotype transitioning during efficient remyelination. Harnessing the regenerative properties of microglia may represent a novel therapeutic target not only for modulating inflammation, but also in promoting remyelination.

Although uncertain, *in vitro* evidence suggests that pharmacological manipulation can 'switch' polarised microglia from one phenotype to another (*80, 152*), therefore the initial hypothesis of this PhD was that microglia undergo a direct phenotypic switch during efficient remyelination.

The aims of this thesis are:

1. To investigate the cellular and molecular mechanisms that drive microglial activation and phenotype transitioning during efficient remyelination
2. To identify immunomodulatory compounds capable of promoting pro-regenerative microglial phenotypes in order to drive efficient remyelination

Chapter 2. Methods

2.1. Animals

All experiments were performed under UK Home Office project licences issued under the Animals (Scientific Procedures) Act (1986) and the EU Directive 2010/63 in accordance with the ARRIVE guidelines. Animals were housed at 6 animals per cage in a 12 hour light/dark cycle with unrestricted access to food and water. Wild type CD1 mice were used for organotypic cerebellar slice cultures and C57Bl6/J mice used for *in vivo* demyelination experiments. To track monocyte infiltration into *in vivo* lesions, we used heterozygous *Ccr2* knockin reporter mice (B6;129(Cg)-*Ccr2*$^{tm2.1lfc}$/J). For lineage tracing, Ai9 (B6;129S6-Gt(ROSA)26Sor$^{tm9(CAG-tdTomato)Hze}$/J) were crossed with C57Bl6-Tg(*Nes*-CreERT2)KEisc/J to induce tdTomato expression in Nestin+ cells, or crossed to *Cx3cr1*-CreER to induce tdTomato expression in microglia. Recombination was induced by overnight treatment with 1 μm 4-hydroxy-tamoxifen (4OHT; Sigma-Aldrich), then washed thrice immediately followed by an additional 3 media changes over the course of the subsequent week prior to demyelination. Sprague-Dawley rats were used for primary microglial cultures. All animals were purchased from Jackson Laboratories.

2.2. Genotyping

Genomic DNA was extracted from ear tissue using the Wizard SV genomic purification system (Promega) according to the manufacturer's instructions. Mice were genotyped using PCR strategies as previously described (*153*).

Briefly, MacGreen (B6N.Cg-Tg(Csf1r-EGFP)1Hume/J) mice were genotyped using primers 79 (ATCATGGCCGACAAGCAGAAGAAC) and 80 (GTACAGCTCGTCCATGCCGAGAGT). NestinCreTdTomato ((B6;129S6-Gt(ROSA)26Sor$^{tm9(CAG\text{-}tdTomato)Hze}$/J) mice were genotyped using primers 1084 (GCGGTCTGGCAGTAAAAACTATC), 1085 (GTGAAACAGCATTGCTGTCACTT), 7338 (CTAGGCCACAGAATTGAAAGATCT) and 7339 (GTAGGTGGAAATTCTAGCATCATCC).

2.3. Primary Rat Microglia Cultures

2.3.1. Isolation and culture

Microglia were derived from mixed glial cultures of P0-P3 Sprague-Dawley rats by differential adhesion, as previously described (*8*). Cells were plated on poly-D-lysine-coated 16 well glass chamber slides (Lab-TEK) at 5 x 10^4 cells per well in Dulbecco's Modified Essential Media (DMEM) containing 4.5 g/L glucose, l-glutamine, pyruvate, 10% fetal calf serum (Gibco 26050088; vol/vol) and 1% penicillin/streptomycin (Life Technologies 15140122; vol/vol). Microglia were then incubated overnight, allowing for adherence to wells before further treatment.

2.3.2. Polarisation and treatment

Treatment included LPC (L4129; 0.5 mg/ml in PBS) or interferon-gamma from mouse (I4777; 20 ng/ml in PBS) and lipopolysaccharide (LPS) (0127:B8; 100

ng/ml in PBS) (all from Sigma-Aldrich) from 2-30 hours prior to fixation with 4% paraformaldehyde (in PBS) for 10 minutes (P6148; Sigma).

2.3.3. Immunostaining

Cells were blocked for 1 hour (5% BSA, 0.03% Triton-X in PBS) and incubated with primary antibodies at room temperature for 1 hour, including mouse anti-iNOS (BD Biosciences, 610329; 1:100), goat anti-Arginase-1 (Santa Cruz Biotechnology, sc-18355; 1:50), rat anti-CD68 (FA-11, Abcam, ab53444; 1:100) and rabbit anti-65 subunit of NFκB (H-4, Santa Cruz Biotechnology, sc-109; 1:100). Alexa Fluor 555 Phalloidin (Thermo Fisher Scientific, A34055; 1:1000) was used to visualise cell cytoskeleton for NFκB translocation studies, and incubated for 1 hour in the dark at room temperature. Following washes in PBS, cells were exposed to fluorescently conjugated secondary antibodies (1:1000, Invitrogen) for 1 hour at room temperature prior to counterstaining with Hoechst and mounting with Fluoromount-G (Southern Biotech).

2.3.4. Imaging

For imaging of primary rat microglia, image acquisition was carried out with a 20x water immersion objective on an LSM 710 confocal microscope with Zen software (Zeiss).

2.3.5. NFκB nuclear co-localisation analysis

Images were exported to Image J and the pixel intensity of the NFκB staining in the nucleus was determined for each cell, with a total average nuclear pixel intensity generated for each field of view. Laser power and laser exposure time were set using IFN-γ/LPS treated microglia samples (as positive control).

2.3.6. ELISA

All reagents from ELISA kits were from R&D Systems. Capture antibodies for IGF-1 and TNF-α were diluted in PBS before coating the wells of a 96 well ELISA plate and left to incubate at RT overnight. The following day, wells were washed with 0.05% Tween (Sigma; P1379) in PBS 3 times before being incubated at RT for 1 hour with blocking solutions consisting of 5% Tween in PBS for IGF-1 or 1% BSA in PBS for TNF-α. Conditioned media were then diluted in 1% BSA in PBS 1:2 for IGF-1 or 1:10 for TNF-α, added to the wells and left to incubate for 2 hours at RT. Standards were diluted in 1% BSA in PBS and a two-fold standard curve was created by diluting the most concentrated standard by half in the following sample, which was further diluted in half in the following sample and so on for 7 wells. Plates were washed thrice in 0.05% Tween in PBS before detection antibodies for IGF-1 and TNF-α were diluted in 1% BSA in PBS and added to each well for a 2 hour incubation at RT. Following a further three washes in 0.05% Tween in PBS, streptavidin was added to each well for 20 mins at RT, followed by a further 3 washes and a 20 min incubation with the substrate (1:1 ratio of luminol and hydrogen peroxide (Glo Reagents; R&D

DY993)) in the dark at RT, at which point 0.16M sulphuric acid was added to stop further reactions was added and plates were immediately taken to the spectrophotometer for analysis. Absorption of substrate reaction was measured for all samples and concentrations of IGF-1 and TNF-α were measured and determined according to the absorption of known standard samples.

2.4. Organotypic Cerebellar Slice Culture Model

2.4.1. Dissection

Cerebellum and hindbrain were isolated from P0–P2 CD1 mouse pups and sectioned sagittally at 300 μm on a McIlwain tissue chopper. Slices were plated onto Millipore-Millicell-CM mesh inserts (Fisher Scientific) in 6-well culture plates at 6 slices per insert for immunofluorescence or 3 slices per insert for live imaging. Slice culture media consisted of 50% minimal essential media, 25% heat-inactivated horse serum, 25% Earle's balanced salt solution (all from GIBCO), 6.5 $mgml^{-1}$ glucose (Sigma), 1% penicillin-streptomycin (Life Technologies 15140122), 1% Glutamax (Life Technologies 35050038) and 1% HEPES (Invitrogen 15630080), and was changed every 2–3 days.

2.4.2. Demyelination with LPC

Demyelination was induced at 21 days *in vitro* by application of 0.5 $mg.ml^{-1}$ lysophosphatidyl choline (LPC; egg yolk, Sigma-Aldrich) for 18-20 hours which was subsequently washed off in media for 10 minutes.

2.4.3. Propidium Iodide

Propidium iodide (25 μg.ml^{-1}, Sigma) was supplemented to the media for the last 1 hour prior to fixation, and slices were washed thrice in PBS before fixation with 4% PFA in the dark.

2.4.4. Necrostatin-1 treatment

Necrostatin-1 (10 μM, Sigma-Aldrich) was supplemented to media upon LPC treatment and in each subsequent media change prior to fixation with 4% PFA. 1mM necrostatin-1 was encapsulated in lipid nanocapsules (LNCs) by Yasmine Labrak (UC Louvrain, Belgium) and used for *in vivo* studies.

2.4.5. Ex vivo lineage tracing

For both NestinCreTdTomato and CX3CR1CreTdTomato slices, 1μM of 4-hydroxytamoxifen (4-OHT, Sigma) was supplemented into the media overnight to allow efficient cre-recombination. Slices were then washed 3 times, once in PBS and twice in fresh media before further incubation for 7 days to allow time for residual 4-OHT to be removed from slices (see 2.5.1).

2.4.6. Immunofluorescent staining of slice cultures

All slices prior to staining were fixed in 4% paraformaldehyde (PFA) for 10 minutes. Slices were then permeabilised and blocked for 1 hour in 5% horse serum and 0.3% Triton-X 100 in PBS, and primary antibodies were applied for 2

nights at 4°C in a humid chamber. All activated microglia were detected with rat anti-CD68 (FA-11, Abcam, ab53444, 1: 100), rabbit anti-IBA-1 (Wako Chemicals, 019-19741, 1:50) and goat anti-PU.1 (D-19, Santa Cruz Biotechnology, sc5949, 1:100). Pro-inflammatory microglia were identified with mouse anti-iNOS (BD Biosciences, 610329, 1:100) and pro-regenerative microglia identified with goat anti-Arginase-1 (M-20, Santa Cruz Biotechnology, sc18355, 1:50). Cell death was assessed using rabbit anti-RIPK3 (Novus Biologicals, NBP1-77299, 1:100), rat anti-MLKL (Merck-Millipore, MABC604, 1:100), rabbit anti-cleaved Caspase-3 (BD Pharmingen, 559565, 1:100) and mouse anti-cleaved Caspase-1 (P20, Santa Cruz Biotechnology, sc22165, 1:100). Remyelination was detected using rat anti-myelin basic protein (MBP) (AbD Serotec, MCA409S, 1:250) and chicken anti-neurofilament heavy chain (NF-H) (Encor Biotechnology, CPCA-NF-H, 1:10,000). Nestin+ cells were detected with mouse anti-Nestin (10c2, Abcam, ab6142, 1:100). Subsequent to washes in PBS, fluorescently conjugated secondary antibodies were applied for 2 h at 20–25°C in a humid chamber (anti-goat IgG (A21432, A11055), anti-rabbit IgG (A11034, A21206, A10042, A11011), anti-rat IgG (A21434, A11006, A21247), anti-mouse IgG (A31570, A21235, A31571, A21042), anti-chicken IgG (A11039)) (1:1000 in block, all from Invitrogen). Slices were counterstained with Hoechst, mounted on slides and coverslipped with Fluoromount-G.

2.5. Focal Demyelinating Lesion Model

2.5.1. Focal demyelination method

10 week-old male C57Bl/6J mice were anaesthetised with isoflurane before being stereotaxically injected with 0.5 mg.ml^{-1} lysophosphatidyl choline (LPC) diluted in sterile PBS (2µl total) into the corpus callosum (coordinates: 0.5 mm lateral, 1.2 mm rostral to Bregma, and 1.4 mm depth to brain surface). Control mice underwent the same procedure with a sham injection of 2µl PBS only. Mice throughout in vivo experiments were randomly selected for either control or treatments, although no particular random selection method was used for this. Mice were allowed to recover before sacrifice by intracardiac perfusion-fixation at 3, 7, and 10 days post LPC (dpl) with 4% paraformaldehyde (PFA) for immunofluorescence, or with cold PBS for flow cytometric analysis. The former were post-fixed overnight with 4% PFA, cryoprotected in sucrose (30% in PBS for 24 hours, followed by 15% sucrose in PBS for a further 24 hours, all at 4 degrees), and cryosectioned at 12 µm thickness. For necrostatin-1 *in vivo* experiments, necrostatin-1 LNCs (1µM, diluted in PBS) or vehicle control LNCs (1µM DMSO in PBS) or diD containing LNCs (to visualise which cells preferentially take up the LNCs; 1µM in PBS) were co-injected with LPC following the same protocol. All LNCs were prepared by Yasmine Labrak and colleagues at UCL Belgium. For flow cytometry experiments, lesioning was carried out by Claire Davies. All other lesioning experiments were carried out by Rebecca Holloway and myself.

2.5.2. In vivo Nestin+ cell lineage tracing

Ai9 (B6;129S6-Gt(ROSA)26Sortm9(CAG-tdTomato)Hze/J) mice were crossed with C57Bl6-Tg(Nes-CreERT2)KEisc/J to induce tdTomato expression in Nestin+ cells. Recombination was induced by 2 subcutaneous injections of tamoxifen (2 mg in 200 µl of corn oil; Sigma-Aldrich T5648) 48 hours apart, 5-7 days prior to brain lesioning as described above.

2.5.3. Immunofluorescent staining of focal lesion tissue

Sections of frozen tissue were air dried for 15 minutes before being permeabilised and blocked for 1 hour at RT (5% horse serum and 0.3% Triton-X-100 in PBS) then incubated with primary antibodies overnight at 4°C in a humid chamber. Microglia were detected with rat anti-CD68 (FA-11, Abcam. Ab53444, 1: 100) and rabbit anti-IBA-1 (Wako Chemicals, 019-19741, 1:50) and cell death was assessed using rabbit anti-RIPK3 (Novus Biologicals, NBP1-77299, 1:100) and rat anti-MLKL (Merck-Millipore, MABC604, 1:100). Nestin+ cells were detected with mouse anti-Nestin (Abcam, ab6142, 1:100). Myelin was detected with mouse anti-MAG (Merck-Millipore, MAB1567 1:100). Subsequent to washes in PBS, fluorescently conjugated secondary antibodies were applied for 2h at RT in the dark in a humid chamber (anti-goat IgG (A21432, A11055), anti-rabbit IgG (A11034, A21206, A10042, A11011), anti-rat IgG (A21434, A11006, A21247), anti-mouse IgG (A31570, A21235, A31571, A21042), anti-chicken IgG (A11039)) (1:1000, Invitrogen). Slices were counterstained with Hoechst, mounted on slides and coverslipped with Fluoromount-G.

2.6. Immunofluorescent Staining of Cuprizone Tissue

2.6.1. Deparaffinisation

Paraffin-embedded sections of tissue from cuprizone-fed mice were generously donated by Tanja Kuhlmann and colleagues (University of Munster). In brief, the copper chelator was supplemented into the chow for 6 weeks before then allowing mice to feed on normal chow for subsequent 4 weeks. Mice were perfused at different time points corresponding to different stages of demyelination and remyelination (see Results Chapter 3, Figure 9A). Tissue sections underwent deparaffinisation using histoclear (2 x 10 min) and a gradient of ethanol (EtOH) concentrations, each for 5 minutes in the following order: 2 x 100%, 1 x 95%, 1 x 70% and 1 x 50%, before being washed in tris-buffered saline (TBS) for 3 x 5 minute washes.

2.6.2. Immunostaining protocol

After deparaffinisation, slides were then placed in vector unmasking solution under high heat and pressure for 20 minutes before a final TBS wash. Slides were then permeabilised and blocked for 1 hour (5% horse serum (Vector Labs S-2012) and 0.3% Triton-X-100 (Fisher Scientific 10254583) in PBS) then incubated with primary antibodies overnight at 4°C in a humid chamber. Microglia were detected with rat anti-CD68 (FA-11. Ab53444, 1: 100) and cell death was assessed using rat anti-RIPK3 (Novus Biologicals, NBP1-77299, 1:100). Slices were counterstained with Hoechst, mounted on slides and coverslipped with Fluoromount-G.

2.7. Image acquisition of *in vivo* tissue

Z-stacks of slices were acquired with an Olympus spinning disk confocal microscope using either a 20X water immersion or a 60X oil immersion objective. Images were collected in Slidebook software (Intelligent imaging innovations) and converted to 16 bit .TIFF files for export and analysis. Super-resolution images were acquired using an LSM880 confocal microscope with AiryScan (Centre for Inflammation Research, University of Edinburgh) and a 63X oil immersion objective. Images were collected in Zen software. For analysis, cell counts were done manually with Image J software using the cell counter macro. To determine the level of remyelination, a measurement of the area of co-localisation of MBP and neurofilament (NFH) staining over the area of total NFH staining, known as the remyelination index using Volocity software (Perkin Elmer). Volocity was also used to determine the percentage of co-localisation between IBA-1 and Nestin, and RIPK3 and CD68 in the focal lesion tissue.

2.8. Flow Cytometry

Focal demyelinated lesions of the corpus callosum were dissected out and homogenised with a 2 ml dounce tissue homogeniser in HBSS (Gibco; 14170088). A Percoll (SLS; 17089102) gradient was used to isolate cells from myelin debris. This was done by re-suspending cell pellet in 100% FBS (in HBSS) and a 33% isotonic Percol solution (1ml 10X HBSS (Invitrogen 14185052), 9ml Percol, 20ml 1xHBSS and HEPES (Invitrogen 15630080), and

1ml of 10% FBS was overlayed on top of each sample before being spun for 15 minutes at 800g at 4 degrees). Samples were blocked with Fc-block (LEAF-purified anti-mouse CD16/32 (Biolegend, 101321)), then incubated with fluorochrome-conjugated antibodies CD11b-PeCy7 (eBioscience, 25-0112-82, 1:100) and CD45-BV605 (Biolegend, 103139, 1:100) for 30 minutes on ice, followed by incubation with FITC Annexin-V apoptosis detection kit with 7-AAD for 15 minutes at room temperature (Biolegend, 640922, 1:20). Single labelled controls were incubated with one antibody only, and an unstained control was incubated in block only. Following washes in FACS buffer (481ml HBSS (Gibco 14170088), 5g BSA (Sigma A1470-25G), 2ml 0.5M EDTA (Ambion AM9260G), 12.5ml 1M HEPES (Invitrogen 15630080), 4.5ml 10% NaN_3 (Sigma-Adrich S8032-25G)), samples were run on the BD LSR Fortessa (6 laser) analyser and analysed using FlowJo software (FlowJo LLC). Gating was based on initial forward and side scatter to eliminate cell debris and clusters, followed by gating for singlet cells, then CD11b to gate for myeloid cells, and then $CD45^{lo}$ for microglia and $CD45^{hi}$ for macrophages, based on positive controls using LPS-injected corpus callosum samples carried out by Claire Davies (Miron lab, data not shown). At this point, the proportion of each cell type being positive for Annexin-V and 7-AAD was analysed to determine proportion of dying cells at each time point.

2.9. Human Tissue

2.9.1. Table of human patients

	Classification	Sex	Age	Disease Duration (yrs)	Block	Lesions Analysed		
						Active	Chronic Inactive	Remyelinated
MS Patients	SPMS	M	64	26	1	1	0	0
	SPMS	M	40	9	1	1	1	3
					2	2	2	2
	PPMS	M	37	27	1	1	0	4
	SPMS	F	57	27	1	1	0	4
	SPMS	F	46	25	1	1	1	0
					2	2	0	0
	SPMS	F	42	19	1	1	0	2
	TOTAL					**10**	**4**	**15**
Control	Carcinoma of the tongue	M	35	-	1	-	-	-
	Myelodysplastic syndrome, RA	M	82	-	1	-	-	-
	Cardiac failure	M	64	-	1	-	-	-
	Ovarian cancer	F	60	-	1	-	-	-
	TOTAL					0	0	0

2.9.2. Immunostaining of human tissue

Post-mortem tissue from multiple sclerosis (MS) patients and controls that died of non-neurological causes were obtained via a UK prospective donor scheme with full ethical approval from the UK Multiple Sclerosis Tissue Bank (MREC/02/2/39). Diagnosis of MS was confirmed by neuropathological means by F. Roncaroli (Imperial College London) and clinical history was provided by R. Nicholas (Imperial College London). Snap frozen unfixed tissue blocks (2 × 2 × 1 cm) were cut at 10 μm and stored at −80°C. Lesions were classified according to the International Classification of Neurological Disease using Luxol Fast Blue staining and CD68+ immunoreactivity (*8, 35*) which was carried out by Anna Williams (Scottish centre for regenerative medicine, university of Edinburgh). Following washes in 0.1% Tween-20 (vol/vol) in Tris-buffered saline (TBS), sections were microwaved in Vector unmasking solution for 10 minutes, washed once, and endogenous phosphatase and peroxidase activity blocked for 5 minutes (Bloxall, Vector). Primary antibodies were incubated with tissue in a humid chamber for 1 hour at RT. Sections were washed in TBS and stains visualized by Vector Blue substrate kit according to the manufacturer's instructions (maximum 15 minutes). For co-staining, sections were washed thrice and re-blocked to quench any remaining phosphatase activity (Bloxall, Vector) prior to application of primary antibody then developed using Vector Red substrate kit according to the manufacturer's instructions (maximum 15 minutes). Following washes in water, the sections were counterstained with Hoechst and mounted with Fluoromount-G. Primary antibodies used include mouse anti- CD68 (Dako, M0814; 1:100), mouse anti-Nestin (Santa Cruz

Biotechnology, sc23927, 1:100), goat anti-PU.1 (Santa Cruz Biotechnology, sc5949, 1:100), and rat anti-RIPK3 (Novus Biologicals, NBP1-77299, 1:100).

2.9.3. Image acquisition and analysis of human tissue

Entire tissue sections were imaged using a Zeiss AxioScan SlideScanner, and lesion maps were prepared for each tissue in Zeiss Zen2 software using Luxol Fast Blue-stained sections. 2 fields of 360µm × 360µm were counted per lesion and counts were multiplied to determine density of immunopositive cells per mm^2. The cell counts from the two fields of view (internal replicates) per lesion were averaged represented as one data point.

2.10. Statistical Analysis

All manual cell counts for slice cultures, *in vivo* lesioned tissue, and MS tissue were performed in a blinded manner. Data are represented as mean ± S.E.M from a minimum of 3 biological replicates unless otherwise stated. One biological replicate is represented by one animal (both *in vivo* and *ex vivo*/ one lesion in a patient. Internal technical repeats are represented by 3 organotypic slices (*ex vivo*) or slides of tissue from the same animal for *in vivo* animal studies. Internal replicates for human data were represented by the mean counts from 2 360µm × 360µm fields of view per lesion. Each lesion was represented as a data point, even if one patient had multiple lesions (due to the heterogeneity of all lesions). All data were first tested for normality prior to

performing statistical analyses using a D'Agostino-Pearson normality test (Graphpad Prism). Although *in vivo* experiments had low (n=3) n numbers due to limited resources and animal deaths in some instances, power calculations showed >80% power at $p<0.05$ using a web-based power calculation software (https://clincalc.com; see examples below). Multiple comparisons in the same data set were analysed by Kruskal-Wallis test with Newman-Keuls post-hoc test if non-parametric, or with a one way ANOVA if normally distributed. Single comparisons to control were made using Mann-Whitney U test (non-parametric) or t-tests (parametric). Human tissue data were compared by Mann-Whitney U test. $P< 0.05$ was considered to be statistically significant. Data handling and statistical processing was performed using Microsoft Excel and GraphPad Prism 6/7 Software.

Experiment	**Figure**	**Comparison**	**Power**	**Variance**
Annexin-V+PI+ microglia *in vivo*	3.3.5	3 dpl v 7 dpl	100%	3.58724 v 8.283
		7 dpl v 10 dpl	88.51%	8.283 v 98.0892
		3 dpl v 10 dpl	95.67%	3.58724 v 98.0892
CD68+ RIPK3+ colocalisation (%) *in vivo*	3.3.7	3 dpl v 7 dpl	100%	2.00223 v 15.5078
iNOS+ CD68+ numbers at 7 dpl *ex vivo*	3.3.10	Veh v Nec-1 at 7 dpl	100%	0.08335 v 4
MS tissue MLKL+ CD68+ counts	3.3.14	Control v Active	98.49%	1.33403 v 289.68

2.11. Table of Antibodies used for Immunostaining

Antigen	Species	Clone	Source	Cat no	Concentration
iNOS	Mouse		BD Biosciences	610329	1µg/ml
CD68	Rat	FA-11	Abcam	Ab53444	5µg/ml
NFκB P65	Mouse	H-4	SCBT	Sc-109	2µg/ml
PU.1	Goat	D-19	SCBT	Sc5949	1µg/ml
Arginase-1	Goat	M-20	SCBT	SC18355	5µg/ml
RIPK3	Rabbit		Novus Biologicals	NBP1-77299	1µg/ml
MLKL	Rat		Merck-Millipore	MABC604	2µg/ml
Caspase-3	Rabbit		BD Pharminogen	559656	1µg/ml
Caspase-1	Mouse	P20	SCBT	Sc22165	2µg/ml
MBP	Rat		AbD Serotec	MCA4095	1µg/ml
NF-H	Chicken		Encor Biotechnology	CPCA-NFH	0.1µg/ml
Nestin	Mouse	10c2	Abcam	Ab6442	0.5µg/ml
IBA-1	Rabbit		Wako	019-19741	0.5µg/ml
CD68	Mouse	ED1	Dako	M0814	1µg/ml

Chapter 3: Investigating the fate of pro-inflammatory microglia during efficient remyelination

3.1. Abstract

Previous work showed that pro-inflammatory microglial activation after demyelination leads to a transition to an anti-inflammatory/ tissue reparative phenotype needed for efficient remyelination. Remyelination failure in MS is associated with lesions with abundant pro-inflammatory microglia, and a lack of pro-regenerative microglia. In order to be able to promote pro-regenerative microglial activation therapeutically in diseases like MS, we first must understand how this transition takes place, particularly focusing on the fate of pro-inflammatory microglia during efficient remyelination. Here, it is shown in multiple models that pro-inflammatory microglia undergo cell death via controlled necrosis (necroptosis). Furthermore, blockade of necroptosis with a small molecule inhibitor lead to prolonged pro-inflammatory microglial activation, consequentially leading to a significant impairment in remyelination. Finally, in MS lesions microglial necroptosis is only a significant feature of acute lesions with high remyelination potential, and not chronic inactive lesions with poor remyelination potential. Taken altogether, this work presents a previously unrecognized mechanism of immunomodulation whereby microglia are able to rapidly shut down inflammation after injury by undergoing necroptosis. Furthermore, impairment of this process may contribute to the prolonged inflammation and lack of remyelination in MS lesions. Therefore, pro-

inflammatory microglial necroptosis may represent a novel therapeutic target in driving remyelination.

3.2. Introduction

Microglia are able to adopt a range of functional phenotypes reflective of their microenvironment; defined by their interactions with other cell types, exposure to particular cytokines, or in response to damage (damage associated molecular patterns (DAMPs), alarmins) or infection (pathogen associated molecular patterns (PAMPs)). In the context of remyelination, two predominant microglia and macrophage phenotypes have been identified by differential gene and protein expression and function. After demyelination, microglia first become 'pro-inflammatory' in phenotype, identified by their expression of inducible nitric oxide synthase (iNOS), tumour necrosis factor alpha (TNF-α), interleukin-6 (IL-6), interleukin 1 beta (IL-1β) and FC gamma receptors CD16/32 (*7, 8*). Although it is unclear their exact role in remyelination, it has been shown that they are able to promote oligodendrocyte progenitor cell (OPC) migration (*in vitro*) and proliferation (*in vitro* and *in vivo*)(*8*). For efficient remyelination to take place however, pro-inflammatory microglia must undergo a transition to a anti-inflammatory/ pro-regenerative phenotype, identified by expression of arginase-1 (Arg-1), mannose receptor, insulin-like growth factor 1 (IGF-1) and transforming growth factor beta (TGF-β), shown experimentally to promote OPC differentiation into mature myelinating oligodendrocytes (*7, 8*). Efficient remyelination is therefore underpinned by precise temporal activation states of microglia, with the resolution of pro-inflammatory microglial responses a vital determinant in driving remyelination.

It is therefore predicted that dysregulation of microglial phenotypes may have a significant impact on remyelination. For example, persistent pro-inflammatory

expression of genes such as CD16/32, CD86 and IFN-γ are seen in the electromechanical displacement spinal cord injury model, which is also associated with poor axonal regeneration/ remyelination (*80*). This suggests that unresolved inflammation and chronic pro-inflammatory microglial inflammation is detrimental for regeneration. Furthermore, a greater ratio of pro-inflammatory microglia compared to pro-regenerative microglia is associated with poor axonal regeneration in spinal cord injury (*80*) and is associated with the peak of clinical severity in experimental autoimmune encephalomyelitis (EAE) (*121*). Moreover, chronic inactive lesions in post-mortem MS tissue (with poor remyelination potential) are associated with an abundance of iNOS+ pro-inflammatory microglia and macrophages, whereas mannose receptor+ macrophages increased predominantly in actively remyelinating lesions (*8, 117*). Co-culture studies have shown that pro-inflammatory microglia secrete many inflammatory and reactive molecules capable of inducing damage to, and death of, oligodendrocytes and OPCs, including nitric oxide (NO_2) (*154*), TNF-α (*155-157*), IL-1β (*156*), and peroxynitrite (*158*). Resolution of inflammatory microglia is therefore important for oligodendrocyte health and efficient remyelination.

Evidence from human tissue and models of CNS demyelination suggests that for efficient remyelination to take place, there must be a transition in microglial phenotypes from an initial pro-inflammatory/ OPC-proliferative phenotype to an anti-inflammatory/ pro-regenerative/ OPC-differentiating phenotype. The mechanisms that underpin microglial activation during remyelination remain unknown. Although thought to be an *in situ* switch in activation in the microglia

themselves, this has never been substantiated. Therefore, uncovering the cellular and molecular mechanisms that underpin microglial activation states during efficient remyelination may represent a novel therapeutic target in driving remyelination.

3.3. Results

3.3.1. Delineating microglial activation dynamics using an explant model of demyelination

To delineate the precise timing of microglial activation in the *ex vivo* model after demyelination, organotypic cerebellar slices derived from developing mouse brain were fixed at various times post-LPC throughout remyelination (Figure 1A). Pro-inflammatory microglia (iNOS+ CD68+) numbers peaked at 12 hours post LPC (hpl; Figure 1B, C) whereas pro-regenerative microglia (Arg-1+ CD68+) numbers peaked at 7 days post LPC (dpl; Figure 1B, C). At 1 dpl there was a significant reduction in CD68+ microglia, a marker of activated microglia (Figure 1B, C), as well as pan microglia marker PU.1 at 24 hpl (Figure 1D, E). PBS was used as a vehicle control and organotypic slice cultures fixed at 1, 7 and 14 days post-treatment and showed no fluctuations in CD68+ microglia numbers over time (See Chapter 9. Appendix, Figure 1) suggesting that no death or repopulation is taking place in the control treated slices, and also demonstrating that LPC is indeed driving the loss of microglia.

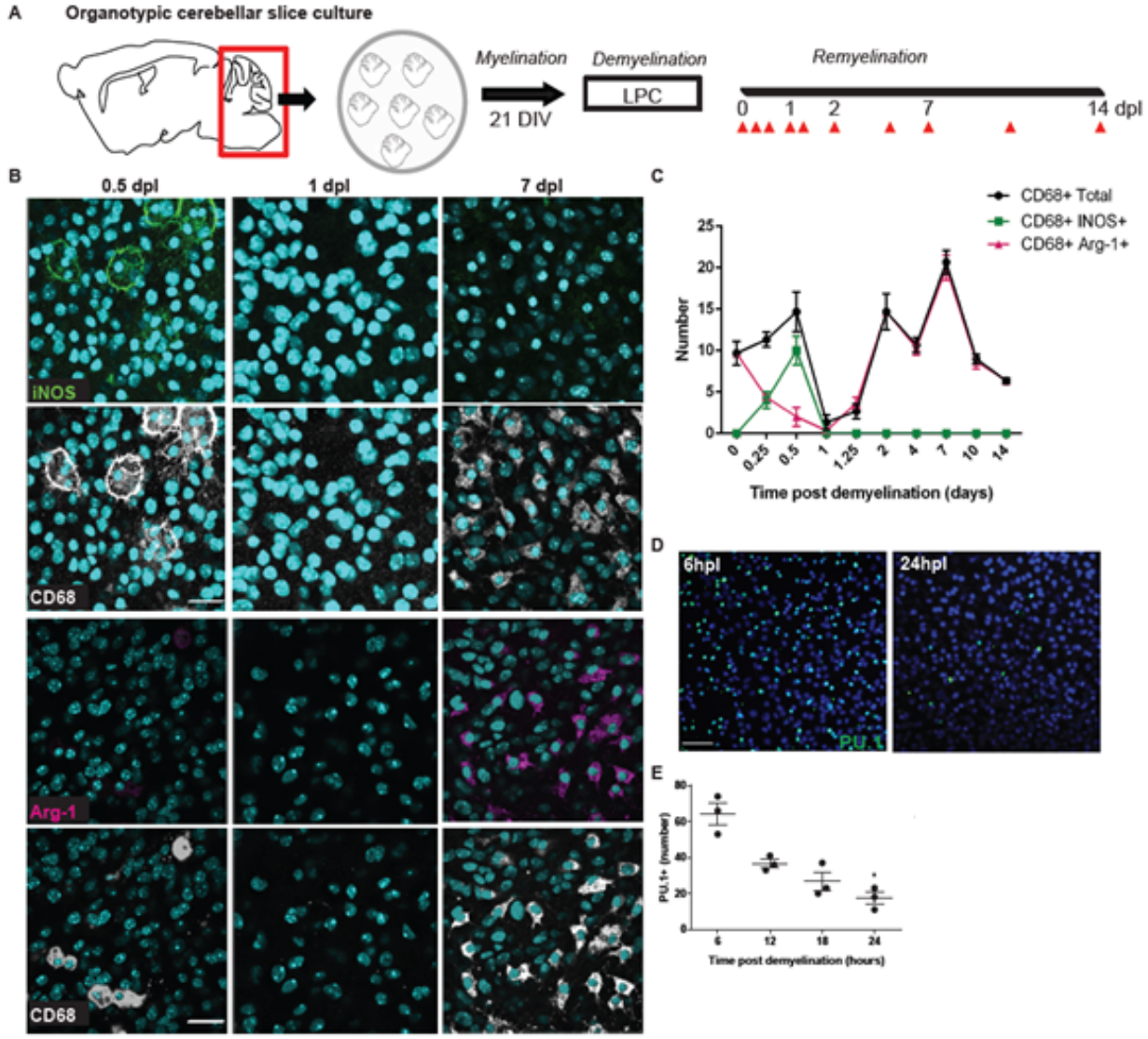

Figure 1. A. Schematic of organotypic cerebellar slice culture model of demyelination and remyelination. Red arrows indicate time points analysed. **B.** Fixed slices at 0.5 dpl, 1 dpl and 7 dpl immunostained for iNOS (green), CD68 (white) and Arg-1 (magenta) and counterstained with Hoechst. Scale bar, 20um. **C.** Mean numbers of microglia from 0 – 14 dpl ± s.e.m.. N=3 biological replicates. **D.** Slices stained for PU.1 (green) at 6 hpl and 24 hpl. Scale bar, 20µm. **E**. Mean numbers of PU.1+ cells in slices from 0 – 24 hpl ± s.e.m.. N=3 biological replicates. *p<0.05 24 hpl v 0 hpl (Kruskal-Wallis test, Dunn's Multiple Comparison post-test). N=3 biological replicates. *p<0.05 18 hpl v 0 hpl (Kruskal-Wallis test, Dunn's Multiple Comparison post-test).

3.3.2. Propidium iodide accumulation in microglia confirms cell death after demyelination in organotypic cerebellar slice culture model

To determine whether cell death was the cause of the reduction in microglia numbers in the explants, propidium iodide (PI), we used a fluorescent DNA-binding dye only able to penetrate cells with a compromised cell membrane, thus indicative of cells undergoing cell death (Figure 2A). Organotypic slices were live-labelled with PI one hour prior to fixation to identify dying cells. Prior to demyelination (0 hpl), very few CD68+ or PU.1+ microglia were PI+ (Figure 2B-E). However, after demyelination, the proportion of PI+ microglia increased over time prior to the observed loss at 24 hpl (Figure 2B-E).

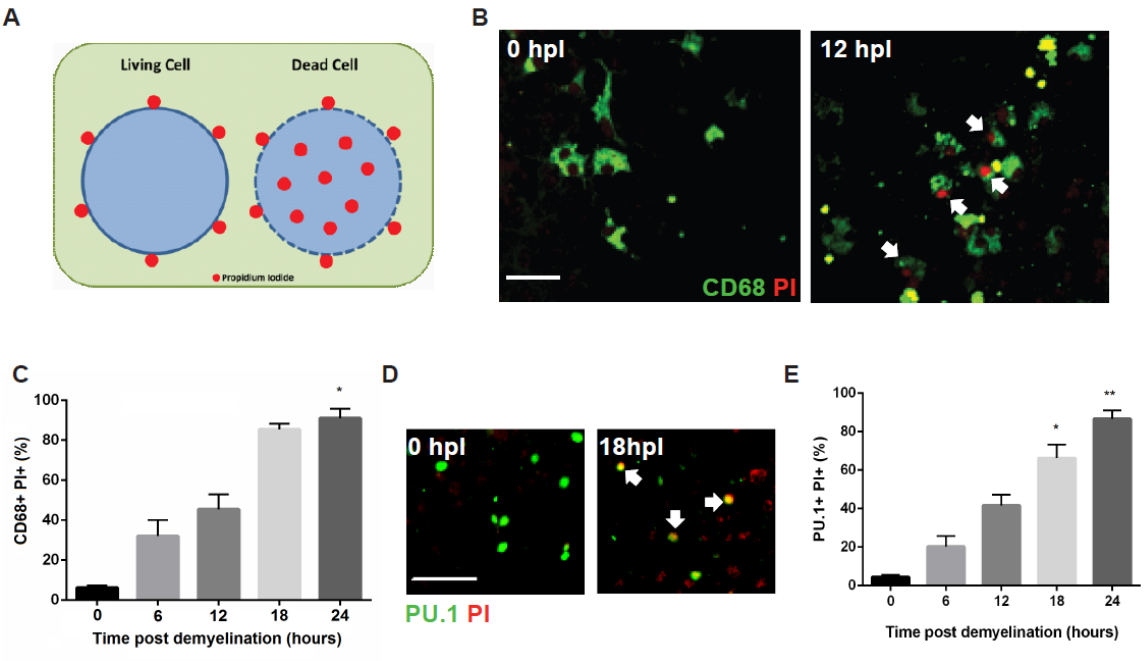

Figure 2. A. Schematic of the mechanism of action of propidium iodide; a fluorescent dye able to penetrate cells with a compromised membrane (cells undergoing cell death). **B**. Organotypic slices stained for CD68 (green) and live labelled with propidium iodide (PI; red) at 0 hpl and 12 hpl. White arrows indicate microglia (CD68+) positive for PI. Scale bar, 20µm. **C**. Mean percentages of PI+ microglia (represented as a percentage of all total CD68+ microglia) from 0 dpl to 24 dpl. * $p<0.05$ 24 hpl vs 0 hpl (Kruskal-Wallis test, Dunn's Multiple Comparison post-test). N=3 biological replicates. **D**. Untreated (0 hpl) and demyelinated (18 hpl) slices live-labelled for PI (red) then immunostained for PU.1 (green), double positive cells indicated (arrows). Scale bar, 10µm. **E**. Mean percentage of PI+ total microglia (represented as a percentage of all total PU.1+ microlglia) from 0 – 24 hpl ± s.e.m.. *$p<0.05$, **$p<0.01$ vs 0 hpl (Kruskal-Wallis test, Dunn's Multiple Comparison post-test). N=3 biological replicates.

3.3.3. LPC does not appear to induce cell death directly in microglia in vitro

To determine if the LPC toxin itself can induce microglial cell death, rather than a consequence of pro-inflammatory activation during remyelination, primary rat microglia were cultured with LPC for 18 hours. Immunostaining revealed no decrease in CD68+ cells, nor did microglia express iNOS or Arg-1 in response to LPC treatment (Figure 5). This preliminary experiment suggests that LPC alone is not sufficient to drive the death or induce the activation of microglia, however greater numbers of biological repeats would be needed to draw definitive conclusions.

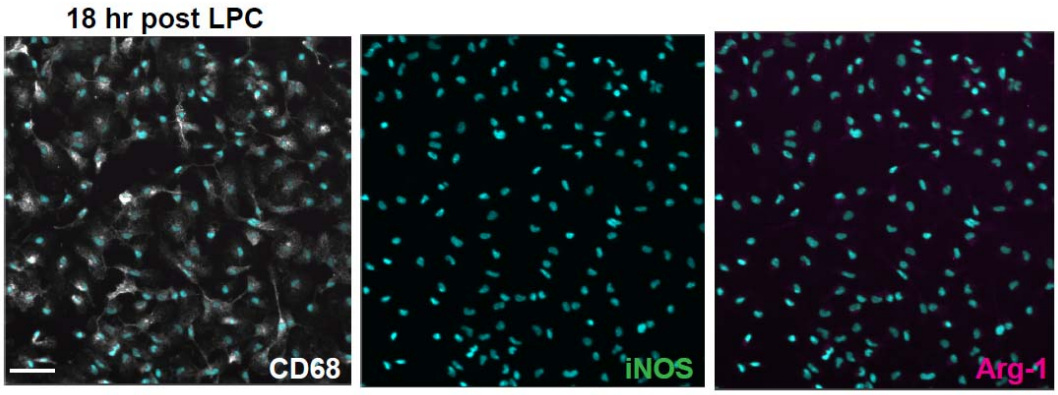

Figure 3. Primary rat microglia treated with LPC for 18 hours immunostained for CD68 (white), iNOS (green) and Arg-1 (magenta). Scale bar, 10μm.

3.3.4. In vivo focal demyelination model and method for microglial identification and cell death analysis by flow cytometry

To analyse microglia in an *in vivo* model of demyelination, LPC was stereotaxically injected into the corpus callosum of adult mice, inducing a focal demyelinating lesion which subsequently efficient remyelinates over the next 14-21 days, as previously demonstrated (*8*). Lesions were analysed by flow cytometry at time points in remyelination corresponding to key events in microglial activation (*8*); 3 dpl associated with a peak in iNOS+ microglia numbers, 10 dpl associated with a peak in Arg-1+ microglia numbers, and an intermediate time of 7 dpl (Figure 4A). Gating for microglia firstly relied on dead cell and cell debris elimination based on forward (FSC-A) and side scatter (SSC-A), followed by gating for CD11b+ cells to identify myeloid cells, followed by $CD45^{lo}$ expression to distinguish microglia from monocyte derived macrophages. $CD11b+CD45^{lo}$ microglia were plotted against 2 cell death markers Annexin-V and 7-Aminoactinomycin D (7-AAD) to identify proportions of dying microglia at each time point post demyelination (Figure 4B). Unfortunately there was no positive control generated for death markers and therefore the gates for Annexin-V and 7-AAD were set based on the sham control population (Figure 5C).

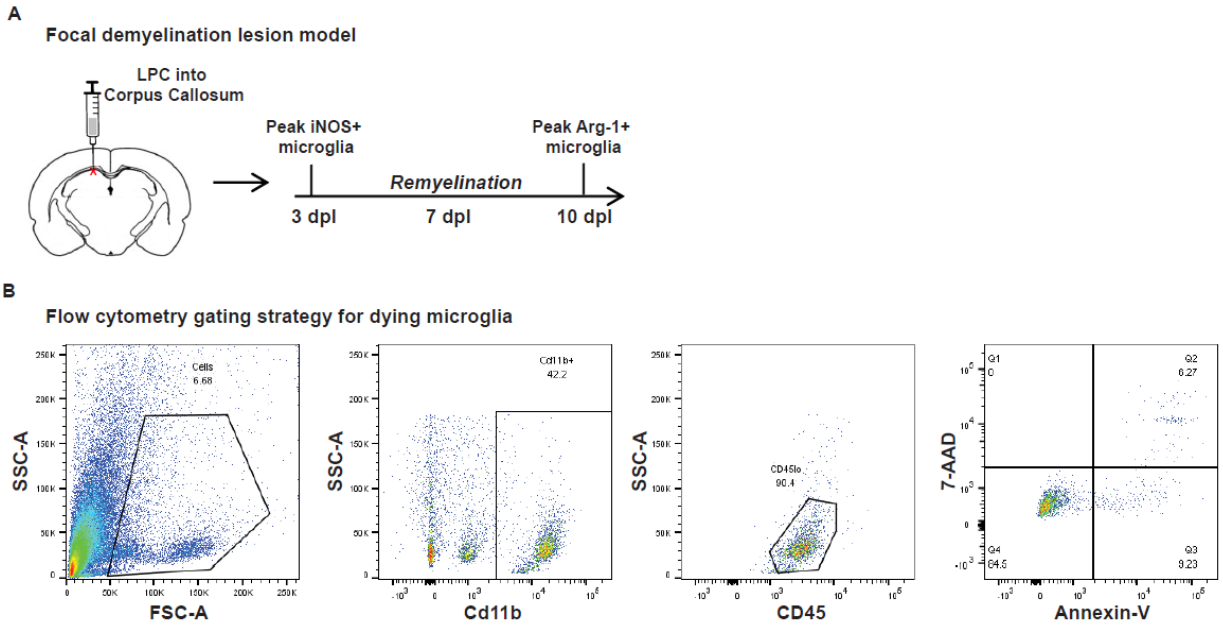

Figure 4. A. Schematic of the *in vivo* focal demyelination lesion model. **B.** Gating strategy for microglia from *in vivo* lesions; using forward (FSC-A) and side scatter (SSC-A) to gate all living cells, excluding debris; myeloid cells detected with CD11b expression; detection of microglia based on low expression of CD45; detection of cell death with Annexin-V and 7-AAD.

3.3.5. Microglia undergo cell death following demyelination in vivo

Analysis of the microglia from the lesion site revealed a significant decrease in microglia numbers from 3 dpl to 7 dpl and 10 dpl (Figure 5A). CD11b+CD45^{lo} microglia were then analysed for cell death using Annexin-V and 7-AAD. There was a significant increase in the proportion of microglia positive for both cell death markers at 7 dpl compared to 3 dpl, which then decreased at 10 dpl (Figure 5B, D, E). Microglial death was not a result of the mechanical injury inflicted by the stereotaxic injection, as microglia from sham control mice (injected with needle containing PBS of the same volume and for the same time as LPC treated mice) at 7 dpl were negative for Annexin-V and 7-AAD (Figure 5C). Therefore, the observed loss of microglia from 7dpl, after the peak in pro-inflammatory microglia activation, is associated with microglial cell death.

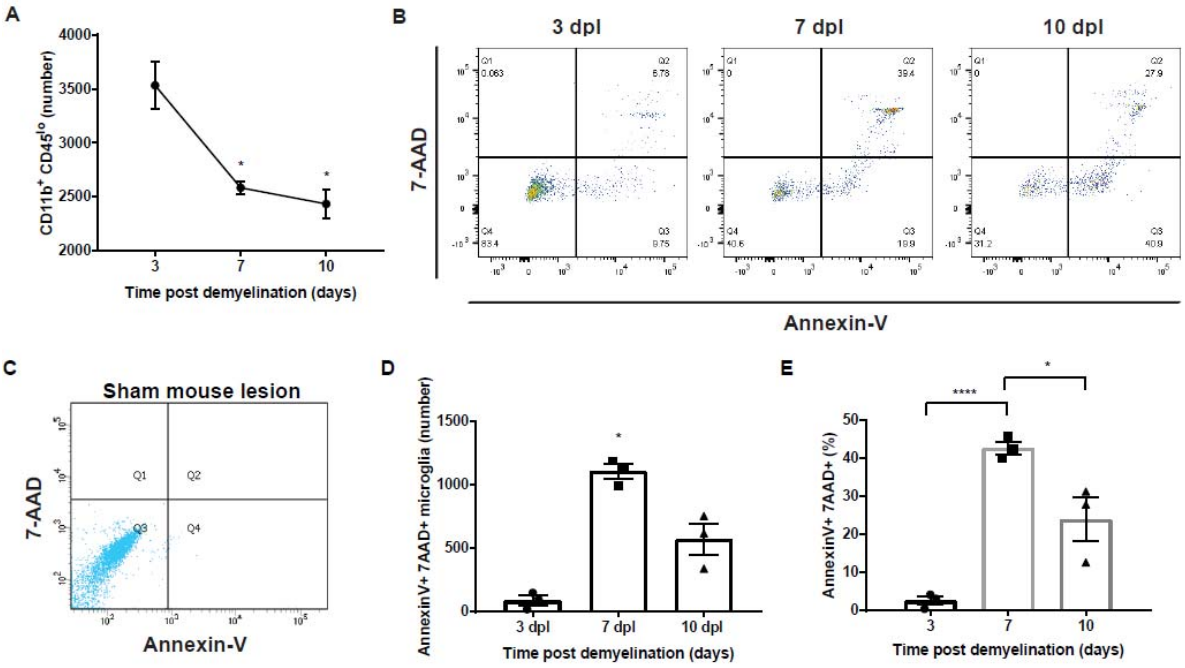

Figure 5. A. Mean numbers of CD11b+CD45lo cells at 3, 7 and 10 dpl ± s.e.m. *P=0.0141 3 dpl vs 7 dpl, *P=0.0127 3 dpl vs 10 dpl (unpaired Student's *t*-test). N=3 mice per time point. **B**. Flow cytometry plots of lesion-isolated microglia (CD11b+ Cd45lo) positive for cell death markers Annexin-V and 7-AAD at 3, 7, and 10 dpl. **C**. Flow cytometry plot of sham injection (7 dpl) mouse tissue gated for microglia and plotted with cell death markers Annexin-V and 7-AAD. **D**. Mean numbers of Annexin-V+7-AAD+ microglia at 3, 7 and 10dpl ±s.e.m. *P=0.029 (Kruskal-Wallis test). N=3 mice per time point **E**. Mean proportion of all microglia which are Annexin-V+ 7-AAD+ (represented as a percentage of total CD11b+CD45+ cells) at 3, 7 and 10 dpl ± s.e.m. ****P<0.0001 3dpl vs 7 dpl , *P=0.0233 7 dpl vs 10 dpl (unpaired Student's *t*-test). N=3 mice per time point.

3.3.6. Microglial cell death is not via apoptosis or pyroptosis

The mechanism by which microglia were dying was investigated. Apoptosis as detected by terminal deoxynucleotidyl transferase dUTP nick-end labelling (TUNEL; red) and cleaved caspase 3 (green) staining revealed the majority of PU.1+ microglia were negative at 12 hpl, compared to ethanol-treated (EtOH) positive control organotypic slices (Figure 6A). Microglia showed constitutive cleaved caspase-1 expression (a marker of inflammatory cell death mechanism pyroptosis) in CD68+ microglia even prior to demyelination (0 hpl, Figure 6B), suggestive of a role in non-death related mechanisms. Microglial death after demyelination therefore is not via apoptosis or pyroptosis.

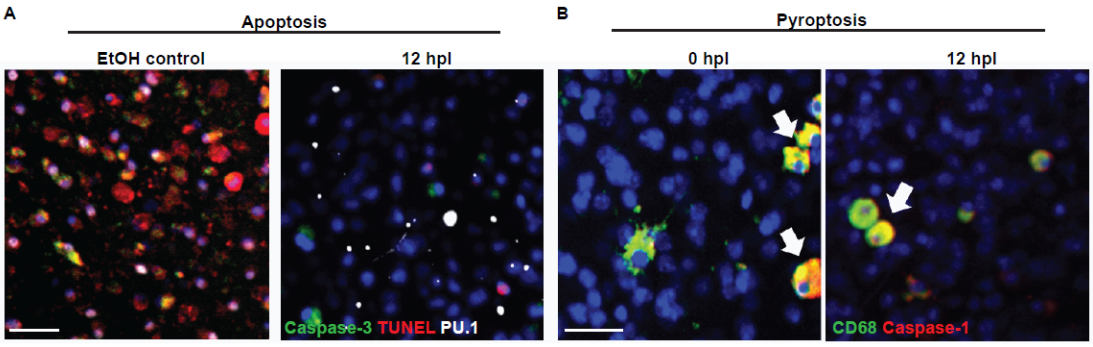

Figure 6. A. Ethanol-treated organotypic cerebellar slice (left) as a positive control to induce apoptosis and demyelinated slice at 12 hpl immunostained for cleaved caspase-3 (green), TUNEL assay (red) and PU.1 (white). Scale bar, 10µm. **B.** Organotypic cerebellar slices untreated (0 hpl) (left) and LPC-treated at 12 hpl (right) immunostained for CD68 (green) and Cleaved Caspase-1 (red). Arrows indicate Caspase-1+ microglia (CD68+) in both untreated and demyelinated slices. Scale bar, 10µm.

3.3.7. Microglial cell death after LPC-induced demyelination ex vivo and in vivo is via necroptosis

We next investigated necroptosis, a programmed necrosis driven by formation of the necroptosome comprised of receptor-interacting serine/threonine-protein kinases (RIPK) 1 and 3, leading to phosphorylation of mixed lineage kinease domain like pseudokinase (MLKL) and formation of pores in the cell membrane (*159*) (Figure 7A). Immunostaining *ex vivo* tissue for MLKL revealed a significant increase in MLKL+IBA-1+ microglia at 12 hpl, prior to the observed loss of cells (Figure 7B, C). Similarly, immunostaining for RIPK3 in the *in vivo* lesion tissue revealed a significant proportion of microglia at 3 dpl that were RIPK3+ compared to 7 dpl and time-matched sham control (3dpl) (Figure 7D, E) as detected by percentage of co-localisation of the two markers. Quantification of 3 sham controls and comparing levels of RIPK3+ microglia from mechanical injury alone would demonstrate basal microglial necroptosis levels, and should be included in future experimentation. Accordingly, high co-localisation of MLKL and IBA-1 was observed at 3dpl compared to 7dpl (Figure 7F, G), although further repeats are warranted. Nevertheless, increased expression of both RIPK3 and MLKL in microglia prior to the loss of the cells in both models therefore suggests that microglial death occurs via necroptosis.

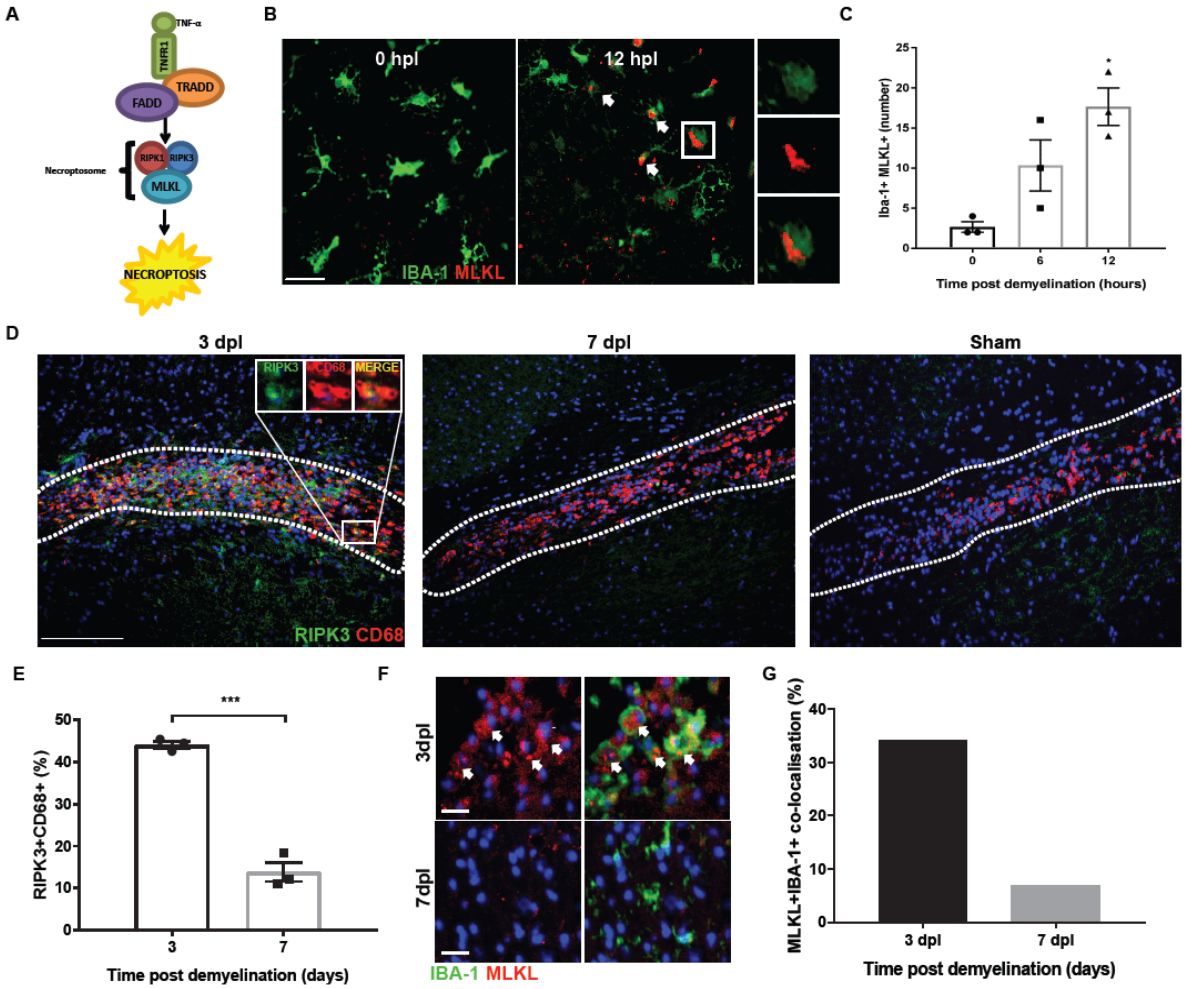

Figure 7. A. Simplified schematic of TNF-α induced necroptosis pathway. **B**. Untreated (0 hpl) and LPC-treated slices (12 hpl) immunostained for IBA-1 (green) and MLKL (red), double positive cells indicated (arrows). Magnified example of a selected IBA-1+ MLKL+ cell (box; right) at 12 hpl. Scale bar, 10µm. **C**. Mean number of MLKL+ microglia (IBA-1+) at 0, 6 and 12 hpl ± s.e.m.. *p<0.05 12 hpl vs 0 hpl (Kruskal-Wallis test, Dunn's Multiple Comparison post-test). N=3 biological replicates. **D**. *In vivo* lesioned corpus callosum (dotted outline) at 3 and 7 dpl, along with a sham injection (7 days post injection) stained for RIPK3 (green) and CD68 (red). Inset at 3 dpl shows RIPK3+ CD68+ cell. Scale bar, 50µm. **E**. Mean percentage of RIPK3+ CD68+ microglia / total

CD68+ microglia at 3 and 7 dpl ± s.e.m.. *P=0.0002 (unpaired Student's *t*-test). N=3 mice per time point. **F**. Image of corpus callosum lesion stained for MLKL (red) and IBA-1 (green) at 3 and 7 dpl. Arrows indicate MLKL+ IBA-1+ microglia. Scale bar, 10μm. **G**. Percentage of MLKL+ IBA-1+ microglia (represented as a percentage of total IBA-1+ cells) at 3 and 7 dpl. N=1 biological repeat.

3.3.8. Monocyte-derived macrophages undergo necroptosis following demyelination in vivo

Monocyte-derived macrophages have been shown to migrate into the demyelinated lesion site in this model (*8*). Therefore, to determine if macrophages also undergo necroptosis in this model, *Ccr2*$^{RFP/+}$ mice underwent LPC-induced demyelination (carried out by Claire Davies, Miron Lab), and *Ccr2*+ macrophages that express RFP can be distinguished from *Ccr2*-RFP negative microglia in the CNS (Figure 8A). Immunostaining of *Ccr2*-RFP lesions with necroptosis marker RIPK3 revealed that *Ccr2*-RFP+ macrophages represented only ~25% of all RIPK3+ cells at 3dpl (Figure 8B, C). Interestingly, at 10dpl, a marked decrease in *Ccr2*-RFP+ macrophages were present, and these cells only represented ~10% of total RIPK3+ cells at this time (Figure 8B, C), suggesting a proportion of macrophages had undergone necroptosis. However, macrophage migration out of the lesion area cannot be ruled out. Overall this demonstrates that the majority of the cells undergoing necroptosis in the lesion are microglia.

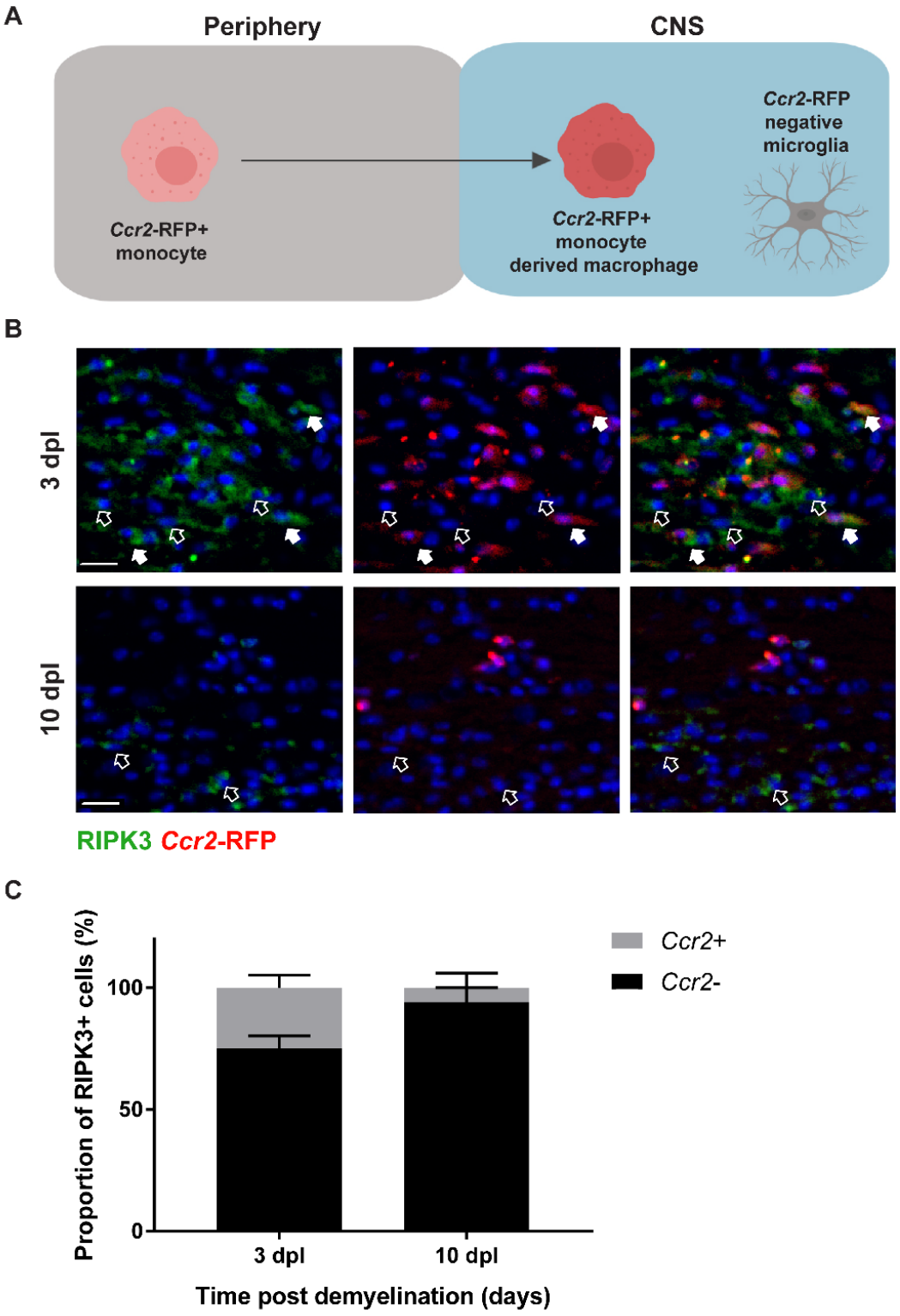

Figure 8. A. Schematic of *Ccr2*-RFP+ monocytes migrating to the CNS and differentiating into *Ccr2*-RFP+macrophages. **B**. Images from lesion areas with Ccr2-

RFP+ macrophages (red) and immunostained with RIPK3 (green) at 3dpl and 10dpl. Scale bar, 20μm. **C**. Quantification of Ccr2+ RIPK3+ cells and Ccr2 negative RIPK3+ cells as a proportion of total RIPK3+ cells in the lesion area at 3dpl and 10dpl ±s.e.m..

3.3.9. Microglial necroptosis takes place in the early stages of remyelination in the Cuprizone model of demyelination and remyelination

To determine whether we could associate microglia necroptosis with remyelination in a distinct model of myelin damage, tissue from the cuprizone model was investigated for necroptotic microglia. In this model, the copper chelator cuprizone is supplemented into the chow of mice for 6 weeks, inducing demyelination particularly in the corpus callosum in the first 3 weeks, followed by concurrent demyelination and remyelination in the second 3 weeks (*160*). At this point, the mice are returned to a normal diet for 4 weeks where remyelination (without demyelination) takes place (Figure 9A).

Immunostaining revealed that RIPK3+ CD68+ microglia were significantly increased at the onset of early remyelination and decreased once remyelination was complete (Figure 9B, C). Staining of tissue during demyelination and early remyelination revealed microglia (IBA-1+) were also MLKL+ (Figure 9D), further supporting evidence for microglial necroptosis at the onset of remyelination.

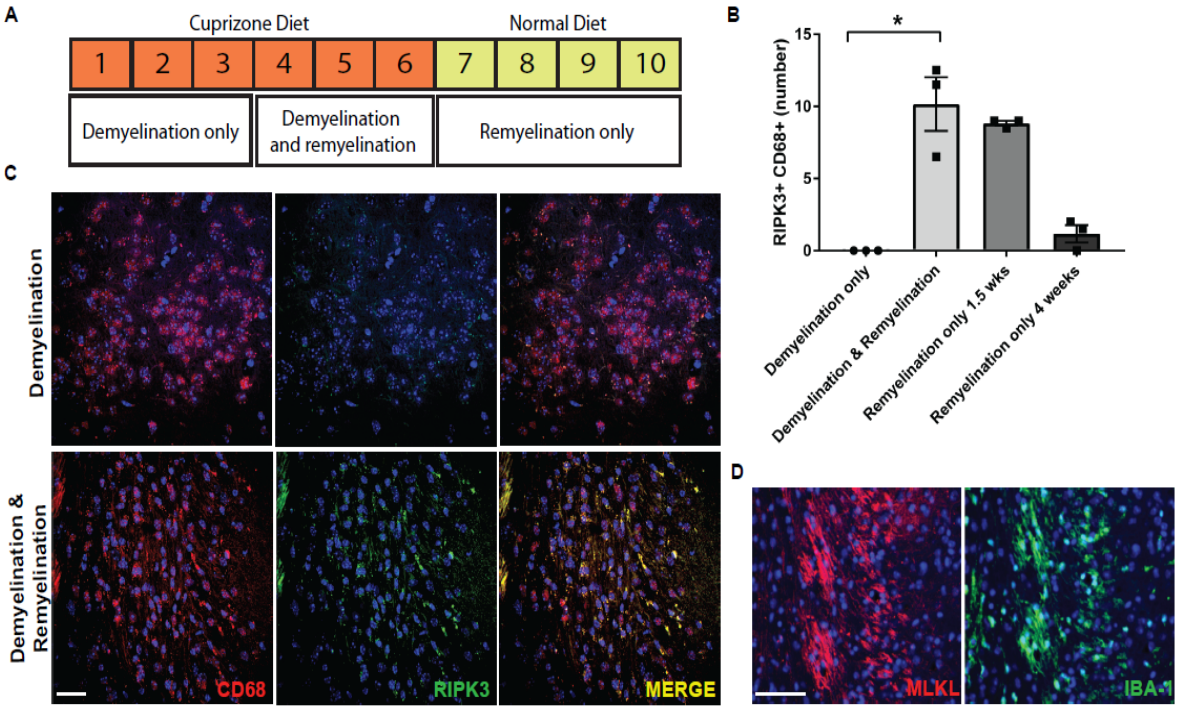

Figure 9. A. Schematic of the treatment regimen for the cuprizone model of demyelination and remyelination. **B**. Number of RIPK3+ CD68+ microglia in mice treated with cuprizone from various phases of demyelination and remyelination: demyelination-only, demyelination and remyelination, remyelination only phases (1.5 wks post return to normal diet, 4 wks post return to normal diet) ± s.e.m.. *P=0.0365 for demyelination & remyelination vs demyelination only (Kruskal-Wallis test, Dunn's Multiple Comparison post-test). N=3 mice per time point and condition. **C**. Images from cuprizone tissue during demyelination only phase (top panel) and ongoing demyelination and remyelination phase (bottom panel) immunostained for CD68 (red) and RIPK3 (green). Scale bar, 50µm. **D**. Representative image from cuprizone tissue during ongoing demyelination and remyelination immunostained for MLKL (red) and IBA-1 (green). Scale bar, 50µm.

3.3.10. Inhibition of necroptosis with small molecule inhibitor necrostatin-1 prolongs a pro-inflammatory phenotype in microglia and hinders remyelination in the ex vivo LPC model of demyelination

To investigate the importance of microglial necroptosis during efficient remyelination, Necrostatin-1, a small molecule inhibitor of necroptosis that prevents necroptosome formation via the inhibition of RIPK1 activity (Figure 10A) was supplemented from the onset of demyelination. Necrostatin-1 treatment prevented microglia (CD68+) loss at 1 dpl compared to vehicle control (Figure 10B, C), and also prolonged iNOS expression in the microglia at 7 dpl when the transition to the pro-regenerative phenotype would normally have taken place (Figure 10B, D). Preventing microglia necroptosis also significantly hindered remyelination in the explants at 7 and 14 dpl, compared to the robust remyelination observed in the vehicle control (Figure 10E, F). Remyelination was detected by measurement of Neurofilament (NF-H) and MBP co-localisation as a proportion of total NF-H staining (remyelination index), with 1.0 being a measurement of total co-localisation of all NF-H+ axons with MBP (Figure 10F). Therefore, inhibition of necroptosis prevented pro-inflammatory microglial death, leading to a significant inhibition of remyelination.

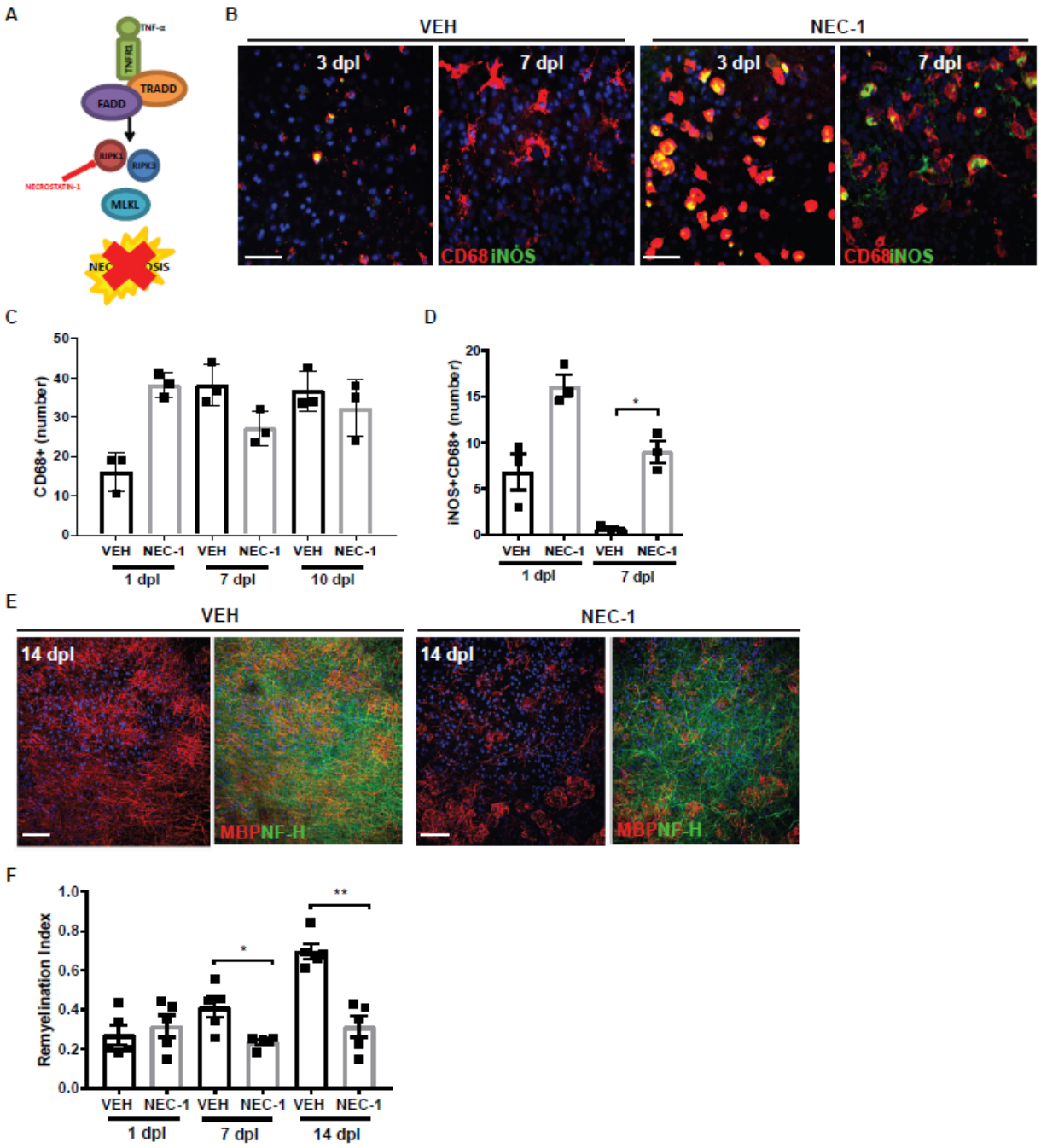

Figure 10. A. Schematic of a simplified necroptosis pathway with small molecular inhibitor of necroptosis, necrostatin-1, inhibiting RIPK1 activation. **B**. Demyelinated slices treated with vehicle (VEH; left) or necrostatin-1 (NEC-1; right) at 1 and 7 dpl immunostained for CD68 (red) and iNOS (green). Scale bar, 10µm. **C**. Mean number of

CD68+ microglia in NEC-1- or VEH-treated conditions at 1, 7 and 10 dpl ± s.e.m.. **D**. Mean number of iNOS+ microglia (CD68+) at 1, and 7 dpl in NEC-1- or VEH-treated conditions ± s.e.m.. *P=0.05 vs VEH (Mann Whitney test). N=3 biological replicates per time point and condition. **E.** Demyelinated slices treated with VEH (left) or NEC-1 (right) at 1 and 7 dpl immunostained for myelin (MBP; red) and axons (NF-H; green). Scale bar, 20µm. **F**. Remyelination index of VEH- and NEC-1-treated slices at 1, 7 and 14 dpl ± s.e.m.. *P=0.0159, **P=0.0079 vs VEH (Mann Whitney test). N=5 biological replicates per time point and condition.

3.3.11. Oligodendrocytes and neurons do not undergo necroptosis in large numbers after demyelination in ex vivo organotypic cerebellar slice cultures

As necroptosis of oligodendrocytes and neurons has been observed in MS (*97*) and Alzheimer's Disease (*161*), respectively, we assessed whether this was occurring in our acute model of demyelination in the slice culture. Demyelinated slices were stained for oligodendrocyte lineage marker Olig2, neuronal marker NeuN, and necroptosis marker RIPK3. At 18 hpl, <3% of total oligodendrocytes or neurons were positive for RIPK3 (Figure 11A-D) showing that necroptosis in our model predominantly occurs in microglia.

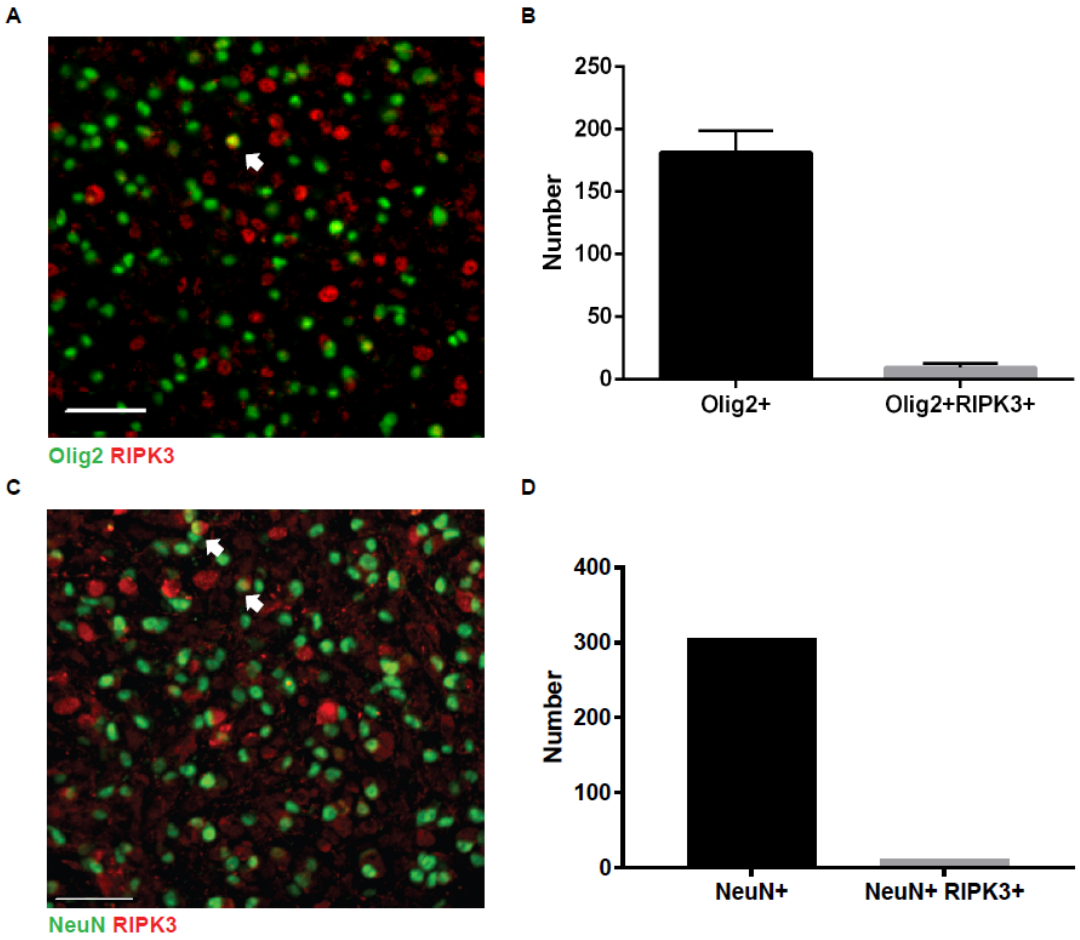

Figure 11. A. Demyelinated slice at 12 hpl immunostained for oligodendrocyte lineage marker Olig2 (green) and RIPK3 (red). Scale bar, 20µm. **B**. Mean numbers of Olig2+ cells and Olig2+RIPK3+ cells ±sem.. N=3 biological replicates. **C**. Demyelinated slice at 12 hpl immunostained for neuronal marker NeuN (green) and RIPK3 (red). Scale bar, 20µm. **D**. Number of NeuN+ cells and NeuN+RIPK3+ cells. N=1 biological replicate.

3.3.12. Using lipid nanocapsules (LNCs) to specifically target microglia in vivo

In order to specifically inhibit microglial necroptosis during remyelination *in vivo*, lipid nanocapsules (LNCs) containing the fluorescent molecule diD (made by Anne des Rieux's lab (Yasmine Labrak); Louvain University, Belgium) were first used to detect specificity of LNC uptake in microglia compared to other cell types during remyelination (Figure 12A). diD (a fluorescent dye) containing LNCs were co-injected with LPC into the corpus callosum to ensure direct lesion penetrance, and lesions were immunostained at 3 dpl to determine if microglia preferentially phagocytosed LNCs over other cell types. At 3 dpl, the majority of diD LNC accumulation was associated with IBA-1+ co-expression, with minimal (>5%) accumulation in astrocytes (GFAP; Figure 12B, D) or cells of the oligodendrocyte lineage (CC1; Figure 12C, D), therefore identifying LNCs as an efficient method to deliver necrostatin-1 specifically to microglia *in vivo*.

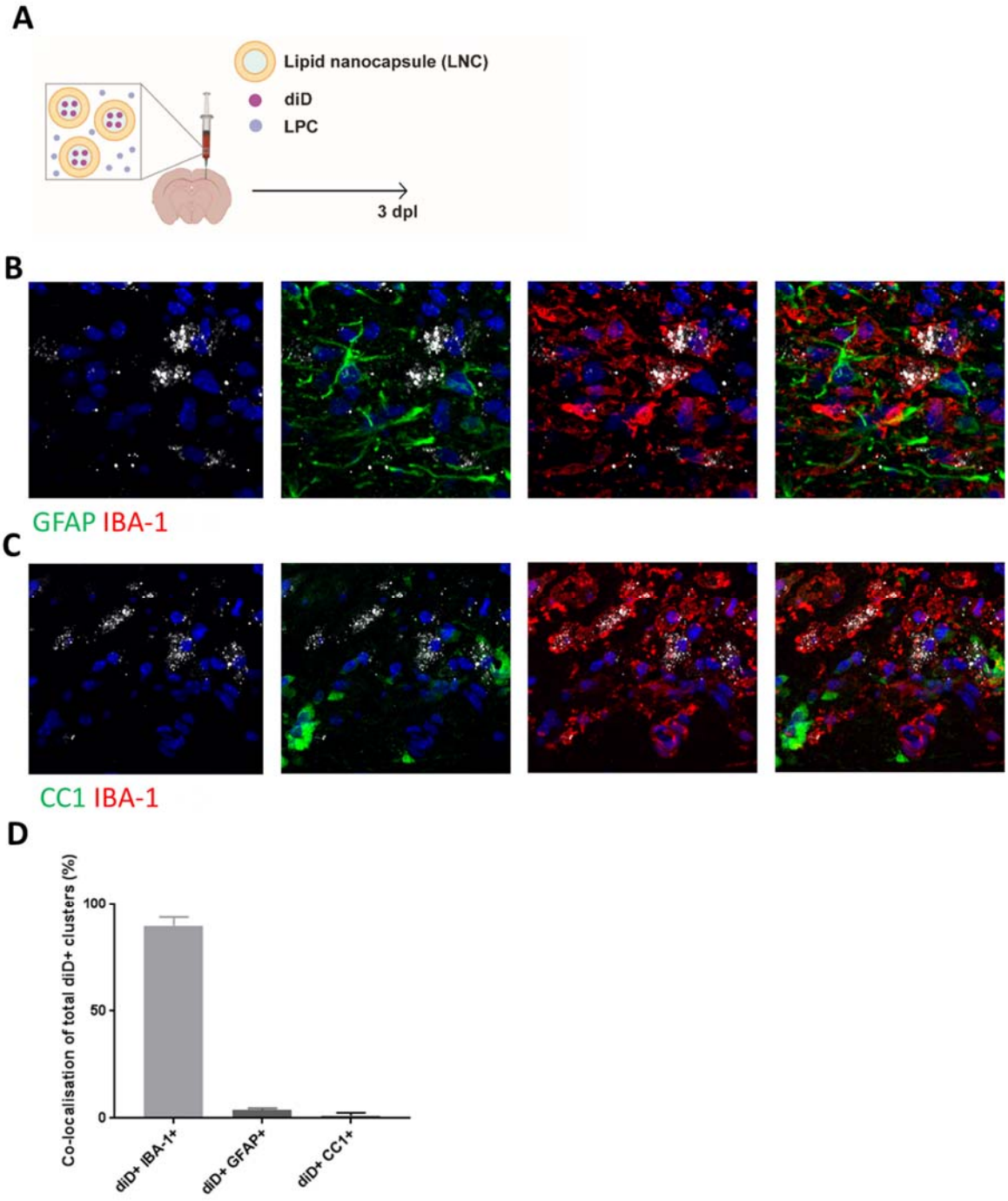

Figure 12. A. Schematic of experimental plan for *in vivo* delivery of LNCs containing diD and LPC via stereotaxic injection into corpus callosum. **B**. Representative image of demyelinated lesion area at 3dpl of mice injected with LNCs containing fluorescent dye

diD (white) and immunostained with IBA-1 (red) and astrocyte marker GFAP (green) to show specificity of LNC delivery. Scale bar, 20μm. **C**. Representative image of demyelinated lesion area at 3dpl of mice injected with LNCs containing fluorescent dye diD (white) and immunostained with IBA-1 (red) and oligodendrocyte lineage marker CC1 (green) to show specificity of LNC delivery. Scale bar, 20μm. **D.** Mean proportion of IBA-1, GFAP and CC1+ cells positive for diD clusters (represented as a percentage of all diD clusters present in the field of view) ± s.e.m.. N=3 biological repeats.

3.3.13. Inhibition of necroptosis with necrostatin-1 LNCs prolongs a pro-inflammatory phenotype in microglia and hinders remyelination in the in vivo LPC model of demyelination

Necrostatin-1 and vehicle control (DMSO) were encapsulated into LNCs and co-injected with LPC (Figure 13A). Compared to vehicle control (Veh LNCs), necrostatin-1 (NEC-1 LNCs) treatment lead to a decrease in IBA-1+/MLKL co-localisation at 3 dpl (Figure 13B), indicative of necrostatin-1 treatment inhibiting necroptosis pathway activation. At 10 dpl, there were 2-fold greater numbers of microglia (identified by expression of microglia-specific marker Tmem119) in NEC-1 LNC treated mice compared to vehicle LNC treated mice (Figure 13C), suggestive of a prevention of microglial death in NEC-1 treated mice. Furthermore, NEC-1 treatment lead to a significant increase in the percentage of iNOS+ Tmem119+ microglia, and a significant reduction in the percentage of Arg-1+ Tmem119+ microglia at 10 dpl compared to vehicle treated demyelinated lesions (Figure 13C, raw values in Chapter 9 Appendix, Figure 2). This suggests that NEC-1 treatment prevented pro-inflammatory microglial necroptosis, leading to a prolonged presence of pro-inflammatory microglia and an inhibition of pro-regenerative microglial activation. Importantly, immunostaining for myelin protein MAG (myelin associated glycoprotein) revealed a stark reduction in NEC-1 treated mice compared to vehicle, as measured by mean MAG pixel intensity of the lesion area at 10 dpl (Figure 13D, E), indicating that NEC-1 treatment in microglia had significantly inhibited oligodendrocyte differentiation (suggestive of remyelination) *in vivo*. Taken altogether, this evidence suggests that we have effectively targeted

microglia using LNCs, and specific inhibition of microglial necroptosis prevents microglial death, maintains pro-inflammatory (iNOS) activation, and prevents pro-regenerative (Arg-1) microglial activation, consequentially inhibiting oligodendrocyte differentiation, and therefore remyelination. However, to definitively show that remyelination is inhibited, electron microscopy would be needed. Unfortunately with time constraints for this project, this was unable to be carried out (see future directions).

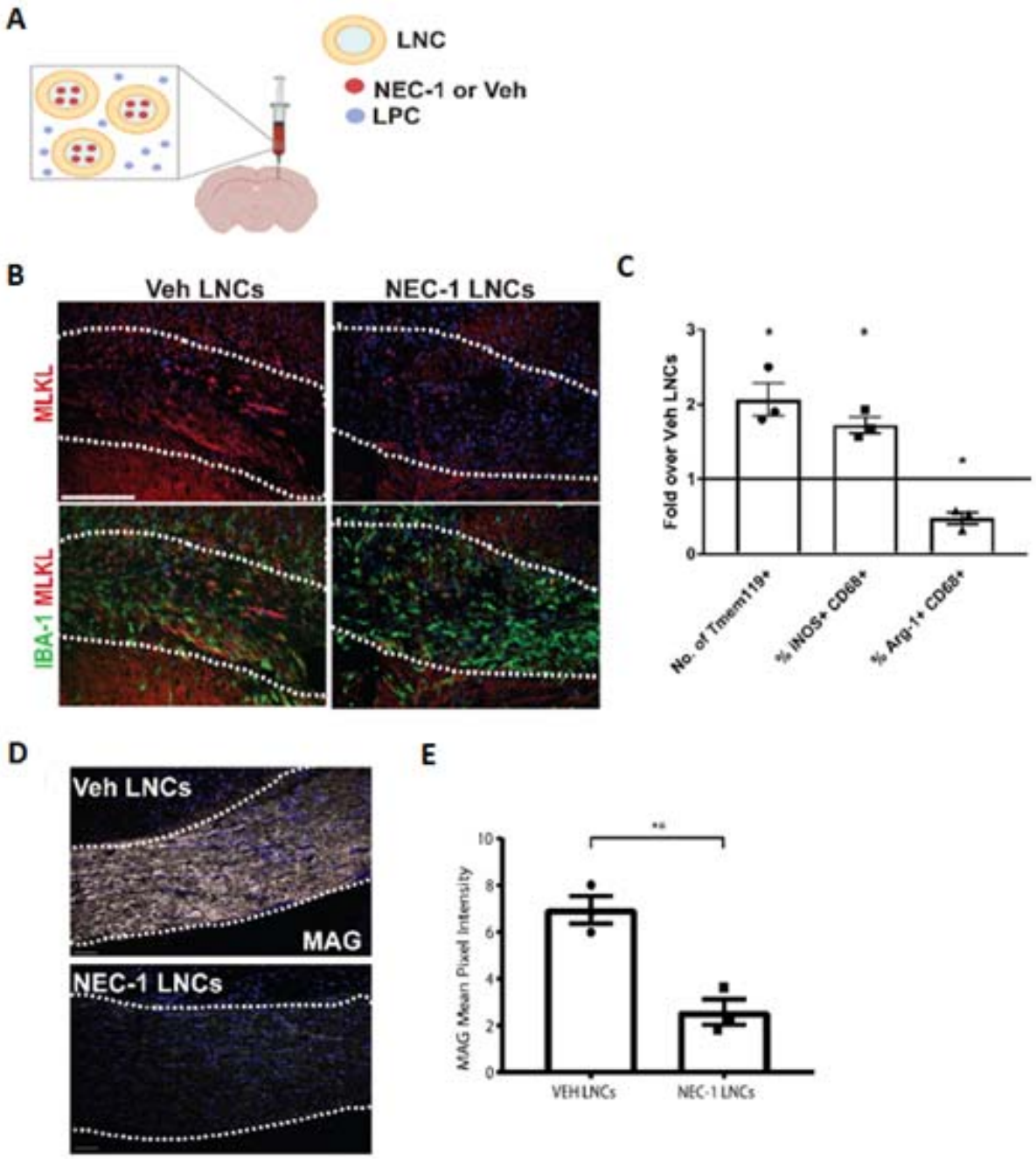

Figure 13. A. Schematic of experimental plan for *in vivo* delivery of LNCs containing Necrostatin-1 or vehicle (Veh; DMSO) control and LPC via stereotaxic injection into corpus callosum **B.** Images of lesions at 3 dpl (dotted outline) subsequent to treatment with Veh LNCs or NEC-1 LNCs, stained for IBA-1 (green) and MLKL (red). Scale bar, 50 µm. **C.** Quantification of the number of Tmem119+ cells, the percentage of iNOS+CD68+

(of total CD68+) cells and the percentage of Arg-1+CD68+ (of total CD68+) cells in 10 dpl lesions subsequent to treatment with NEC-1 LNCs, represented as fold change over values in Veh LNC treated mice. One sample *t*-test compared to a hypothetical value of 1: *P=0.0395 for Tmem119+ cells, 0.026 for percentage of iNOS+CD68+ cells, and 0.0224 for percentage of Arg-1+CD68+ cells. N=3 mice per stain. **D.** Images of corpus callosum at 10 dpl (dotted outline) subsequent to treatment with Veh LNCs or NEC-1 LNCs stained for myelin protein MAG (white). Scale bar, 20 μm. **E.** Mean MAG pixel intensity in lesions at 10 dpl following injection with Veh LNCs or NEC-1 LNCs. 2-tailed unpaired Student's *t*-test, **P=0.0055. N=3 mice per condition.

3.3.14. Microglial necroptosis is a prevalent feature in active multiple sclerosis lesions

To investigate the importance of microglial necroptosis during remyelination in the human disease, MS lesions of different subtypes including remyelinated lesions, lesions with ongoing remyelination/ high potential for remyelination ("active"), and lesions with failed remyelination/ low potential for remyelination ("chronic inactive"), as described previously (*162*) were analysed and compared to the white matter of post mortem tissue from patients who had died of non-neurological causes ("control") (see Chapter 2: Methods, Table 1 for all human tissue information). Only in active lesions were there signicant increases in RIPK3+ and MLKL+ CD68+ microglia compared to control white matter (Figure 14A-E). Therefore, microglial necroptosis is a feature of active MS lesions associated with high numbers of macrophages and a high incidence of remyelinaton (*163*), whereas inactive lesions have signfiicantly fewer necroptosing microglia. Therefore, there may be an association of microglial necroptosis with remyelination potential in human disease.

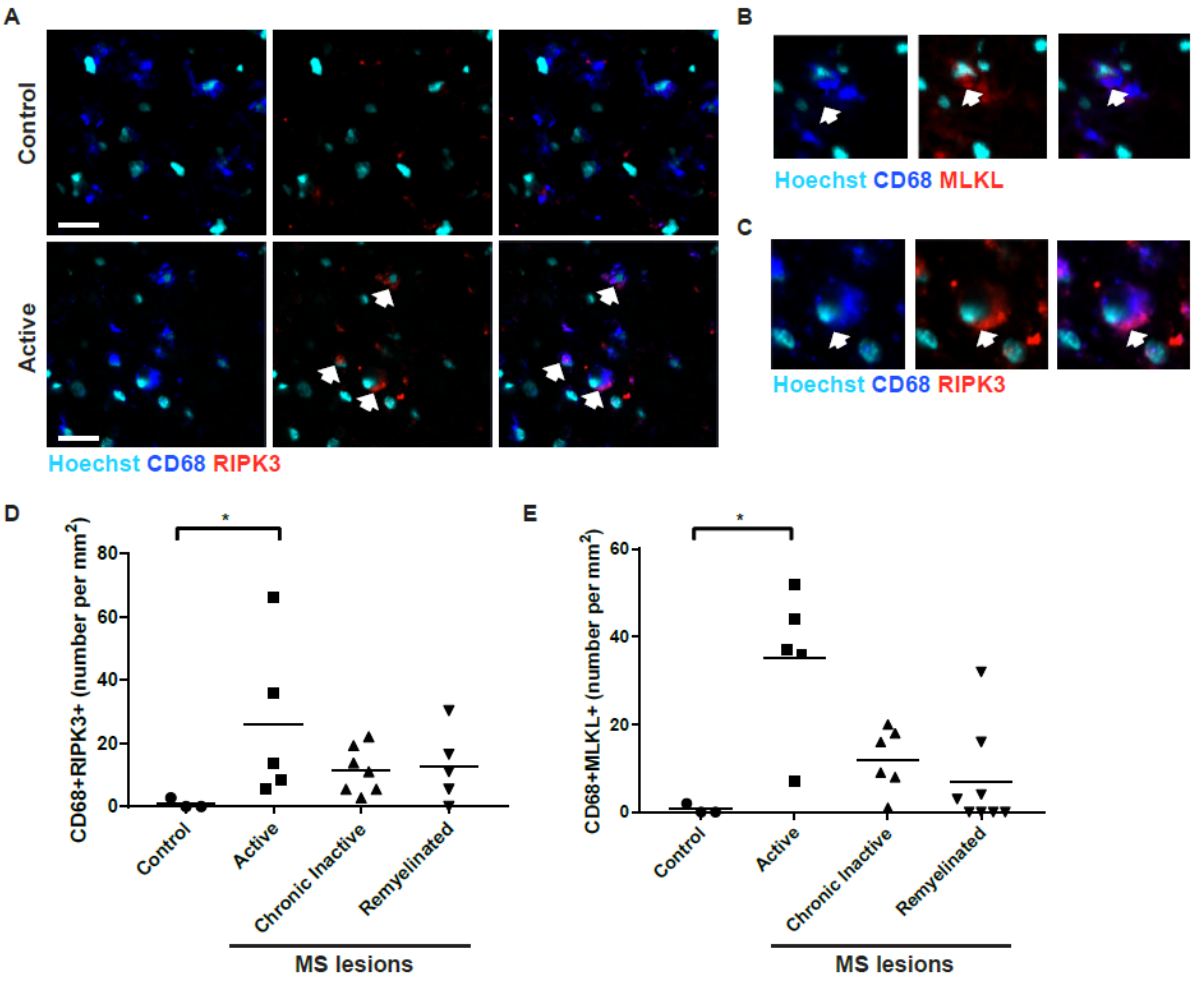

Figure 14. A. Control brain tissue and active MS lesion immunostained for CD68 (blue) and RIPK3 (red), counterstained with Hoechst (turquoise). White arrows indicate CD68+RIPK3+ cells. Scale bar, 20µm. **B**. Magnified view of MLKL expression (red) in a microglia (CD68+; blue) in an active lesion, counterstained with Hoechst (turquoise). White arrows indicate CD68+MLKL+ cells. **C**. Magnified view of RIPK3 expression (red) in a microglia (CD68+; blue) in an active lesion, counterstained with Hoechst (turquoise). White arrows indicate CD68+RIPK3+ cells **D**. Mean density of RIPK3+ microglia (CD68+) per mm^2 in control, active, chronic inactive and remyelinated MS lesions. Individual data points represent separate lesions. *P=0.0357 active lesions vs

control (Mann-Whitney test). Remyelinated v control p=0.1429; chronic inactive v control p=0.1029 (Mann-Whitney test). **E**. Mean density of MLKL+ microglia (CD68+) per mm^2 in control, active, chronic inactive and remyelinated MS lesions. Individual data points represent separate lesions (see Table 1). *P=0.0226 active lesions vs control (Mann-Whitney test). Remyelinated v control p=0.4169; chronic inactive v control p=0.1683 (Mann-Whitney test).

3.4. Discussion

I sought to determine the cellular and molecular mechanisms underpinning microglia transition during efficient remyelination from an initial pro-inflammatory phenotype to a pro-regenerative phenotype. Prior to this transition in phenotype, pro-inflammatory microglia undergo necroptosis, as shown by a loss of microglia after the peak of pro-inflammatory microglial activation, the expression of necroptosis markers MLKL and RIPK3, and the inhibition of death using an inhibitor of necroptosis. By blocking microglial necroptosis, microglia persist in a pro-inflammatory activation state for significantly longer and as a consequence, remyelination is hindered. Therefore, for efficient remyelination to take place, pro-inflammatory microglia must undergo necroptosis, which may play a role in rapidly shutting down inflammation and allowing for the activation of pro-regenerative microglia to drive remyelination. I propose that pro-inflammatory microglial necroptosis is a previously unrecognised mechanism in which microglial phenotypes are regulated during remyelination.

Using LPC to induce demyelination in the *ex vivo* and *in vivo* models permits investigations of efficient remyelination without concurrent demyelination. Although LPC is a myelin toxin, there is evidence to show how it can directly influence microglial activation and behaviour. For example, LPC has been shown to activate caspase-1 in microglia pre-stimulated with inflammatory lipopolysaccharide, a bacterial membrane protein known to induce a potent inflammatory response in immune cells including microglia (*164*). In the developing zebrafish brain, LPC released from apoptotic neurons is required at

least in part to promote the migration of microglia precursors to colonise the brain (*165*). However, I did not observe a toxic effect of LPC directly on microglia *in vitro* (Figure 3), and also associated microglial necroptosis with initiation of remyelination in a model without LPC (Cuprizone, Figure 9). Additionally, microglia from demyelinated slices at 12 hpl were negative for apoptosis markers TUNEL and cleaved caspase-3 (Figure 6A), and displayed constitutive caspase-1+ expression even prior to demyelination (0 hpl, Figure 6B). Indeed, cleaved caspase-1 has been previously shown to be upregulated in LPS and ATP- treated activated microglia *in vitro,* indicative of activated inflammasome in the absence of cell death (*166*). Furthermore, activated (CD68+) microglia are prevalent in myelinated slices prior to demyelination (Figure 6B). This may be in response to the mechanical damage associated with slicing of the brain sections for culture, and therefore may explain the presence of cleaved caspase-1 expression and inflammasome activation in microglia from non-demyelinated slices.

Necroptosis has only recently been identified as a type of programmed cell death involved in many pathologies (*97, 167, 168*). Attention was brought to this mechanism when *in vitro* experiments with TNF-α treatment caused cultured cells to exhibit features of both apoptotic and necrotic death; they appeared to have a swollen 'balloon-like' morphology (a necrotic cell characteristic), yet underwent autophagy (commonly seen in apoptotic cells; (*169*)). Now it is appreciated that many other factors can trigger cells to undergo necroptosis including ischemia-reperfusion (*170*), viral and bacterial infection (*171-173*)

and it has been observed in neurodegenerative diseases including amyotrophic lateral sclerosis (ALS) (*168*), MS (*97*), and Alzheimer's Disease (AD) (*161*).

Although similar factors can trigger other cell death mechanisms, the downstream molecular pathways underpinning necroptosis distinguish it as a unique controlled cell death mechanism (Figure 7A, *Diagram 4*). Similarly to apoptosis, necroptosis can be initiated by the binding of CD95 and CD95L (FAS and FASL), TNF receptor 1 and 2 (TNFR1 and TNFR2), TNF-related apoptosis inducing ligand receptor 1 and 2 (TRAIL1 and TRAIL2), and pathogen recognition receptors (PRRs) involved in the detection of pathogens or PAMPs (*174*), with TNFR1 mediated necroptosis being the most extensively studied. Although each trigger will initiate a distinct downstream activation pathway, all can converge to activate the necroptosome, and ultimately, necroptosis.

Comprised of receptor interacting protein kinase-1 and 3 (RIPK1 and RIPK3) and pseudokinase mixed lineage kinase like (MLKL), the necroptosome is the most downstream, and ultimate initiator of necroptosis (Figure 7A). In response to receptor activation, and intracellular death domains including TNFR-associated death domain (TRADD), caspase-8 cleaves both RIPK1 and RIPK3, rendering them inactive, either eliciting an inflammatory response (if cellular inhibitors of apoptosis (cIAPs) or and linear ubiquitin chain assembly complex (LUBAC) are present) or by driving apoptosis (if deubiquitilyases are present, leading to the destabilisation of the inflammatory complex). In the absence of caspase-8 activity, deubiquitilyated RIPK1 can form a complex with RIPK3 which is then able to interact via the RIP homotypic interaction motif (RHIM)

present on both kinases (*175*) leading to the auto-phosphorylation of RIPK3, and subsequently leading to the phosphorylation of MLKL. Upon phosphorylation, MLKL forms a large oligomeric complex, thought to function as a platform at the plasma membrane, allowing for the recruitment of Ca^{2+} or Na^{+} ion channels (*176, 177*), and also as a direct pore-forming complex that is recruited to the cell membrane causing direct damage (*178*). Not only the executioner of necroptosis, MLKL has also been shown to trigger the formation of the NLR family pyrin domain containing 3 (NLRP3) inflammasome, required to process and activate interleukin-1 beta (IL-1β), a potent inflammatory mediator (*179*). The membrane disruption caused by MLKL then allows efficient efflux of IL-1β (*179*), suggesting a mechanism responsible for the inflammatory response elicited as a consequence of necroptosis.

Although inflammasome activation is an important part of pro-inflammatory microglial responses (*180*), the loss of microglia and confirmation of cell death with PI, 7-AAD and Annexin-V in our models (Figure 5) suggest that MLKL is also initiating necroptosis during remyelination, not just inflammasome activation. However, this highlights the need to detect necroptosis not just by marker expression, but also by detection of loss of cells.

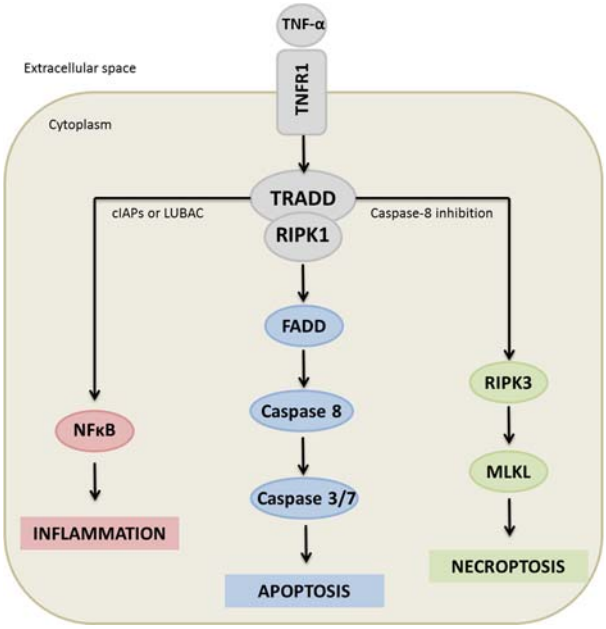

Diagram 4. Outline of how a single stimuli can trigger inflammation, apoptosis or necroptosis. In this example, TNF-α bound to TNFR1 can recruit TRADD and RIPK1. cIAPs and LUBAC can stabilise the complex, leading to recruitment of NFκB, and activation of its signalling pathway complexes involved in cell survival, inflammation and proliferation. Further stimulation leads to deubiquitylation of this complex and initiation of caspase-8 dependant forms of apoptotic cell death. In the absence of caspase-8 activity, deubiquitylated RIPK1 can recruit RIPK3, leading to the recruitment and phosphorylation of MLKL that can initiate necroptosis.

It is important to note however that activation of necroptosis markers does not always lead to death of the cell. For example, RIPK1 plays promiscuous roles in regulating inflammation and apoptosis as well as necroptosis (Figure 14) (*174*). Post-translational modifications of RIPK1 means there are 4 variants involved in different processes, including TNFR1 dependent pro-inflammatory signalling by its role in a receptor-bound complex known as complex 1 (*181*), leading to the activation of MAPK and NFκB and their consequential roles in survival and inflammation. De-stabilisation of complex 1 leads to cell death, either by a caspase-8 dependent and RIPK1-independent form of apoptosis, a RIPK1 and caspase-8 dependant form of apoptosis, or by necroptosis via the necroptosome (*174, 182*). In some circumstances, such as in the presence of viral DNA, necroptosis can take place independent of RIPK1 (*183*). Therefore, this further highlights that the detection of necroptosis should include the assessment of expression of multiple markers of necroptosis (particularly MLKL), the detection of cell death itself, and the inhibition of death by necroptosis inhibitors such as necrostatin-1.

Although RIPK3+ *Ccr2*-RFP+ macrophages were present in the lesion site at 3 dpl, (Figure 8B, C), it cannot be fully determined if macrophages also undergo necroptosis during this time. Indeed, there is a reduction in the number of *Ccr2*-RFP+ cells at 10 dpl compared to 3 dpl, although migration out of the lesion site cannot be ruled out. There is evidence that macrophages can undergo necroptosis, and evidence to suggest that this mechanism is important in regulating macrophage phenotypes. Liver-resident macrophages (Kupffer cells) from mice infected with *Listeria monocytogenes* undergo necroptosis after

phagocytosis of the bacteria, as shown by detection of PI+ Kupffer cells and inhibition of death by flow cytometry with necrostatin-1 treatment (*172*). Furthermore, Kupffer cell necroptosis then leads to recruitment of monocytes able to differentiate into tissue-reparative macrophages, as shown by upregulation of *Arg-1* and *Ym1* (*172*). Whether macrophages in the CNS can definitively undergo necroptosis, and its importance in driving a pro-regenerative environment remains to be determined (*see future directions*).

Inhibition of cell death with necrostatin-1 supports the hypothesis that pro-inflammatory microglia undergo cell death via necroptosis during remyelination. However, supplementing necrostatin-1 treatment into explant culture media exposes all cells to potential necrostatin-1 treatment, which may confound any observable results on remyelination if other cell types are also undergoing necroptosis during this time. Indeed, expression of RIPK1, RIPK3 and MLKL is prevalent in oligodendrocytes in post mortem MS tissue and in EAE (*97*). However we found that only ~3% of Olig2+ cells were RIPK3+ after LPC treatment of slices (Figure 10A, B) and therefore unlikely to impact remyelination. Additionally, neuronal necroptosis has been shown to drive neurodegeneration in AD (*184*), however we found minimal NeuN+ neurons positive for RIPK3 after LPC treatment (Figure 10C, D).

Although my *ex vivo* evidence suggests that necroptosis in remyelination is predominantly in microglia, I aimed to produce a specific microglial-targeted inhibition of necroptosis *in vivo*. For this, necrostatin-1 encapsulated inside lipid nanocapsules (LNCs) were produced by Yasmine Labrak (UC Louvain,

Belgium), shown previously to be preferentially taken up by phagosomes (*185*), and therefore predominantly by microglia in the CNS. To my knowledge, this was the first time that LNCs have been administered at the onset of demyelination (by co-injection with LPC) and therefore presented potential logistical issues, such as toxicity at high doses, and unknown degradation rates *in vivo*. Although toxicity of LNCs alone was not measured in these experiments, prior experiments from the des Rieux lab concluded that concentrations of LNCs above 1μM were cytotoxic, and therefore a maximum concentration of 1μM was used for these experiments. Although Veh LNC treated mice showed similar microglial activation dynamics and remyelination to LPC treatment alone, toxicity of empty LNCs alone and with LPC should be investigated (*see future directions*). Nonetheless, a single treatment of necrostatin-1 LNCs was sufficient to prevent pro-inflammatory microglial necroptosis, as shown by reduction in loss of microglia (Tmem119+), prolonged expression of iNOS and reduction of Arg-1 at 10 dpl compared to vehicle (Figure 13B, C, Chapter 9 Appendix figure 2). NEC-1 LNC treatment also significantly reduced remyelination at 10 dpl, as shown by intensity of MAG staining (indicative of oligodendrocyte maturation and potential remyelination; Figure 13D, E) compared to vehicle, suggesting that remyelination is significantly inhibited by specific inhibition of microglial necroptosis. Although the differences in MAG pixel intensity are stark in NEC-1 LNC treated mice compared to Veh LNC treated mice at 10 dpl, closer inspection of remyelination by electron microscopy, the gold standard in measuring remyelination, should be used in the future (*see future directions*).

It cannot be underestimated however that necrostatin-1 itself may have some off-target effects including the inhibition of indoleamine-2,3-dioxygenase (IDO), an immunomodulatory enzyme found to be important particularly in inflammation-associated tumorigenesis (*186*), and therefore inhibition of which may have the potential to affect inflammatory activation in microglia outside of modulation of necroptosis. In more recent years, more specific necrostatins have been synthesised, including necrostatin-1s which does not interact with IDO (*186*), and therefore any future studies inhibiting necroptosis should be carried out using the newer generation of more specific necrostatins. However, the various roles of RIPK1 in non-necroptosis pathways may result in off-target effects of necrostatins despite greater RIPK1 specificity (*159*). Although necrosulfonamide has been identified as a potent inhibitor of necroptosis via its selective inhibition of MLKL, and therefore a more specific inhibitor of necroptosis in general, it is unclear if the small molecule inhibitor is able to target mouse MLKL, as studies to identify the compound were done in human cell lines (*187*). However, a recent paper reported how necrosulfonamide treatment in a mouse model of spinal cord injury is protective for spinal cord neurons, although its direct effect on reducing MLKL activity was not measured (*188*). Therefore, the lack of uncertainty to the specificity of necroptosis specific inhibitors warrants a genetic mouse model. For example the use of a microglial-specific inducible *Mlkl* knockout mouse may provide an even more specific and straightforward means of inhibiting microglial necroptosis in the future (*see future directions*).

It is now appreciated that necroptosis is a common feature in many neurodegenerative diseases and in different cell types. Evidence suggests that neuronal necroptosis potentiates the progression of disease in AD. Indeed, post mortem analysis of brains from AD patients revealed significantly increased levels of necroptosis proteins RIPK3 and MLKL, as well as phosphorylated, and therefore active MLKL compared to control (*161*). Co-staining revealed ~60% of pMLKL+ cells were neurons (indicated by NeuN staining), 28% were microglia (IBA-1+) and 11% were astrocytes (GFAP+)(*161*). Furthermore, mRNA expression levels of necroptosis markers *Ripk1* and *Mlkl* correlated negatively with brain weight and Braak staging, a measurement of pathology, suggesting a detrimental effect of necroptosis on the progression of AD (*161*), although individual cell type gene expression was not assessed, and therefore the role of microglial necroptosis remains unclear. Moreover, post mortem MS samples showed an increase in necroptosis proteins RIPK3, MLKL and pMLKL, and importantly, increases in protein aggregates of MLKL compared to control (*97*), indicative of MLKL oligomerisation and execution of necroptosis (*159, 178*). Immunostaining revealed increases in RIPK1+ and MLKL+ CC1+ oligodendrocytes in MS tissue and cuprizone-induced demyelinated mouse tissue. Inhibition of necroptosis by necrostatin-1 analogue 7N-1 or RIPK3 knockout mice protected oligodendrocytes from death in cuprizone model, showing how necroptosis can be detrimental and blocking necroptosis may be of therapeutic benefit in some cell types (*97*). MS tissue samples also revealed RIPK1+ and MLKL+ IBA-1+ microglia, albeit to a much lesser extent, although different lesion types were not analysed. Evidence from this thesis suggests that

there are indeed significant differences in RIPK3+ and MLKL+ microglia depending on lesion types, with more RIPK3+ and MLKL+ microglia present in active lesions associated with high macrophage infiltration and potential for remyelination (*163*) (Figure 14), suggesting a role of microglial necroptosis in efficient remyelination in MS. Importantly, global inhibition of necroptosis in the cuprizone model increased the fraction of myelinated axons, most likely protecting oligodendrocytes from demyelination (*97*); however the role of microglial necroptosis was not investigated, and therefore its potential beneficial role in remyelination was not determined. Mining of RNA sequencing data from microglia in another EAE study (data not shown) revealed that both *Ripk3* and *Mlkl* expression is prevalent in late stages of the disease (*189*), correlating with when remyelination has been shown to take place in this model (*18*). Although merely correlative, this may suggest that microglial necroptosis may be an important factor for remyelination in EAE. On the contrary, microglial necroptosis has been suggested to contribute to inflammation-induced retinal neurodegeneration in the rd1 mouse model and in the NMDA model of acute retinal injury (*190*). Indeed, inhibition of necroptosis with necrostatin-1 attenuated retinal inflammation and prevented degeneration, although neuronal necroptosis was not measured; therefore the effects of necrostatin-1 on preventing neuronal death as a protective outcome in this model cannot be ruled out.

Findings in this thesis may suggest that for efficient remyelination to take place, pro-inflammatory microglia must undergo necroptosis, potentially as a way of effectively shutting down inflammation and promoting the activation of pro-

regenerative microglia supportive of remyelination. Also for the first time, it is proposed that necroptosis in the CNS may be of benefit, as blocking microglial necroptosis prolongs pro-inflammatory microglial activation for a significantly longer time and hinders remyelination experimentally, supported by human tissue evidence indicating that necroptosing microglia are present in significant numbers in lesions with a potential for remyelination.

3.5. Future Directions

I have demonstrated that by blocking microglial necroptosis, remyelination is significantly hindered, however a key experiment to provide greater translational evidence would be to promote or accelerate microglial necroptosis in order to enhance remyelination. Although the LPC model is a reliable model of efficient remyelination, a more suitable model for this experiment would be one where persistent pro-inflammatory microglial activation is prevalent, as well as having a poor remyelination potential in order to observe considerable differences. For example, spinal cord injury (SCI) models have poor regenerative potential (*80, 191*), as well as persistent pro-inflammatory microglia and macrophages throughout (*192*), and therefore have the potential to show profound differences in microglial activation and regeneration. Moreover, remyelination in aged mice following spinal cord demyelination is significantly impaired compared to young mice (*193*) and is associated with persistent inflammation in microglia (*193, 194*) and would therefore also be an interesting model to determine if promoting microglial necroptosis could accelerate remyelination (although the role of microglial necroptosis in both of these models needs to be characterised). The chemotherapeutic agent Shikonin has been shown to induce necroptosis of glioma and non-small cell lung cancer cells (*195, 196*) and would therefore be a potential candidate to promote microglial necroptosis, although targeted delivery such as via LNC encapsulation may be necessary.

Although necrostatin-1 LNCs were shown to be relatively microglia-specific (by diD LNC co-localisation with IBA-1), there was still a small proportion of diD+

clusters not localised to IBA-1+ cells. Furthermore, with evidence suggesting that necrostatin-1 may have off-target effects such as IDO inhibition (*186*), a genetic mouse model may provide a more straightforward inhibition of necroptosis. For example, an inducible knockout of *Mlkl* driven by the *Csf1r* promoter would allow specific timing of necroptosis inhibition, specifically in microglia and macrophages. Although inducible Cre models have limitations, such as limited recombination efficiency, spontaneous recombination and the use of tamoxifen to induce Cre-recombination (which has been shown to accelerate remyelination experimentally (*197*)), it would be interesting to investigate if this model is more effective at inhibiting microglial/macrophage necroptosis and its effects of remyelination compared to necrostatin-1 LNC treatment.

As high concentrations of LNCs have been shown to be toxic to cells by the des Rieux lab, it needs to be ensured that the LNCs in these experiments are not causing toxicity, and therefore affecting necroptosis or microglial activation alone. Therefore, administration of empty LNCs at the same 1:100 dilution should be carried out with and without LPC to see if there is an increase in microglial death or a change in activation compared to LPC alone. This could be determined by isolation of microglia at 7dpl when a significant decrease in microglia is observed in demyelinated lesions and comparing numbers of microglia to LPC alone by flow cytometry, and also by looking at death markers by flow cytometry at this time, as well as immunostaining for activation markers (such as iNOS, Arg-1, CD68 for example). In the empty LNCs without demyelination, there should be no observed loss of microglia and minimal cell

death marker-positive microglia, comparable to time-matched mice without demyelination. Similarly, one would expect no change in the number of activated (CD68+) microglia, or the proportions of iNOS+ and Arg-1+ microglia at all time points compared to LPC alone.

Although I have demonstrated the importance of microglial necroptosis, the molecular mechanism driving this process is still unknown. Indeed, TNF-α has been shown to induce necroptosis in a multitude of cell types (*198-201*), and microglia-secreted TNF-α has been shown to induce necroptosis in oligodendrocytes (*97*). Whether microglial TNF-α release causes an autocrine response to regulate microglial inflammation remains to be determined. Using neutralising antibodies against secreted TNF-α would block its activity and could be used to assess the role of secreted TNF-α in driving microglial necroptosis. Furthermore, it could be that microglia are more resistant to necroptosis in disease models with chronic pro-inflammatory microglial responses, and the mechanisms that underpin this would could be explored in order to uncover novel therapeutic targets aimed at promoting remyelination. This could be assessed by looking in models where chronic pro-inflammatory microglial activation occurs, such as in ageing mice after demyelination (*8, 193, 194*) or in SCI (*192*). Firstly, immunostaining with necroptosis markers would determine if pro-inflammatory microglia do not undergo necroptosis, or if they do but either i) repopulation does not take place or ii) repopulation takes place but the inflammatory environment leads to pro-inflammatory microglial activation in repopulated microglia. If pro-inflammatory microglia in these models do not undergo necroptosis, RNA sequencing of microglia in these

models could be conducted and compared to RNA sequencing datasets from microglia in the LPC model during peak of pro-inflammatory activation (3 dpl). This may highlight differences in activation, phenotypes and death and survival pathways for example that could explain why pro-inflammatory microglia in some models do not undergo necroptosis.

The importance of monocyte-derived macrophages in this model needs to be determined. Firstly, evidence demonstrates that *Ccr2*-RFP+ macrophages express necroptosis marker RIPK3, however it is uncertain if this represents pro-inflammatory activation or necroptosis. Analysis of *Ccr2*-RFP+ by flow cytometry with death markers Annexin-V and 7-AAD would determine if macrophages are undergoing cell death in this model. Furthermore, selective blocking of macrophage necroptosis by a macrophage-specific *Mlkl* knockout (driven by the *Ccr2* promoter, for example), would determine if macrophage necroptosis is necessary for i) microglial necroptosis to take place, ii) for pro-regenerative microglial activation to take place and iii) for efficient remyelination to take place. If a persistent pro-inflammatory macrophage activation phenotype occurs in this knockout mouse model, it would be interesting to observe how this impacts microglial activation and if they can still undergo necroptosis and a transition to a pro-regenerative phenotype, and if this is sufficient to drive remyelination. Furthermore, a microglial-specific *Mlkl* knockout (driven by the *Tmem119* promoter for example) would also determine the importance of microglia death for macrophage infiltration and necroptosis in this model. For example, if microglia cannot undergo necroptosis and have a persistent pro-inflammatory phenotype, can peripheral macrophages promote

remyelination alone? These studies will determine the importance of microglial and peripheral macrophage necroptosis in driving remyelination.

Lastly, the gold standard for detection of remyelination is electron microscopy. Although a significant difference in MAG pixel intensity in lesions at 10 dpl treated with necrostatin-1 LNCs compared to vehicle was detected, suggesting that inhibition of microglial necroptosis prevents efficient remyelination, the detection of differences in remyelination would be more convincing with electron microscopy demonstrating thinner myelin.

Chapter 4: Investigating the mechanisms underpinning microglial repopulation and activation to a pro-repair phenotype during efficient remyelination

4.1. Abstract

Microglia are the resident macrophages of the CNS. Although considered long lived cells with low turnover, many studies have now demonstrated how rapidly microglia can repopulate the brain after depletion (*68-70, 202, 203*). However, the roles of microglial death and repopulation are understudied. Indeed, I found that pro-inflammatory microglial death by necroptosis plays an important role regulating microglial phenotypes during remyelination, but the mechanisms that underpin how microglial repopulation takes place are unclear. Here, I show that repopulation of microglia takes place rapidly after pro-inflammatory microglial necroptosis during remyelination. Lineage tracing revealed that the source of microglial repopulation is primarily via the expansion of residual Nestin+ microglia and supplemented by the differentiation of Nestin+ cells. Furthermore, repopulating (Nestin+) microglia are significantly increased in MS lesions with high remyelination potential but not in lesions that fail to remyelinate, suggesting the importance of these cells in remyelination. This data therefore demonstrates how microglial repopulation can take place outside of experimental depletion models, and is a feature of remyelination in a demyelination model and in MS.

4.2. Introduction

Microglia have a low turnover under physiological conditions, both in the mouse (1.38% of microglia proliferating (BrdU+ incorporation) and 1.23% of microglia undergoing apoptosis at all times (*66*)), and in humans (28% of microglia turnover per year (*204*)), a major difference compared to the rapid turnover of peripheral macrophages (*205*). However, in response to experimental depletion it has been shown that microglia can rapidly repopulate the CNS, both in the embryo and in the adult (*68-70, 202, 203, 206*). Whereas monocytes are the source of peripheral macrophage replenishment, isolation of microglia from the periphery results in the reliance on self-renewal. As a result, the source of repopulating microglia after depletion has been hotly debated.

Although under normal conditions, microglia progenitors originate from the yolk sac during embryogenesis, depletion studies have sought to determine if additional sources of microglia can arise outside of the yolk sac. Depletion of primitive embryonic microglia in the yolk sac at E6.5/ E7.5 with a CSF1R inhibitor results in a complete lack of microglia in the developing CNS at E10.5 – E14.5 when primitive microglia would normally penetrate the rudimental brain (*206*). However, by E17.5 some Cx3cr1-GFP+ microglia were observed to be in the brain, and full repopulation occurred by birth (*206*), suggesting that microglia can arise outside of the yolk sac if this source is depleted, potentially via definitive haematopoiesis.

Microglial depletion studies in the adult CNS revealed how repopulation differs from the original seeding in development. Two depletion studies relying on

different methods, *Cx3cr1*-CreERT2;iDTR genetic depletion mouse model (*68*) compared to CSF1R inhibition (*69*), revealed a role for Nestin+ cells in microglial repopulation, albeit with different conclusions. After depletion of microglia in the *Cx3cr1*-CreERT2;iDTR mice with diphtheria toxin, residual microglia expressed Nestin, as shown by immunohistochemical IBA-1/Nestin co-localisation at 7 days post depletion (*68*). However, by CSF1R inhibition-mediated microglial depletion, repopulation was suggested to occur via Nestin+ cell differentiation (*69*); BrdU incorporation in proliferating cells revealed the majority of BrdU+ cells prior to repopulation were negative for microglia markers such as IBA-1, and mice sacrificed during repopulation showed the majority of BrdU+ cells were IBA-1+ suggesting that these cells could have come from non-microglial BrdU+ origin (*69*). Although different sources for repopulating microglia may reflect differences in depletion methods, it highlights the need for definitive lineage tracing studies. Indeed, a recent study sought to uncover the source of repopulating microglia by lineage tracing of Nestin+ cells using the Nestin-CreERT2::Ai14 reporter mouse and CSF1R-mediated microglia depletion (*70*). Nestin+ cell lineage tracing revealed that microglia did not arise from tdTomato(Nestin)+ cells, although the recombination efficiency of this reporter was not noted. Furthermore, the induction of Cre-recombination before depletion, and not during repopulation, could theoretically miss a transient Nestin+ cell population arising during this time. Nevertheless, lineage tracing of microglia using Cx3cr1-CreER::Ai14 reporter mice showed that after repopulation, all IBA-1+ cells were tdTomato(Cx3cr1)+ and therefore must have originated from microglia.

Although spontaneous recombination was not assessed, a potential issue with inducible Cre-recombinase based reporter models, the authors convincingly show that microglial self-renewal is most likely the source of repopulating microglia in the CSF1R inhibition-mediated depletion model. However, it is unclear if this is the case for all methods of microglial depletion in the adult CNS, and whether this extends to white matter injury.

Although microglial depletion studies have highlighted the rapid responsiveness of microglia to repopulate the CNS, there is no evidence to show how microglia repopulate after microglial death without experimental depletion, such as during remyelination. Understanding how repopulation takes place during efficient remyelination may uncover potential therapeutic targets aimed at promoting microglial repopulation to a tissue-repair phenotype that can drive remyelination.

4.3. Results

4.3.1. Nestin and microglia marker co-localisation is observed during microglia repopulation during remyelination in vivo

To determine if Nestin expression in plays a role in repopulation in the LPC model of demyelination and remyelination, *in vivo* focal demyelinated tissue from 3, 7 and 10 dpl was stained for Nestin and microglia marker IBA-1. Prior to microglial death at 3 dpl (when the peak in iNOS+ microglia occurs), and at 10 dpl (when the peak of Arg-1+ microglia occurs) (*8*) there was little Nestin+IBA-1+ microglia present (Figure 1A, C), as was the case in the sham control (Figure 1A). However, at 7 dpl, a significant proportion of IBA-1+ microglia expressed Nestin (Figure 1A-C). Z-plane orthogonal images were obtained at 7 dpl to show IBA-1 and Nestin co-localisation (Figure 1B).

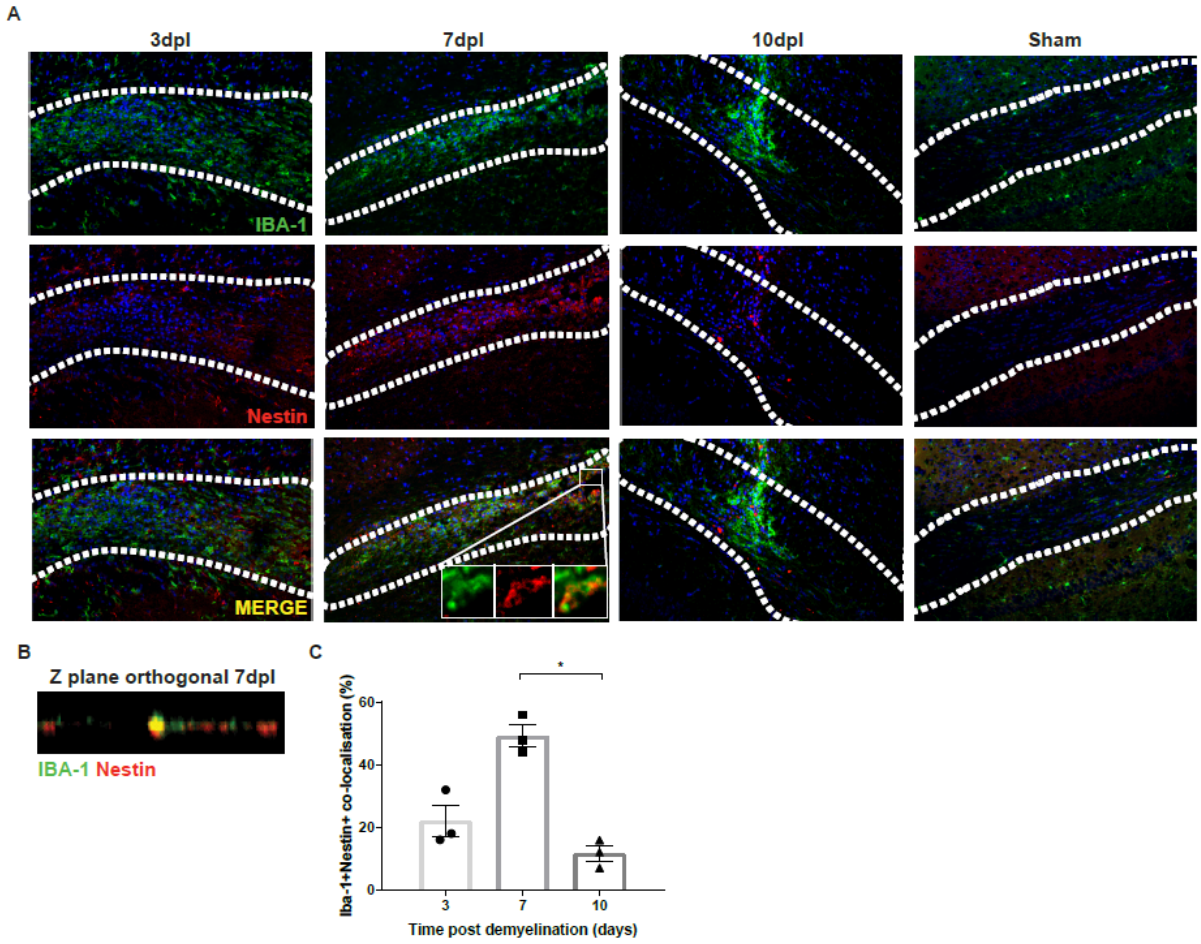

Figure 1. A. *In vivo* lesioned corpus callosum (dotted line) at 3, 7 and 10 dpl and a sham control stained for Nestin (red) and IBA-1 (green). Scale bar, 50µm. **B.** Z-plane orthogonal view of 7 dpl lesioned corpus callosum stained for Nestin (red) and IBA-1 (green) demonstrates co-expression. **C**. Mean percentage co-localization between IBA-1 and Nestin staining normalized to total IBA-1 signal ± s.e.m.. *P=0.0219 7 dpl vs 10 dpl (Kruskal-Wallis test, Dunn's Multiple Comparison post-test). N=3 mice per time point.

4.3.2. Lineage tracing of Nestin+ cells to determine the fate of Nestin+ cells during microglial repopulation in organotypic cerebellar slice cultures

Although we have observed Nestin expression in microglia during repopulation after demyelination, the source of repopulating cell types was still to be determined; be it Nestin+ progenitor cells or residual microglia expressing Nestin. Therefore, lineage tracing was conducted first on Nestin+ cells to determine the proportion of these progenitor cells able to differentiate into microglia during repopulation. Slices from *Nes*-CreERT2;RCL-tdT mice were cultured and tdTomato expression was induced in Nestin+ cells by 4-hydroxytamoxifen (4-OHT) prior to demyelination with LPC (Figure 2A). Recombination efficiency was observed by immunostaining for Nestin (Figure 3B) where it was shown to occur in almost all Nestin+ cells.

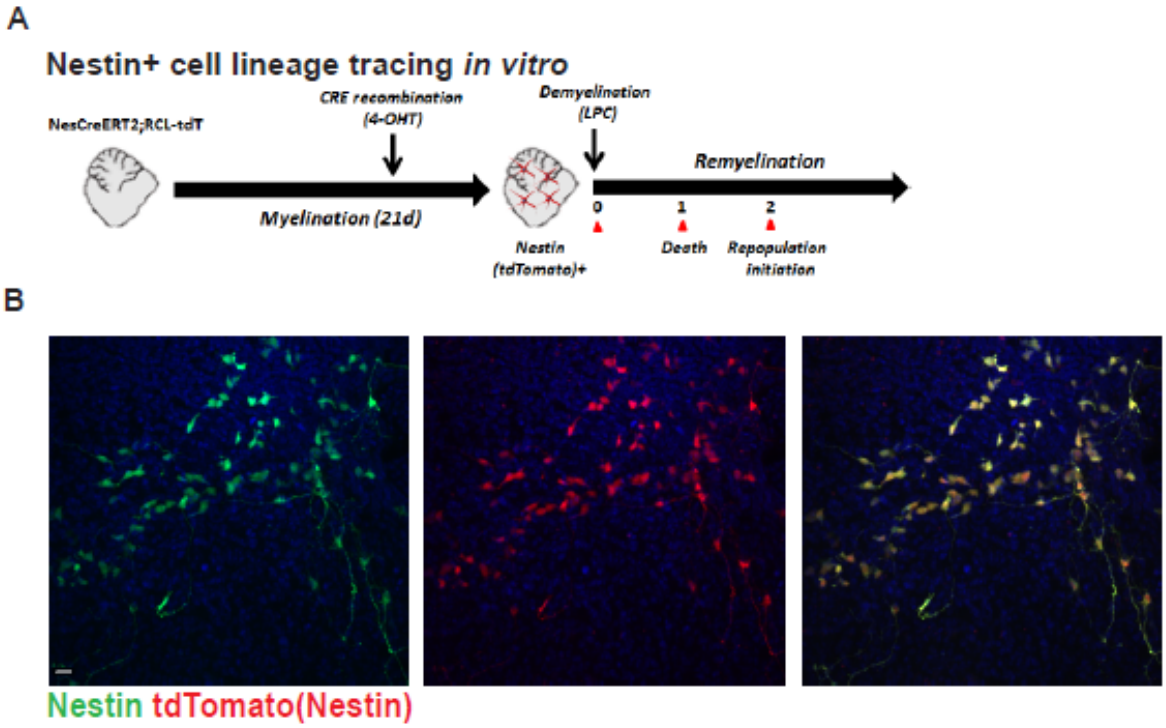

Figure 2. A. Schematic of 4-hydroxytamoxifen (4-OHT) treatment in *Nes*-CreERT2;RCL-tdT slices. **B**. Representative slice from *Nes*-CreERT2; RCL-tdT mice at 21 DIV with 4-OHT treatment immunostained with Nestin (green) shows high recombination efficiency. Scale bar, 20µm.

4.3.3. Lineage tracing of Nestin+ cells to determine the fate of Nestin+ cells during microglial repopulation in vivo

In vivo lineage tracing of Nestin+ cells was also conducted by giving *Nes*-CreERT2;RCL-tdT mice two sub-cutaneous injections of tamoxifen 5-7 days prior to lesioning (Figure 3A), followed by perfusion of mice at 3, 7 and 10 days post demyelination, dissection of lesioned corpus callosum and analysis of Nestin+ cells by flow cytometry. Firstly, viable cells were determined by forward and side scatter (FSC-A and SSC-A, respectively), followed by gating of viable tdTomato(Nestin)+ cells using DAPI, a DNA binding dye that can only enter cells with a compromised cell membrane (indicative of cells undergoing cell death). DAPI+ tdTomato+ cells were therefore excluded from the gating. tdTomato+ cells were gated based on expression of 10^3 or greater, as a wild-type (non-tdTomato+) control was not available. A major disadvantage of gating without a negative control is that this population can be overestimated, which must be noted. Lastly, tdTomato(Nestin)+ cells were plotting against myeloid cell markers CD11b and CD45 (Figure 3B). Therefore, it could be determined by flow cytometry the proportion of tdTomato(Nestin)+ cells that expressed microglia and macrophage markers CD11b and CD45.

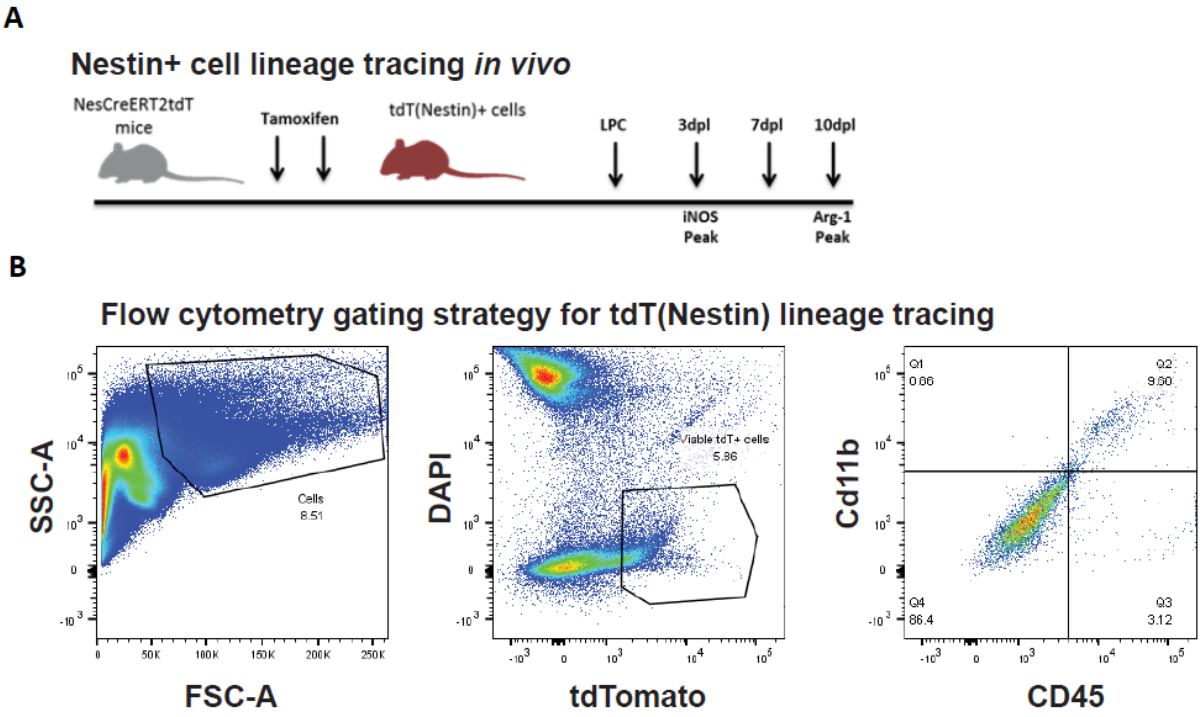

Figure 3. A. Schematic of tamoxifen treatment in *Nes*-CreERT2;RCL-tdT mice. **B.** Gating strategy for to determine the proportion of tdTomato(Nestin)+ cells that express microglia markers CD11b and CD45 during repopulation *in vivo*.

4.3.4. A proportion of Nestin+ cells differentiate into microglia during efficient remyelination

Immunostaining *Nes*-CreERT2;RCL-tdT *ex vivo* slices with IBA-1 revealed a significant proportion of IBA-1+ cells expressing tdTomato at 2dpl during repopulation (Figure 4A, B). Interestingly, at 7dpl there were very few IBA-1+ tdTomato(Nestin)+ cells (Fig. 4A), suggesting the Nestin+ microglial population is transient. Furthermore, analysis of tdTomato(Nestin)+ cells from *in vivo* demyelinated lesions revealed a significant proportion (~20%) of tdTomato(Nestin)+ cells expressing microglial/ macrophage markers CD11b and CD45 at 7dpl which was maintained at 10dpl (Figure 4C, D). Therefore evidence from *ex vivo* and *in vivo* lineage tracing of Nestin+ cells reveals a small population of Nestin+ cells capable of differentiating into microglia as evident by the expression of microglia markers IBA-1, CD11b and CD45, all of which are not expressed by Nestin+ cells during homeostasis (0 dpl, Figure 4A). It would be important to include sham injected (mechanical injury from the needle only, or a PBS (vehicle) loaded needle injection) mice in this study to determine the baseline numbers of tdTomato(Nestin)+ cells that express microglia/ macrophage markers during these time points, however this was not possible during this time with limited mice available, however this should be done in the future to definitively determine if Nestin+ cells differentiate into microglia only in the context of death and repopulation in disease/ injury models such as the LPC model used here.

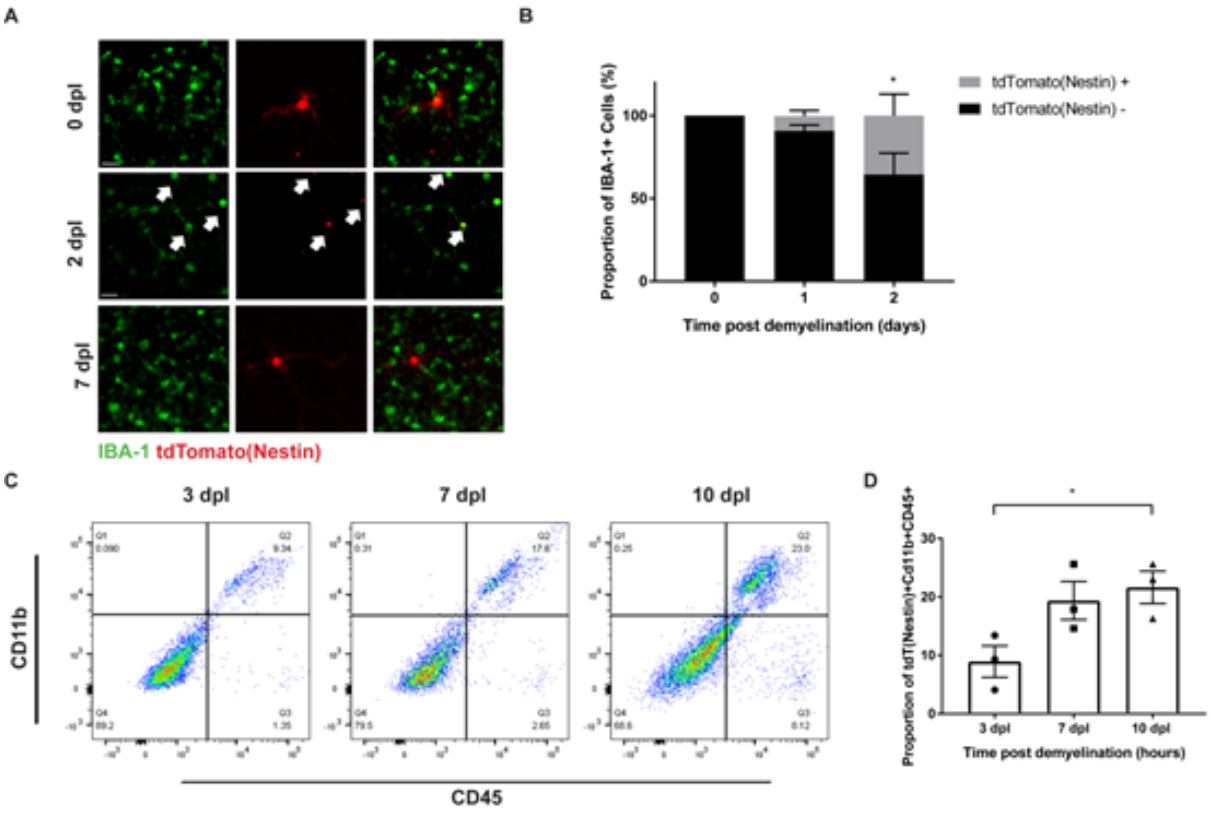

Figure 4. A. Slices from *Nes*-CreERT2;RCL-tdT mice at 0, 2 and 7dpl immunostained for IBA-1 (green). Scale bar, 20µm. **B.** Proportion of IBA-1+ cells positive and negative for tdTomato(Nestin) represented as a percentage of total IBA-1+c cells at 0-2 dpl ± s.e.m. *P=0.0154 0 dpl vs 2 dpl (Kruskal-Wallis test, Dunn's Multiple Comparison post-test). N=4 mice per time point. **C.** Representative flow plots to show the proportion of tdTomato(Nestin)+ cells that express CD11b and CD45 at 3, 7 and 10dpl. **D.** Mean numbers of CD11b+ CD45+ tdTomato(Nestin)+ cells at 3, 7 and 10 dpl ±s.e.m.. N=3 mice per time point. *P=0.0496 (one-way ANOVA, Tukey's multiple comparison post-hoc test).

4.3.5. Lineage tracing of microglia during repopulation reveals that residual microglia represent the majority of repopulating microglia during remyelination

As only small proportion of Nestin+ cells expressed microglia markers during repopulation (Figure 4), it was important to determine what proportion of total repopulating microglia this population represented. Flow cytometric analysis of total microglia revealed that tdTomato(Nestin)+CD11b+CD45lo microglia represented only approximately 4% of total microglia at 7dpl (Figure 5A), suggesting repopulation is likely to mostly result from expansion of the residual microglia pool. To address this, lineage tracing of microglia using *Cx3cr1*-CreER;RCL-tdT was carried out in slices, whereby treatment of slices with 4-OHT induced tdTomato expression specifically in Cx3cr1+ cells (Figure 5B). Immunostaining of *Cx3cr1*-CreER;RCL-tdT slices with IBA-1 revealed that a proportion of microglia do not undergo necroptosis after demyelination (Figure 5C, D), as there were tdTomato(Cx3cr1)+ cells present prior to demyelination (0 dpl) that were still present by 2 dpl when microglial necroptosis had taken place. Furthermore, a significant proportion of tdTomato(Cx3cr1)+ microglia express Nestin at 2 dpl (Figure 5C, E). Overall this data shows that some microglia evade necroptosis and are the primary contributors to repopulation, with many expressing Nestin during this process.

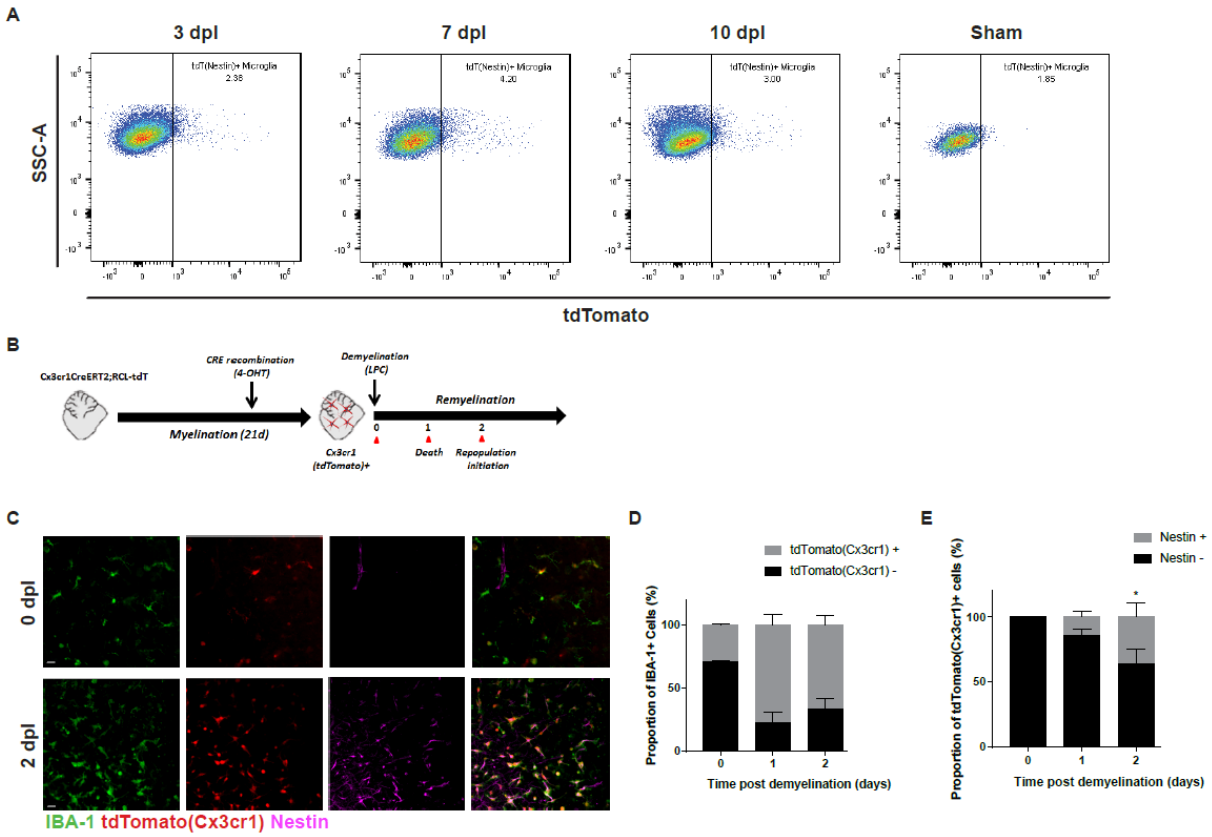

Figure 5. A. Representative flow plots of CD11b+CD45+ microglia plotted against tdTomato to determine the proportion of total microglia positive for tdTomato(Nestin) at 3, 7 and 10dpl and a sham control. **B.** Schematic of 4-OHT treatment in *Cx3cr1*-CreER;RCL-tdT slices. **C.** Slices from *Cx3cr1*-CreER;RCL-tdT mice at 0 dpl and 2 dpl immunostained for IBA-1 (green) and Nestin (magenta). Scale bar, 20µm. **D.** Proportion of IBA-1+ cells positive and negative for tdTomato(Cx3cr1) represented as a percentage of total IBA-1+ cells at 0-2 dpl ± s.e.m. N=4 mice per time point. **E.** Proportion of tdTomato(Cx3cr1)+ cells positive and negative for Nestin represented as a percentage of total tdTomato(Cx3cr1)+ cells at 0-2 dpl ± s.e.m. *P=0.0106 0 dpl vs 2 dpl (Kruskal-Wallis test, Dunn's Multiple Comparison post-test). N=4 mice per time point.

4.3.6. High resolution imaging of Nestin+ cells shows co-localisation with microglia markers as well as microglial phagocytosis of Nestin+ cells in organotypic cerebellar slice cultures

Super resolution imaging of *Nes*-CreERT2;RCL-tdT slices was carried out to determine if Nestin+ cells truly expressed IBA-1, or if microglia phagocytosis of Nestin+ cells was the reason for co-localisation of markers. This revealed Nestin+ IBA-1 marker co-localisation (Figure 6A), however in rare cases microglial phagocytosis of Nestin+ debris was also observed (Figure 6B). Single labelled controls were not carried out to determine channel bleed-through, however areas of IBA-1+ only and tdTomato(Nestin)+ only are observed, suggesting that bleed-though is not taking place.

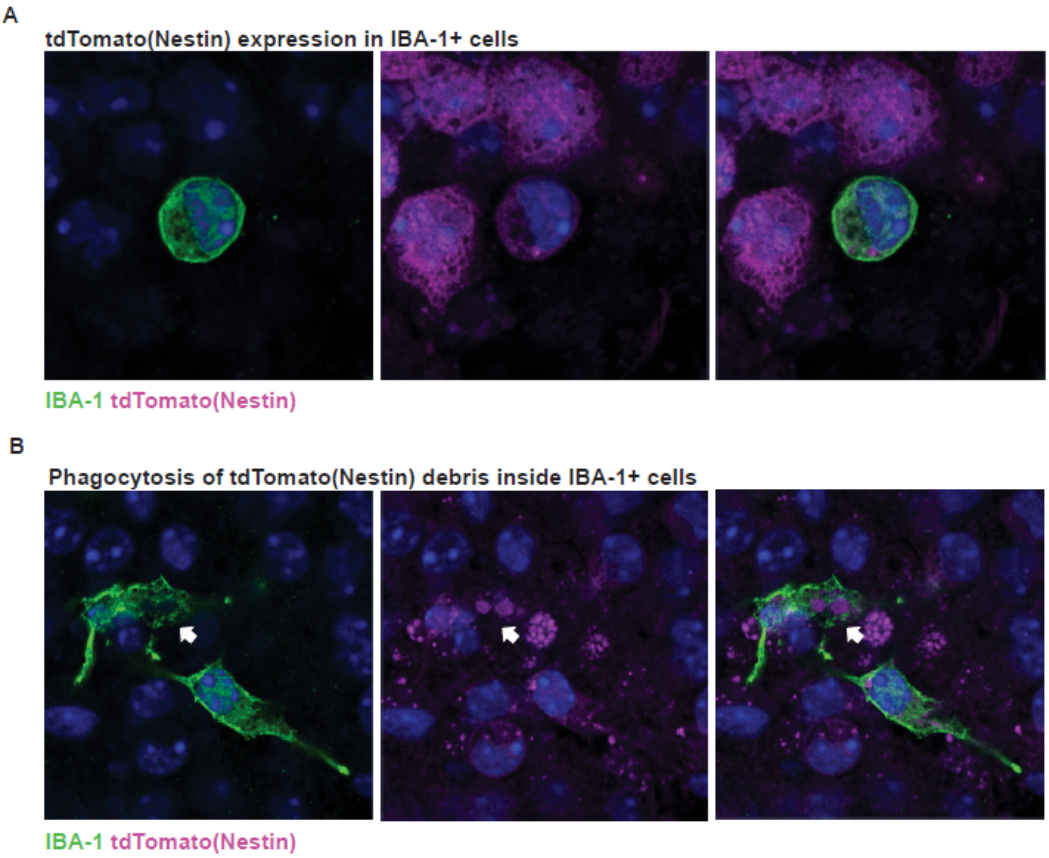

Figure 6. A. Super resolution image of tdTomato(Nestin)+ cell (magenta) expressing IBA-1 (green). **B.** Example of tdTomato(Nestin)+ cell fragments (magenta) having been phagocytosed by IBA-1+ microglia (green; arrow).

4.3.7. Nestin+ cells express markers of neural stem cells but not astrocyte markers

To understand the identify of the Nestin+ cells with capacity to differentiate into microglia, *Nes*-CreERT2;RCL-tdT slices were immunostained for neural stem cell marker mushashi-1 (Msh-1; Figure 7A) and SOX-2 (Figure 7B), as well as astrocyte marker glial fibrillary acidic protein (GFAP; Figure 7C) prior to demyelination. Immunostaining revealed that tdTomato(Nestin)+ cells expressed Msh-1 and Sox-2 but not GFAP, suggesting they may be of neural stem cell origin, and not trans-differentiated astrocytes (Figure 7A-C). However,

GFAP is a marker of activated astrocytes, therefore a pan astrocyte marker such as ALDH1L1 could be used to determine if any tdTomato(Nestin)+ cells express pan astrocyte markers.

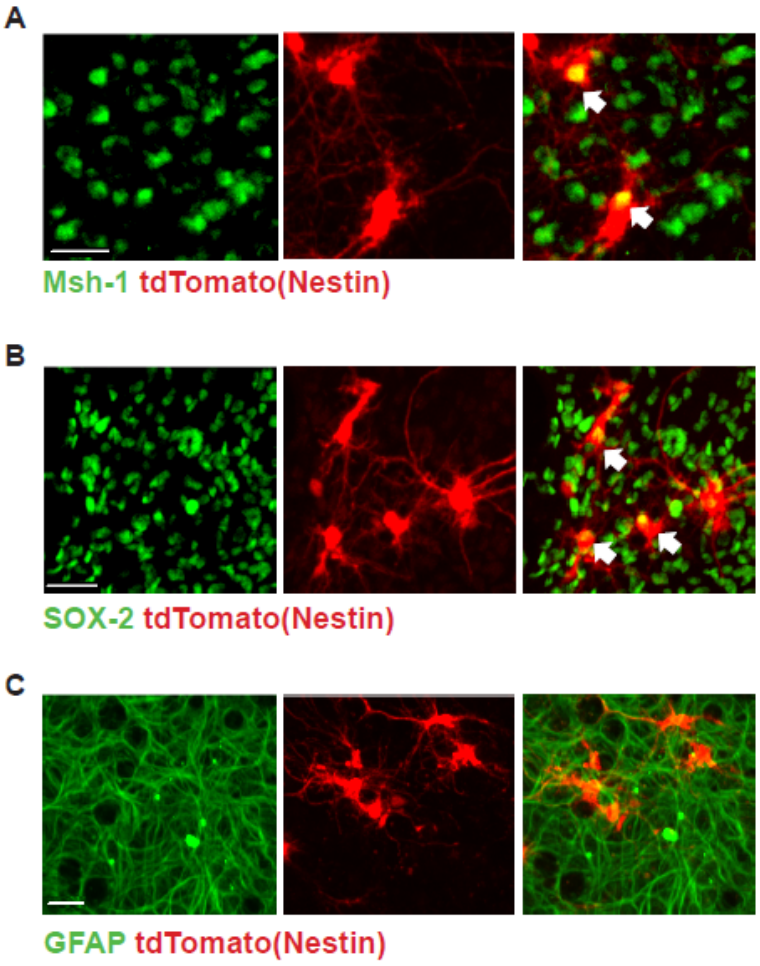

Figure 7. A. Representative image from *Nes*-CreERT2;RCL-tdT slices immunostained for Msh-1 (green). Scale bar, 20µm. **B.** Representative image from *Nes*-CreERT2;RCL-tdT slices immunostained for SOX-2 (green). Scale bar, 20µm. **C.** Representative image from *Nes*-CreERT2;RCL-tdT slices immunostained for GFAP (green). Scale bar, 20µm.

4.3.8. Oligodendrocytes do not express Cx3cr1 after demyelination in organotypic cerebellar slice cultures

It has previously been shown that oligodendrocytes can express Cx3cr1 (*207*). Therefore, to determine if oligodendrocytes are contributing to the tdTomato(Cx3cr1)+ population, slices from *Cx3cr1*-CreER;RCL-tdT were cultured for 21 days in vitro, fixed and immunostained for oligodendrocyte lineage marker Olig2 which revealed that there were no tdTomato(Cx3cr1)+ cells expressing Olig2 (Figure 8) prior to demyelination. Although demyelinated slices were not analysed for tdTomato(Cx3cr1)+ Olig2+ cells, there is no evidence to suggest that Olig2+ cells upregulate Cx3cr1 in during differentiation. Therefore, our lineage tracing using *Cx3cr1*-CreER;RCL-tdT mice is specifically tracing microglia.

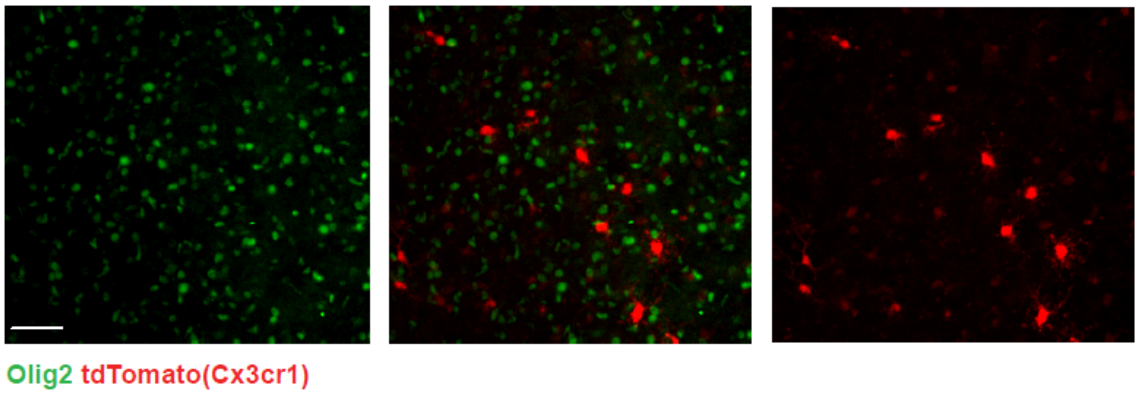

Figure 8. Representative slice from *Cx3cr1*-CreER; RCL-tdT stained for Olig2 (green) shows no co-localization with tdTomato(Cx3cr1) (red). Scale bar, 50µm.

4.3.9. Repopulating microglia are present in active multiple sclerosis lesions

To determine if microglial repopulation is a feature of multiple sclerosis lesions, post mortem tissue was stained for macrophage marker PU.1 and Nestin. Lesion subtypes were explained in Chapter 3 (see results, section 3.3.13). Active lesions show significantly increased density of PU.1+Nestin+ cells compared to control white matter tissue (Figure 9A-C), suggesting that microglial repopulation may be a feature seen in remyelinating lesions. Interestingly, some remyelinated lesions had a high density of PU.1+Nestin+ cells, and some lesions had very few. This may represent differences in the stage of remyelination of each lesion. It is important to note that PU.1 is not microglial specific, and that further analysis with a microglia-specific marker such as Tmem119 or P2ry12 could be used instead. However, it has been shown that microglia downregulate these homeostatic markers when activated (*103*) and therefore there are limitations of using microglia-specific markers in such conditions. Furthermore, our *ex vivo* evidence of Nestin+ PU.1+ cells suggests that it is microglia that do indeed express Nestin (Figure 4, 5), as peripheral cells capable of expressing Nestin would not be present in the explant model.

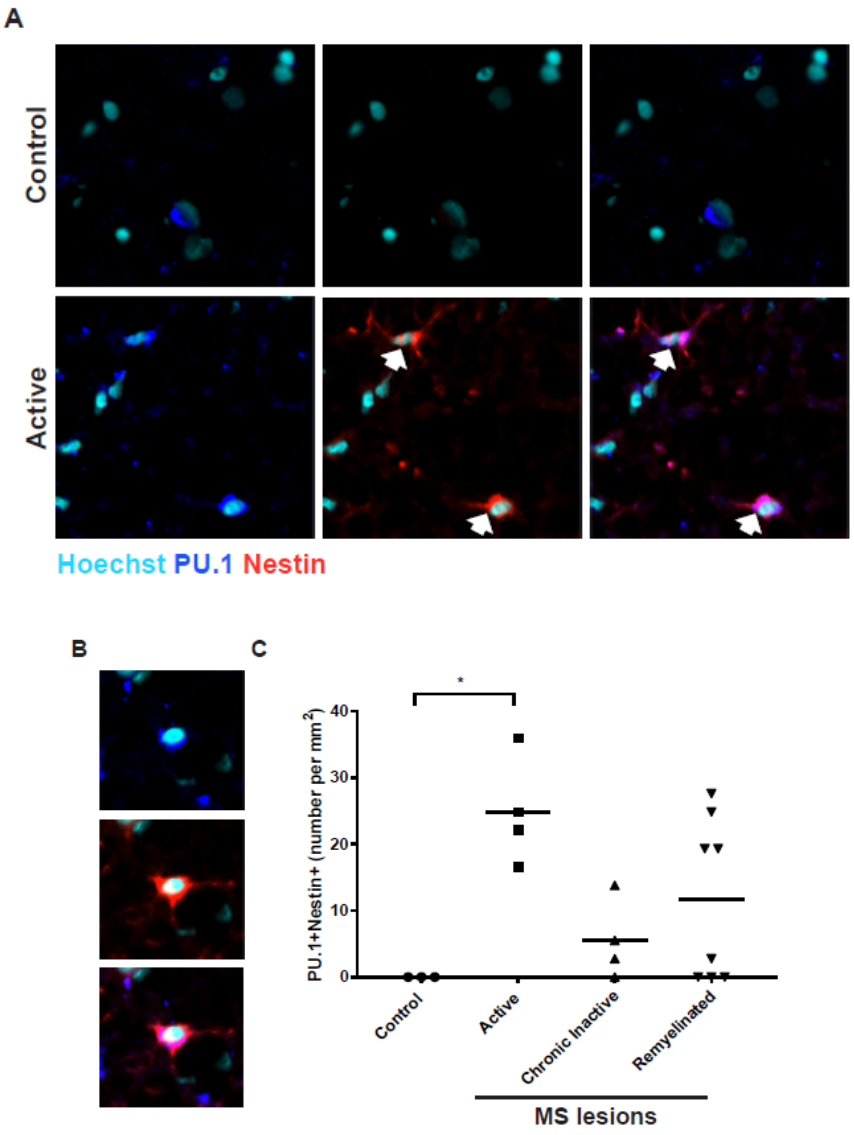

Figure 9. A. Control brain and active MS lesion tissue immunostained for PU.1 (blue) and Nestin (red), counterstained with Hoechst (turquoise). Scale bar, 20µm. **B**. Magnified view of a Nestin+ (blue) and PU.1+ (red) cell in an active lesion, counterstained with Hoechst (turquoise). **C**. Mean density of Nestin+ PU.1+ cells per mm^2 in control, active, chronic inactive and remyelinated lesions. Individual data points represent separate lesions (See *Results Chapter 1, Table 1*). *P=0.0329 active lesions vs control (Mann-Whitney test). Remyelinated v control p=0.5523; chronic inactive v control p=0.6552 (Mann-Whitney test).

4.4. Discussion

As I showed that microglial necroptosis is important in the regulation of pro-inflammatory microglia, I next determined how microglial repopulation takes place during efficient remyelination. Understanding how microglia repopulate may uncover a potential therapeutic target in driving pro-regenerative microglial activation in diseases where chronic pro-inflammatory microglial activation and failed remyelination feature, including MS and spinal cord injury (SCI) (*8, 192, 208*).

After pro-inflammatory microglial necroptosis, I found that rapid repopulation occurred in both *ex vivo* and *in vivo* models prior to the onset of remyelination. During repopulation, microglia were found to express the neural stem cell marker Nestin, and lineage tracing confirmed that a small proportion of repopulating microglia are derived from Nestin+ progenitor cells (also expressing SOX2 and Msh1). However the primary source of repopulating microglia were found to be derived from residual microglia, as shown by lineage tracing using Cx3Cr1 (a proportion of which expressed Nestin during this repopulation phase). Furthermore, in MS lesions, a significantly higher density of PU.1+Nestin+ cells was observed in active lesions compared to white matter from controls. Importantly, this research has shown for the first time that microglia repopulate during efficient remyelination (without experimental microglial depletion), and that this can occur from various sources.

A recent study was the first to investigate the role of repopulating microglia in a model of CNS damage. Depletion of ~90% of pro-inflammatory microglia by a

CSF1R inhibitor in a diphtheria toxin model of hippocampal neuronal loss lead to repopulation of microglia that were less activated, as shown by morphological analysis (more branched and less amoeboid) and a reduction in expression of CD68, a marker of activated microglia and macrophages. Furthermore, repopulated microglia did not become pro-inflammatory as shown by a significant reduction in expression of inflammatory genes and pathways including NFκB, TLR4 and IL-1 compared to mice without microglia depletion. Importantly, microglial depletion and repopulation in this disease model also lead to an increase in synaptic plasticity as shown by increased spine number, as well as a rescue of behavioural deficits (*202*). This work was the first to show a beneficial role of depleting pro-inflammatory microglia to shut down inflammatory responses in a model of neurodegeneration, and to suggest a potential role for repopulating cells in promoting CNS health.

Microglial repopulation has not always been shown to be beneficial. For example, depletion of spinal cord microglia with Mac-1-saporin lead to the depletion of 50% of microglia as well as an acute inflammatory response, as shown by increases in gene expression of TNF-α, IL-1β, CCR2 and IL-6 in spinal cord lysates (*203*), although it is unclear which cell types are responsible for this inflammatory response. In the same study, peripheral nerve injury was induced after microglial repopulation occurred to investigate the beneficial effects of repopulated microglia on regeneration. However, microglial depletion and repopulation prior to injury resulted in a lack of beneficial responses (such as no differences in pain perception). As spinal cord injury models are associated with chronic pro-inflammatory microglial responses (*192*), depletion of

microglia during the peak of pro-inflammatory microglial activation may have been a more physiologically relevant experiment. Therefore, it is uncertain if depletion and repopulation of microglia after injury would benefit peripheral nerve regeneration in the spinal cord (*203*). Furthermore, differences in CNS regions, methods of depletion and level of depletion achieved may account for differences in repopulation and regenerative benefits, and therefore such differences and their impacts on microglia repopulation and activation need to be elucidated.

There is evidence demonstrating how microglia are able to express markers of other cell types in response to activation and injury. For example, microglia have been shown to express markers of haematopoietic stem cells such as CD34 (*209*) and c-kit (*210*) in response to neuronal injury *in vivo*. Primary microglial cultures treated with IFN-γ can also express neural lineage markers β-III tubulin, doublecortin (DCX) and Nestin (*79*). However, mature neuronal markers such as NeuN, NF-H and MAP2 were not expressed by IFN-γ treated microglia. Furthermore, mature myelin marker MBP was not expressed in IL-4 treated microglia despite an increase in oligodendrocyte lineage marker NG2 expression. Therefore, activated microglia do not express mature cell markers of other cell types, suggesting that microglia express progenitor markers in response to activation rather than microglia undergoing trans-differentiation in response to injury/ activation.

Classically, Nestin expression is associated with neural stem cells (NSCs), expressed by mitotically active NSCs in neurogenic niches like the hippocampus

(*211*), and is downregulated in mature neurons (*212*). Nestin is an intermediate filament, and represents a major structural protein in the cytoskeleton (*213*), having an important role in structural organisation and reorganisation of cells, particularly in progenitor cells (*214*). Nestin expression may also be associated with activated cells requiring a degree of plasticity, such as in mature neurons and astrocytes during glial scar formation after spinal cord injury (*215*), and therefore is not solely a marker of neural stem cells in the CNS. Nestin expression in microglia has been studied for the last decade, although little is definitively known about its role in microglial activation or repopulation. Indeed, Nestin expression may be important for cytoskeleton rearrangement in proliferating microglia, although it is uncertain yet if Nestin is essential for proliferating microglia during repopulation in my models (*see future directions*). tdTomato(Nestin)+ cells from *ex vivo* cultures express additional neural stem cell markers Msh-1 and SOX2, suggesting these cells may be neural stem cells, however further analysis of these cells by gene expression profiling will aid in identifying their identity, and if all Nestin+ cells have the potential to differentiate into microglia.

In the adult rat cerebral cortex it has been reported that ~20% IBA-1+CD11b+ microglia also express Nestin under normal conditions, and of these Nestin+ microglia, the majority also express the astrocyte marker vimentin, and NG2 (*216*). However, it is now appreciated that a proportion of microglia turn over at any given time (*66, 204*) and therefore this subpopulation of microglia expressing intermediate filament and progenitor cell markers may represent microglia actively turning over. Although Nestin+IBA-1+ microglia were only

observed in demyelinated lesions and not in sham lesions or outside of the lesion area in our model (Figure 1A), the discrepancy with the previous study could also represent regional differences in microglial activation and rates of turnover (*1, 66, 147, 217*). Indeed, as much as 60% of microglia in the retina express Nestin under normal conditions, which increases in response to optic nerve transection (*218*). Furthermore, microglia positive for Nestin and Bromodeoxyuridine (BrdU), a synthetic analogue of thymidine incorporated into actively proliferating cells, significantly increased in response to injury leading to an expansion of Nestin+ microglia (*218*), suggesting a role of Nestin in the proliferation of microglia. Moreover, evidence from this thesis suggests that Nestin expression in microglia may represent proliferation after injury, specifically due to pro-inflammatory microglial death, and therefore as a repopulation mechanism, which may represent a previously unappreciated role for microglial proliferation after injury. However, microglial proliferation (identified by Ki67 expression or BrdU incorporation, for example) was not directly measured, and will need to be carried out in order to confidently assess proliferation in repopulating microglia (see *future directions*).

Nestin expression has also been shown to be an indicator of astrocyte activation in response to mechanical injury of the mouse hippocampus (*219*), as well as being associated with microglial activation *in vitro* (*220*) and *in vivo* (*218*). However, at the peak of iNOS+ microglial activation there were significantly fewer Nestin+ microglia compared to during repopulation (7 dpl *in vivo;* Figure 1A, C), suggesting that Nestin expression in microglia is associated with repopulation rather than solely microglial activation.

My lineage tracing results revealed that although residual microglia represent the major source of repopulating microglia, there is a small population of Nestin+ cells capable of differentiating into microglia (Figure 4C, D). Although repopulation via Nestin+ progenitors has been reported previously after microglial depletion in the mouse CNS (*69*), it is unclear why both residual microglia and Nestin+ cells would contribute to repopulation. It may be that regional differences, depletion methods, mechanism of cell death and extent of microglial depletion may result in differences in repopulation mechanisms, although this need to be thoroughly explored before any conclusions can be made. Furthermore, differences in methods of progenitor cell detection and their sensitivities (such as reporter cell lineage tracing compared to fate mapping with BrdU, for example) may also lead to differences in findings. Indeed, incomplete recombination or spontaneous recombination with inducible-Cre driven reporter mice may conceivably lead to under- or over-representation of a particular population, respectively, and therefore both recombination efficiency and levels of spontaneous recombination should be assessed.

It is unclear if all Nestin+ cells are capable of differentiating into microglia, as only a proportion of tdTomato(Nestin)+ cells expressed IBA-1 during repopulation (Figure 4) and therefore there may be a degree of heterogeneity in Nestin+ cells. Moreover, the signals that drive a Nestin+ progenitor cell to differentiate into a microglia remain unknown, and it is unclear if Nestin+ cell-derived microglia permanently reside in the CNS after repopulation. Microglia repopulation may take place in response to signals from dying cells, and could

potentially lead to differences in repopulation sources based on how the microglia died (by apoptosis or necroptosis for example). Alternatively, microglia repopulation studies have shown that initially excess microglial proliferation occurs and is followed by a decrease in microglia to levels similar to pre-depletion levels (*68*). This suggests that repopulation may be in response to detectable changes in microglial numbers, either by residual microglia and/or Nestin+ cells. Lineage tracing of tdTomato(Nestin) slices after repopulation has taken place *in vivo* (7dpl) revealed that very few tdTomato(Nestin)+ IBA-1+ cells are present (Figure 4A). As tdTomato expression will persist in cells even if these cells no longer express Nestin, one would expect to see tdTomato+ microglia after repopulation if these cells persist, however my preliminary findings suggest that this population is transient. It is unclear why a small proportion of Nestin+ cells would differentiate into microglia, to then die days later. This may represent a microglial repopulation overcompensation mechanism, where excess microglia undergo death, however the half-life of tdTomato will also need to be investigated in order to determine if this population is truly lost after repopulation.

The role of monocyte-derived macrophages (MDMs) during microglial repopulation has not been fully addressed. Indeed, microglial depletion via CSF1R inhibition does not alter BBB integrity as shown by Evans Blue staining (*69*), although not all depletion studies report BBB integrity. Disruption of BBB integrity has been shown to lead to peripheral monocyte invasion of the CNS that can contribute to the microglial pool in irradiated mice by bone marrow

adoptive transfer (*68, 217*). Furthermore, recent experimental evidence using an inducible knockout of *Csf1r* in Cx3cr1+ cells (leading to 25% depletion of microglia in the CNS) reported that adoptive transfer of GFP+ bone marrow derived macrophages leads to their invasion of the CNS after microglial depletion, despite an intact BBB (*221*). Interestingly, bone marrow-derived monocytes in the CNS can also express Nestin (*68*) which begs the question: what is the contribution of MDMs to microglial repopulation during efficient remyelination? Although microglial repopulation in the *ex vivo* model occurs devoid of peripheral cell contributions, *in vivo* demyelination of *Ccr2*$^{RFP/+}$ reporter mice leads to a small population of RFP+ MDMs in the lesion (See *Chapter 3*); however I have not yet uncovered whether these cells express Nestin during remyelination or contribute to microglial repopulation in the long-term (see *future directions*).

Lastly, although Nestin+PU.1+ cells are observed in MS lesions with high capacity for remyelination (active lesions), it is unclear if these cells represent Nestin+ cells which have differentiated into microglia, or microglial expression of Nestin. Nestin expression in activated astrocytes in the formation of glial scars in MS lesions has been reported previously (*222, 223*), but evidence for the role of microglial Nestin expression in MS is lacking. Furthermore, my observation of a decrease in Nestin+PU.1+ cells in lesions with limited remyelination capacity (chronic inactive) could represent a block in repopulation, or a consequence of a lack of pro-inflammatory microglial necroptosis (See *Results Chapter 1*). Therefore, there is still a great deal of

information regarding the role of Nestin expression in microglia in the human context that needs to be uncovered.

Taken together, I present evidence to show that microglia repopulate after pro-inflammatory necroptosis during efficient remyelination. Lineage tracing of Nestin+ cells and microglia reveals that the majority of repopulation originates from residual microglia, with a small contribution of Nestin+ cells differentiating into microglia. Lastly, active MS lesions were associated with Nestin+ microglia, whereas other lesion types have significantly fewer Nestin+ microglia. Given that active lesions are associated with higher macrophage infiltration and a greater potential for remyelination (*163*), this could suggest that repopulating microglia may be important in remyelination in the human disease.

4.5. Future Directions

There are a few key experiments needed to definitively show the importance of repopulating microglia in regulating microglial phenotypes and remyelination. Firstly, although it is suggested that repopulating microglia represent the pro-regenerative microglial population based on the timing of repopulation during efficient remyelination, lineage tracing of repopulating microglia and immunostaining of these cells with pro-regenerative markers (such as Arg-1 and CD206) would definitively show if repopulating microglia become pro-regenerative. Furthermore, by knocking out Nestin, it would be interesting to see if repopulation takes place, firstly to determine if Nestin+ cells are needed for repopulation, and if microglia need to express Nestin to proliferate and repopulate the lesion. As Nestin is vital for neural stem cell development (*224*) a microglial-specific, inducible knockout (K/O) may be the most suitable transgenic K/O mouse to use in this circumstance, as this would determine the role of Nestin specifically in microglia during microglial repopulation. On that matter, it would be important to determine if microglial proliferation is an important driver of microglial repopulation, or whether microglia from outside of the lesion site are able to migrate into the lesion site to assist with repopulation. The use of microfetti mice (*225*) would be able to determine if repopulation occurs inside of the lesion by expansion of residual microglia in close proximity. This may be more realistic than tracking microglia outside of the lesion, which may be possible using *in vivo* live imaging (which has limitations on size of area able to be observed, resolution of deep brain structures, and length of time able to track microglia (which may be days)).

Although I have shown that by blocking microglial necroptosis there is a persistence in iNOS+ microglial activation, it would be interesting to see if repopulation is also blocked as result. Although this may seem like a logical consequence of preventing microglial death, it would also rule out a role of LPC or demyelination in promoting microglial proliferation or Nestin expression, independent of microglial numbers.

As mentioned in the discussion, it is unclear if peripheral macrophages contribute to microglial repopulation during efficient remyelination. Lineage tracing of macrophages using *Ccr2*$^{RFP/+}$reporter mice would address this. Firstly, immunostaining for Nestin would determine if MDMs express Nestin in the demyelinating lesions, and for how long. Furthermore, imaging lesion areas after remyelination is complete for RFP+ cells would show how long MDMs persist in the brain; whether they exit after inflammation subsides and remyelination is complete, or whether they stay in the brain and contribute to the microglial population. Furthermore, staining for microglial-specific markers TMEM119 and P2RY12 (*103*) could potentially show if MDMs adopt microglial markers once in the brain, and therefore contribute to the microglial population.

In light of evidence showing regional differences in microglial gene expression (*147*) and suggestions that microglia in some regions of the brain can express Nestin under homeostatic conditions (*216, 218*), it would be interesting to see if there are regional differences in microglial repopulation during remyelination, and if there are differences in microglial repopulation/ remyelination efficiency in grey matter compared to white matter. This could be done by similar lineage

tracing and immunostaining techniques as used in our *ex vivo* and *in vivo* models, but in different areas of the brain.

Lastly, the identity of these Nestin+ cells capable of microglial differentiation is still uncertain. Indeed, if only a subset of Nestin+ cells are capable of differentiation into microglia, it would be important to know differences in these cells compared to other Nestin+ cells, and whether or not Nestin+ neural stem cells can indeed differentiate into microglia. By FACS sorting out tdTomato(Nestin)+ cells at different stages during remyelination (un-demyelinated corpus callosum, during demyelination, during repopulation and after repopulation) for RNA-sequencing and comparing tdTomato(Nestin)+-CD45- cells to tdTomato(Nestin)+CD11b+CD45+ Nestin+ cell-derived microglia, and to tdTomato(Nestin)-CD11b+CD45+ microglia, I could uncover key pathways involved in Nestin+ cell microglial differentiation.

Chapter 5: The use of immunomodulatory compounds to 'switch' pro-inflammatory microglia to an anti-inflammatory/ pro-repair phenotype

5.1. Abstract

During remyelination, microglia switch their phenotype from pro-inflammatory to pro-regenerative and failure of this switch leads to a sustained pro-inflammatory response and poor remyelination, associated with diseases like multiple sclerosis (MS). Therefore, targeting microglia to promote a pro-regenerative phenotype may be of therapeutic value. Here, we screened immunomodulatory compounds known to have regenerative properties *in vivo* (*136, 140, 144, 145*) in an attempt to promote a pro-repair phenotype in primary rat microglia. Co-treatment of primary rat microglia cultures with 4 known immunomodulatory compounds and LPS and IFN-γ reduced microglial TNF-α secretions compared to LPS and IFN-γ treatment alone, although further analysis by immunostaining revealed an accelerated reduction of pro-inflammatory microglia compared to IFN-γ/LPS treatment alone. This correlated with an inhibition of NFκB activation, suggesting that immunomodulation may be taking place through inhibition of pro-survival NFκB signalling leading to cell death of the microglia, rather than an immune-resolution or switch in phenotype. Therefore I reveal a previously unappreciated mechanism of immunomodulation distinct from the conventional idea of dampening activation, and may represent a novel therapeutic strategy for targeting pro-inflammatory microglia.

5.2. Introduction

Microglia are highly dynamic, able to alter their genetic, phenotypic and functional behaviours in response to changes in their microenvironment. A prime example of this is during remyelination, where microglia firstly activate to become pro-inflammatory in phenotype in response to demyelination, then at the initiation of remyelination, microglia change their phenotype to an anti-inflammatory/ pro-regenerative in phenotype (*8*).

My data in Chapters 3 and 4 of this thesis demonstrate that during efficient remyelination, pro-inflammatory microglia undergo necroptosis leading to repopulation of microglia prior to the peak in pro-regenerative microglial activation that initiates remyelination (*8*). Furthermore, I had observed that in MS tissue, active lesions that can undergo remyelination had significant levels of necroptotic (RIPK3+ MLKL+ CD68+) and repopulating (Nestin+ PU.1+) microglia compared to white matter control tissue (*see Chapter 3 and 4*), suggesting that a block in microglial death and /or repopulation may contribute to the persistent pro-inflammatory phenotype in lesions that fail to remyelinate. Although microglial death may not regulate phenotypic changes in all models, this work highlighted a potential novel therapeutic avenue of targeting pro-inflammatory microglial death in order to promote faster repopulating and remyelination.

One potential molecular candidate involved in regulating macrophage activation and survival is the transcription factor NFκB, associated with susceptibility for

Multiple Sclerosis (MS) (*130, 131, 133, 226*). Indeed, compounds that modulate macrophage activation and inflammation in EAE and spinal cord injury models, including 17-β Estradiol (*143*), substance P (*140*), PPARγ agonists (*227*) and Rho kinase inhibitors (*138*) also have converging downstream mechanisms of action through inhibiting the function of NFκB (*141, 228-230*). For example, 17-β Estradiol pretreatment of microglia prevents LPS-induced translocation of the P65 subunit of NFκB by directly interfering with transport microtubules that guide the NFκB subunit to the nucleus (*141*) as well as having indirect effects on NFκB via interacting with PPARγ (*231*), a transcription factor that may act by promoting its ubiquitination and degradation (*232*). Furthermore, Rho kinase inhibition prevents proliferation, survival and cell contractility via inhibition of NFκB activation and translocation into the nucleus (*228*). Lastly, the role of substance P in attenuating inflammation remains controversial; there is *in vivo* evidence that substance P treatment ameliorates severity of disability and promotes anti-inflammatory macrophage activation in a model of spinal cord injury in mice (*140*). However, *in vitro* work has shown that substance P can promote NFκB activation (*229*), suggesting that substance P may drive immunomodulation via an NFκB-independent manner.

Altogether, evidence suggests that manipulation of microglia/ macrophages by manipulation of the NFκB pathway can lead to anti-inflammatory activation, here I asked whether use of such compounds could affect pro-inflammatory microglia death, and could therefore potential therapeutic avenues.

5.3. Results

5.3.1. IFN-γ/LPS-treated primary rat microglia produce a robust pro-inflammatory response early after treatment but decline in numbers within 30 hours of treatment.

Primary microglia were first polarised to a pro-inflammatory phenotype *in vitro* by standard treatment with IFN-γ and LPS, as done previously (*8*). Microglia rapidly activated to a pro-inflammatory phenotype, as indicated by iNOS expression and loss of anti-inflammatory associated marker mannose receptor expression at 8 hours post-treatment (Figure 1A-D) and production of TNF-α (Figure 1F). Interestingly, a significant loss of microglia (quantified as number of cells per field) treated with IFN-γ/LPS began at 16 hours post-treatment (Figure 1E) relative to an untreated, time-matched control, such that by 24 hours very few microglia remained. Untreated microglial numbers remained constant throughout, therefore loss of microglia in IFN-γ/LPS treated microglia was due to treatment with pro-inflammatory stimuli.

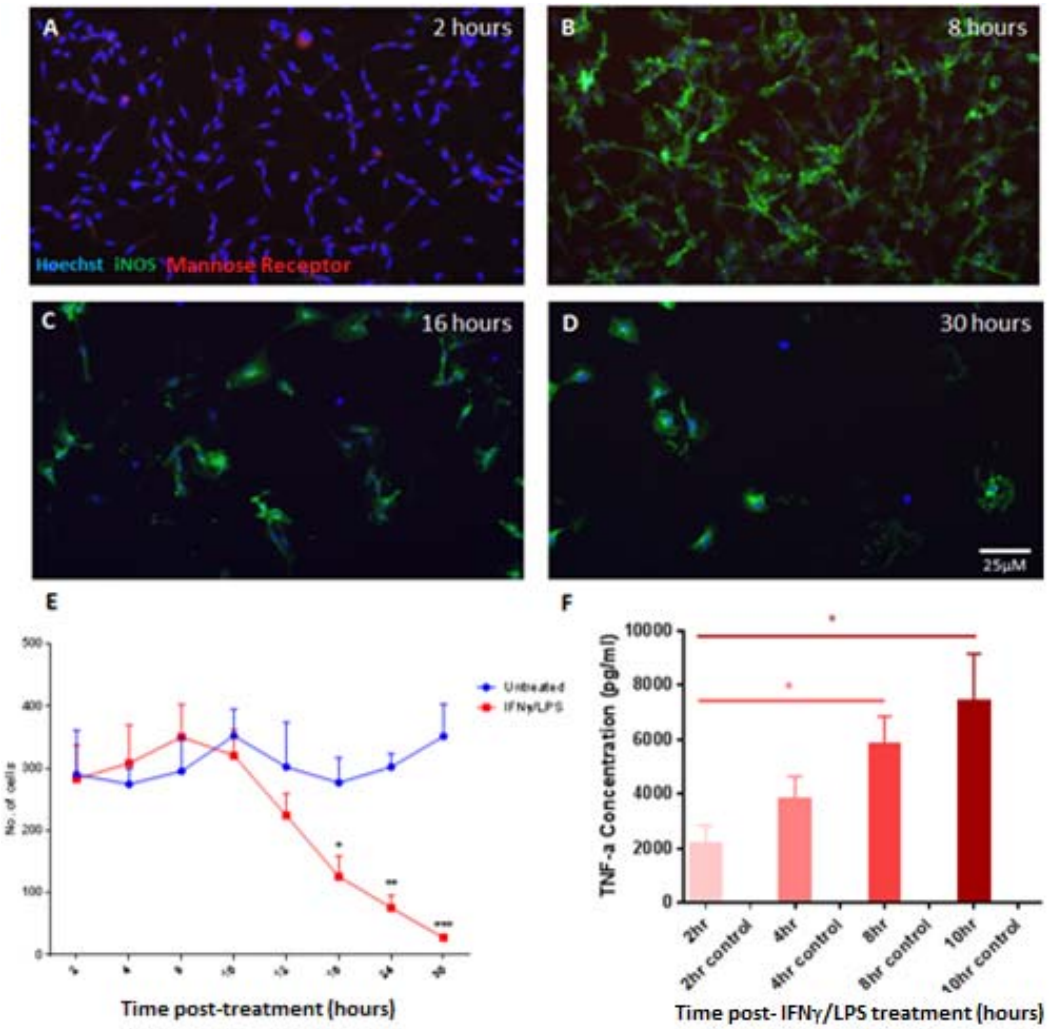

Figure 1. A-D. Microglia stained for iNOS (green) and mannose receptor (red) at 2, 8, 16 and 30 hours post IFN-γ/LPS treatment. Scale bar, 25μm. **E**. Microglia cell count over 30 hours post IFN-γ/LPS treatment (red line) and time matched untreated controls (blue line) ±s.e.m.. *P<0.05, **P<0.01, ***P<0.001 (Mann-Whitney test, IFN-γ/LPS v control). N=3 biological repeats. **F**. Concentration of secreted TNF-α from IFN-γ/LPS treated microglial conditioned media at 2-10 hours post treatment compared to time-matched untreated controls ±s.e.m.. *P<0.05 (Mann-Whitney test). N=3 biological repeats.

5.3.2. Pro-inflammatory microglial death is accelerated by immunomodulatory compounds in vitro.

Screening of 4 different compounds with immunomodulatory properties in models of CNS injury (17-β Estradiol, Substance P, Rho kinase inhibitor HA-1077 and PPAR-γ agonist Rosiglitazone) (*140, 144, 145, 227*) was carried out to determine if pro-inflammatory microglia death is accellerated. Concentrations for each compound were chosen based on previous *in vitro* experiments, although a wide range of concentrations have been used in the literature, and therefore a broader range of concentrations were also used here. 5 concentrations of each compound and their respective vehicle controls (ethanol (17b-estradiol), DMSO (Rosiglitzone and HA-1077) and PBS (substance P)) were used to treat microglia at the time of polarisation with IFN-γ/LPS. Analysis of conditioned media collected from treated cultures prior to cell loss in IFN-γ/LPS condition (10 hours post treatment) revealed a significant decrease in TNF-α production with 3 of the 4 compounds with at least one concentration compared to vehicle control (Figure 2A). Concomitantly, all compounds showed an increase in IGF-1 production with at least one concentration (Figure 2B). However, this decrease in TNF-α levels may have reflected microglial loss, as analysis of microglia numbers revealed an accelerated decrease with each compound compared to IFN-γ/LPS + vehicle (Figure 2C-F). Interestingly, the highest dose of 17-β Estradiol significantly increased TNF-α production (Figure 2A) which may reflect polarising differences in immune responses in low dose compared to high dose, as shown previously (*233, 234*).

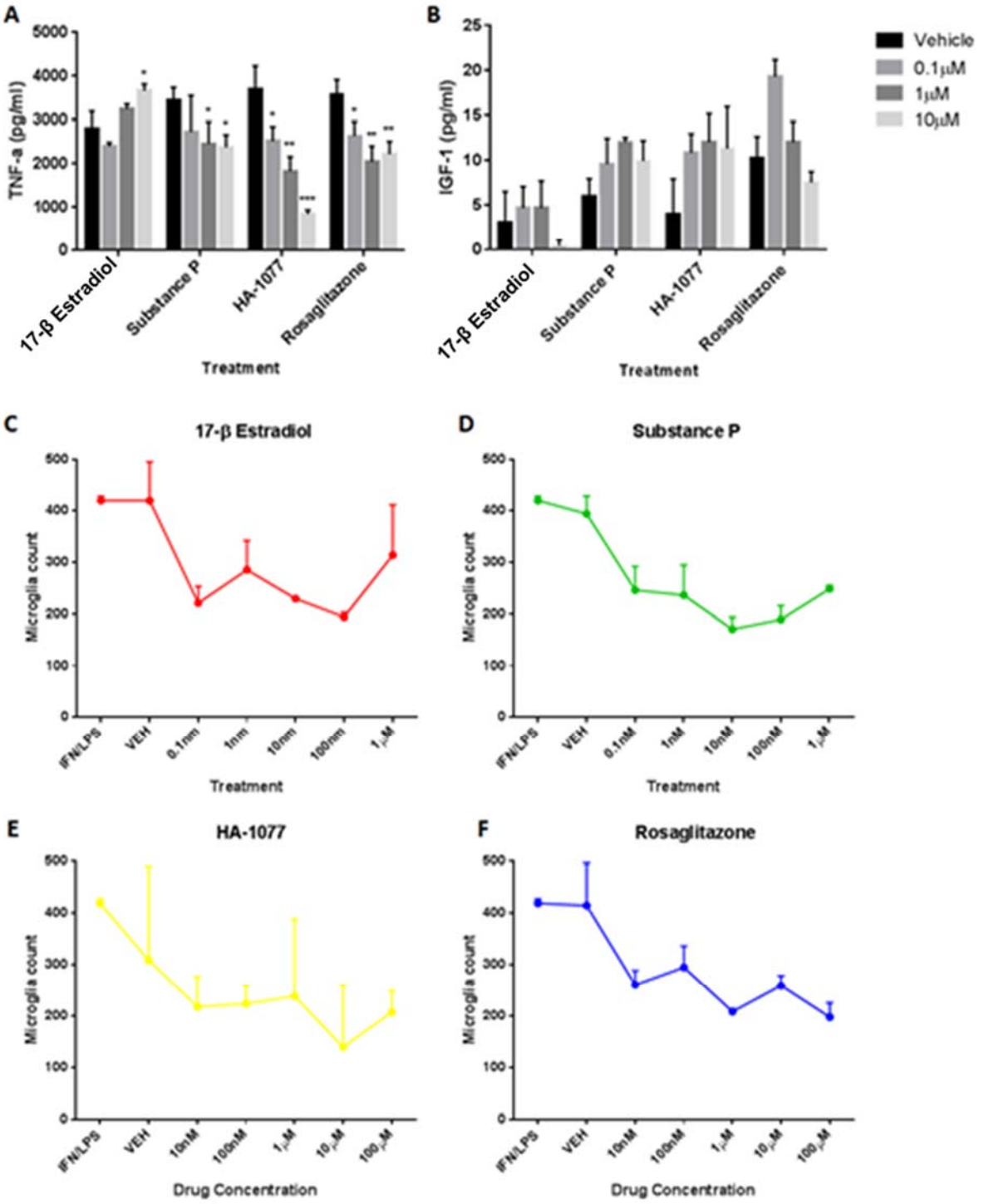

Figure 2. A. Mean concentration of TNF-α in conditioned media of pro-inflammatory microglia co-treated with 17-β Estradiol, Substance P, HA-1077 and Rosiglitazone at 10 hours post treatment ±s.e.m.. *P<0.05, **P<0.01, ***P<0.001 (Mann-Whitney test

compared to vehicle). N=3 biological repeats. **B**. Mean concentration of IGF-1 in conditioned media of pro-inflammatory microglia co-treated with 17-β Estradiol, Substance P, HA-1077 and Rosiglitazone at 10 hours post treatment. N=3 biological repeats. **C-F**. Mean microglia numbers at 10 hours post IFN-γ/LPS treatment alone or co-treated with vehicle control or immunomodulatory compound at concentrations from 0.1nM to 100μm ±s.e.m.. N=3 biological repeats.

5.3.3. NFκB activation in microglia is visualised by intensity of nuclear NFκB translocation in vitro

As each immunomodulatory compound accelerated microglia cell loss and have been shown to regulate the activation of the pro-survival factor NFκB, their effects on NFκB activity in pro-inflammatory microglia were investigated. When activated, NFκB subunit P65 translocates to the nucleus and binds to NFκB DNA binding sites to initiate transcription (*235*). Therefore, nuclear P65 can be used as a readout of NFκB activity. For this, microglia were treated with IFN-γ/LPS for 1 hour prior to fixation and immunostaining with P65 and counterstained with the actin cytoskeleton dye phalloidin to visualise the whole cell membrane, and Hoechst to visualise the nucleus (Figure 3A, B). Image analysis quantified the nuclear pixel intensity of P65 with Image J software (indicative of nuclear translocation and therefore NFκB activity) in microglia treated with IFN-γ/LPS, IL-4, IL-13 or combinations of each to identify basal levels of P65 nuclear co-localisation in pro-inflammatory microglia (IFN-γ/LPS) compared to pro-regenerative microglia (IL-13, IL-4) (Figure 3C). Nuclear pixel intensity was measured as a mean of the whole nucleus, and then recorded as nuclear pixel intensity relative to IFN-γ/LPS treated microglia (used as a positive control). IL-13 and IL-4 are used classically to induce an anti-inflammatory microglial phenotypes (*8, 220*), and were therefore used as the negative controls. Untreated cultures exhibited around 40% lower P65 nuclear co-localisation compared to IFN-γ/LPS treated cultures, as did IL-4 and IL-13 treated cultures (Figure 3C). Furthermore, IFN-γ/LPS treated microglia co-treated with IL-4 and IL-13 also showed decreased P65 nuclear co-localisation, suggesting that potent

immunomodulation can be visualised by inhibition of P65 translocation. Although baseline nuclear NFκB levels were relatively high in untreated cultures, there was enough of a distinction between baseline and IFN-γ/LPS-treated microglia to use this assay to investigate the effect of our candidate compounds on preventing NFκB activity.

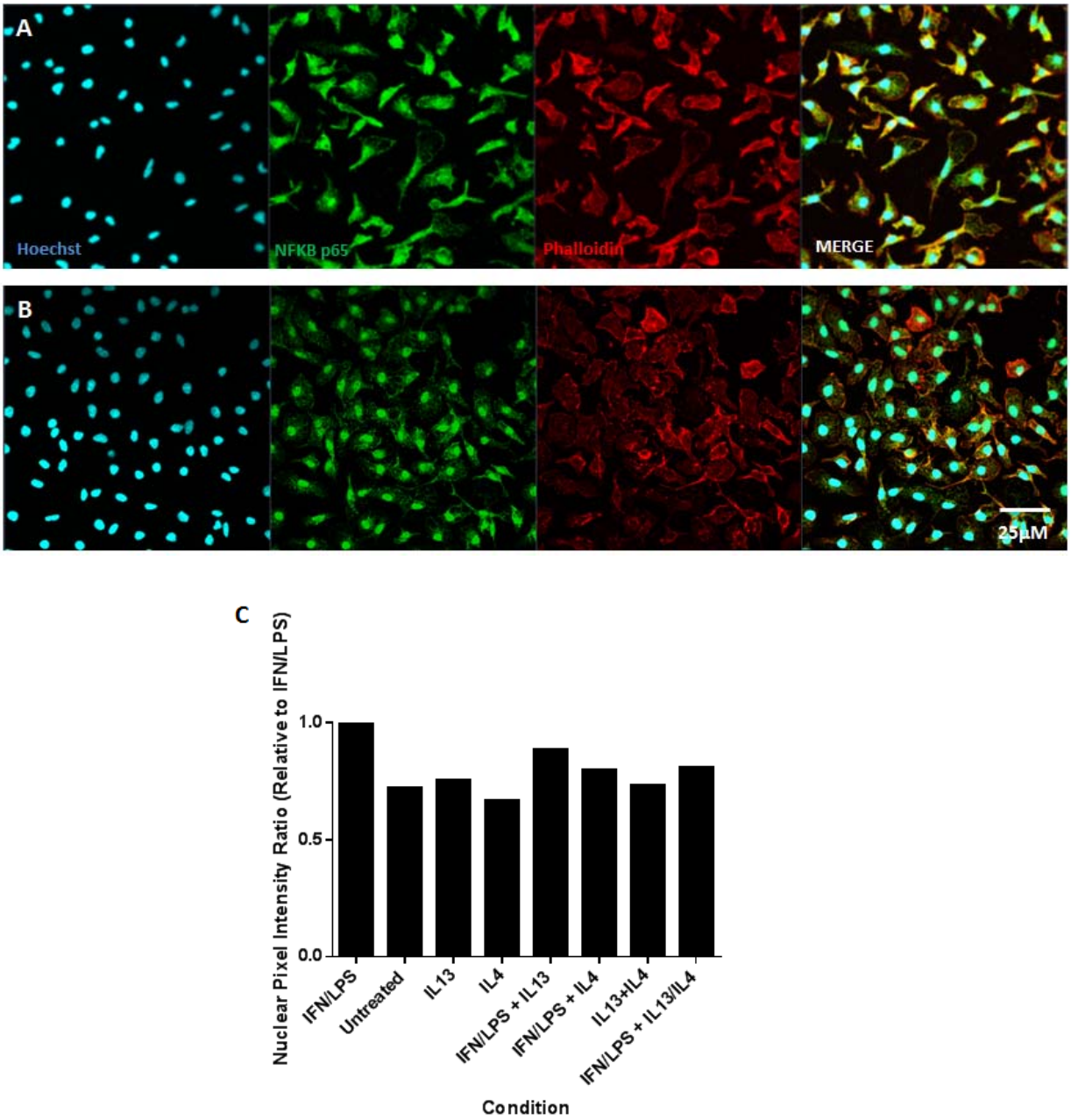

Figure 3. A. Immunostaining of untreated microglial cultures with NFκB subunit P65 (green), with cytoplasm stained using phalloidin (red). Scale bar, 25µm. **B.** Immunostaining of IFN-γ/LPS microglial cultures with NFκB subunit P65 (green), with cytoplasm stained using phalloidin (red). Scale bar, 25µm. **C**. Nuclear pixel intensity of P65 staining in untreated microglia or microglia treated with IFN-γ/LPS, IL-13, IL-4 or

a combination of treatments, relative to IFN-γ/LPS treated cultures. N=1 biological repeat.

5.3.4. NFκB activation in microglia is inhibited by immunomodulatory compounds in vitro

A smaller range of concentrations of each compound were chosen based on those most effective at inhibiting TNF-α production in microglia co-treated with IFN- γ/LPS. Co-treatment of IFN-γ/LPS treated microglia with immunomodulatory compounds lead to a significant reduction in NFκB P65 nuclear translocation indicated by pixel intensity in 3 of the 4 compounds (Figure 4A-D). However, as rosiglitazone does not inhibit nuclear translocation of NFκB, rather it binds to the P65 subunit preventing binding to DNA binding sites, it was expected to have no effect on nuclear translocation of P65 (Figure 4D).

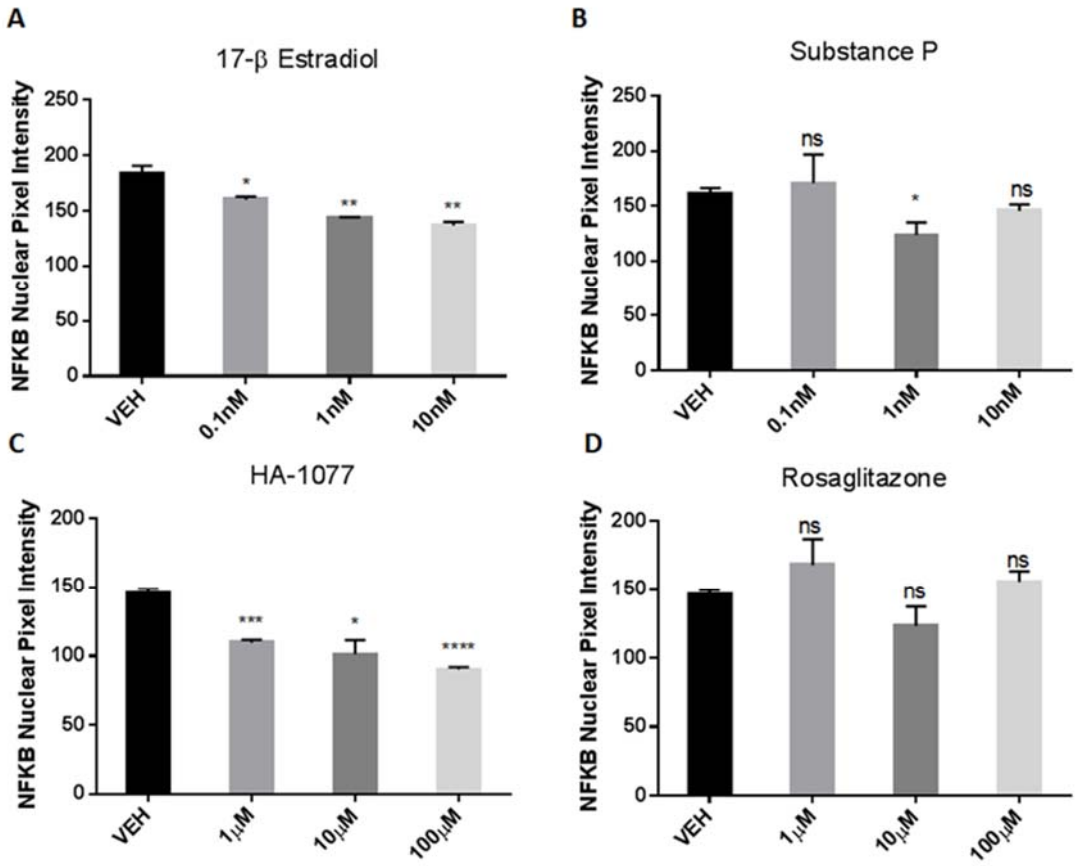

Figure 4. A-D. Mean NFκB P65 nuclear pixel intensity in pro-inflammatory microglial cultures co-treated with 17-β Estradiol, Substance P, HA-1077 and Rosiglitazone ±s.e.m.. *P<0.05, **P<0.01, ***P<0.001 (Mann-Whitney test compared to vehicle). N=3 biological repeats.

5.4. Discussion

Effective therapies that attenuate inflammation and promote remyelination are currently lacking, yet this represents a promising therapeutic strategy for diseases like progressive MS. A potential cellular target for such a therapy is the microglia, as a switch in activation from pro-inflammatory to pro-regenerative phenotypes is essential for remyelination to take place (*8*). I investigated four compounds known to have immunomodulatory properties and promote repair in various experimental models of CNS injury (*136, 138, 140, 236*). Using an established *in vitro* method of inducing pro-inflammatory activation in microglia (IFN-γ/LPS), I set out to investigate if these compounds can directly influence the activation properties of microglia, either by inducing cell death or by promoting a pro-repair phenotype.

Co-treatment of compounds with IFN-γ/LPS showed significant decreases in the production of TNF-α compared to IFN-γ/LPS alone. Known to further potentiate the inflammatory response (*237, 238*), microglial-derived TNF-α has also been shown to induce death of hippocampal neural progenitor cells *in vitro* (*239*), as well as oligodendrocytes in EAE and MS (*97*), therefore indicating one way in which chronic pro-inflammatory microglial activation can be detrimental for neural health. Interestingly, at least one concentration of each compound caused an accelerated loss of microglia, suggesting that decreases in TNF-α may be due to less pro-inflammatory microglia being present, and inducing microglial death may represent a novel mechanism for immunomodulation. 3 out of 4 compounds also significantly inhibited NFκB nuclear translocation representative of activation, suggesting a role of NFκB in microglial

inflammation and survival, and may represent a novel therapeutic avenue in pro-inflammatory microglial immunomodulation.

I now have evidence suggesting that pro-inflammatory microglial undergo cell death in another model *in vitro,* although definitive proof of cell death (by propidium iodide incorporation, for example) is needed before we can fully conclude this. Furthermore, microglia underwent cell death 8 hours earlier when co-treated with each of the 4 immunomodulatory compounds (Figure 2C-F), suggesting that these compounds can accelerate pro-inflammatory microglial death. Although microglial death leads to repopulation *in vivo* (*68-70, 202, 203*), and repopulation may support a pro-regenerative microglial phenotype (*202*), it is most likely that our *in vitro* experimental set up will be unable to investigate the effects of these compounds on promoting a pro-regenerative microglial phenotype. Although, *in vitro* repopulation has not been assessed; indeed microglia that do not die after treatment may be able to repopulate the cultures and become pro-regenerative, which could be explored, yet microglial proliferation *in vitro* takes place regardless of microglial numbers and may be too far removed from the *in vivo* environment for any relevance. However, given my evidence for microglial necroptosis being important for remyelination (*see Chapter 3*) and selective depletion of microglia in the adult mouse leading to rapid repopulation (*68-70, 202, 203*), promoting pro-inflammatory microglial death therapeutically may be of benefit for disorders where chronic pro-inflammatory microglial activation occurs, such as in MS (*8, 240-242*), ageing (*91, 147*) and spinal cord injury (*192, 208, 243, 244*). Therefore, I focused on the

molecular mechanisms that underpin the accelerated cell death caused by these compounds on pro-inflammatory microglia.

NFκB activation is vital for the initiation and potentiation of inflammatory responses in macrophages and microglia (*235, 245*) as well as being a potent pro-survival mediator (*246*). For these reasons I investigated the effect the compounds on inhibiting NFκB activation in pro-inflammatory microglia. This family of transcription factors comprised of 5 subunits; RelA (p65), Rel B, c-Rel, p50 and p52, are ubiquitous to most cells in mammals and are involved in a wide range of responses including survival, proliferation, differentiation and inflammation. The canonical pathway activated by most NFκB-stimuli is the most extensively studied, induced by activation of tumour necrosis factor alpha receptor (TNFR1), interleukin-1 receptor (IL-1R), and pattern-recognition receptors (e.g. toll-like receptor 4 (TLR-4)) (*235*). When inactive, subunits in the canonical pathway are sequestered in the cytoplasm by inhibitory IκB proteins. However, upon stimulation, IκB proteins are phosphorylated by the IκB kinase (IKK) complex (made up of IKKα and IKKβ, and regulatory subunit NEMO), which leads to ubiquitination and subsequent proteasomal degradation of the inhibitory IκB complex, freeing the NFκB subunits (primarily p65 and p50 subunits) to translocate to the nucleus and initiate transcription (see *Diagram 5*). Although NFκB is active in most cell types, its inducible activation has been shown to be vital in microglial activation, function and survival (*231, 235*).

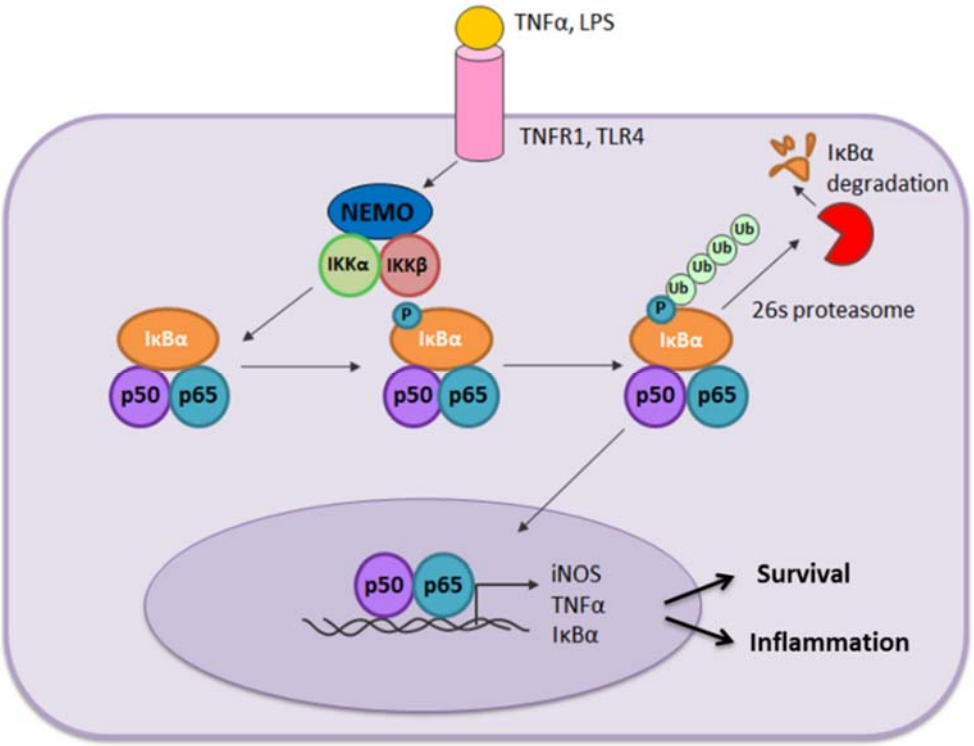

Diagram 5. Schematic representation of the canonical NFκB pathway. Inhibitory IκBα sequesters NFκB subunits in the cytoplasm until a stimulus promotes IκBa ubiquitination and degradation, allowing nuclear translocation of NFκB proteins. NFκB regulates many genes vital for an inflammatory response and survival.

Dysregulation of NFκB has been implicated in a wide range of diseases, more recently in autoimmune diseases such as MS. In EAE, high levels of NFκB have been detected in the spinal cord, the primary area of demyelination in this model (*247*). Additionally, CNS-specific IKK2 and NEMO knockout mice subjected to EAE have ameliorated clinical scores and reduced expression of pro-inflammatory cytokines (*248*). In post mortem MS brain tissue, NFκB is localized to glial cells and macrophages near lesions (*133*), although it is uncertain if NFκB activity in macrophages and microglia has been shown to differ in lesions with differing levels of remyelination potential. Furthermore, genetic screening of blood samples from MS patients showed genes involved in the inhibition of NFκB activity were altered in MS patients, which were also shown to increase susceptibility for the disease (*130*). In addition, a genome-wide association study (GWAS) identified a polymorphism in the TNFRSF1A locus which encodes TNF-α receptor 1 (TNFR1) and Mucosa-associated lymphoid tissue lymphoma translocation protein 1(MALT1) as an MS susceptibility loci (*131, 226*). This polymorphism has been shown to affect the function of TNFR1 (*249*), known to be an upstream activator of the NFκB pathway, and is therefore a possible mechanism by which this polymorphism contributes to the pathogenesis of the disease. Inhibition of NFκB activity may therefore be a promising target in modulating microglial inflammation, and potentially in driving a pro-regenerative phenotype.

At least one concentration in 3 of the immunomodulatory compounds used in this study significantly inhibited NFκB nuclear translocation compared to IFN-γ/LPS alone at 1 hour post treatment (Figure 4A-C). The PPAR-γ agonist

Rosiglitazone does not inhibit NFκB nuclear translocation, but rather directly binds to the NFκB binding sites on DNA to inhibit activity (*127*) and indeed there were no significant changes in NFκB nuclear translocation compared to vehicle (Figure 4D). Although Rosiglitazone therefore serves as a negative control here, it represents a major limitation of this assay in detecting reductions in NFκB activity; the assay is only suitable for compounds that prevent NFκB translocation. Therefore, a more suitable readout would most likely be the expression of proteins associated with inflammation downstream of NFκB activation such as IL-2 (*250, 251*), IL-6 (*252, 253*) or TNF-α (*254, 255*).

Although the loss of microglia began at 16 hours post IFN-γ/LPS treatment, translocation of P65 occurred rapidly (within 1 hour), presumably to initiate transcription of inflammatory mediators in response to the pro-inflammatory stimulation. Without NFκB inhibition, IFN-γ/LPS-treated microglia still underwent cell death, albeit later, which may be explained by the high concentration of TNF-α produced by the microglia that may indeed cause their own death in culture (*97, 256*). Although my evidence suggests pro-inflammatory microglia undergo necroptosis in *ex vivo* and *in vivo* environments (*see Chapter 3*), it is unclear if microglial TNF-α is the direct cause, and would need to be investigated further to determine if TNF-α is indeed the initiator of pro-inflammatory microglial necroptosis.

In conclusion, I have shown in some preliminary *in vitro* studies that by inhibiting NFκB activity, pro-inflammatory microglia are susceptible to an accelerated cell death, which may be a novel and beneficial therapeutic strategy

for promoting microglial phenotypic switching, and consequently, remyelination. Furthermore, for the first time I suggest that immunomodulation can involve inducing death of pro-inflammatory microglia to rapidly shut down inflammation, a previously unappreciated mechanism for immunomodulation.

5.5. Future Directions

Although preliminary, I have evidence that immunomodulatory compounds can accelerate pro-inflammatory microglial loss which may provide rapid resolution of inflammation in disease contexts. Firstly, an important immediate experiment would be to show that microglia are indeed dying *in vitro* after IFN-γ/LPS and this is accelerated with the immunomodulatory compounds, and not just a loss of cellular adhesion (if microglia were just losing adhesion, they would be washed away during fixation and washing). A propidium iodide assay would address this; propidium iodide could be supplemented into microglial media 1 hour prior to fixation, and the number of PI+ microglia could be quantified over time post-IFN-γ/LPS + compound treatment and compared to time-matched untreated/ vehicle treated and IFN-γ/LPS + vehicle treated microglial cultures. To follow on, screening compounds in an *ex vivo* model of remyelination would allow me to look at the effect of these compounds on pro-inflammatory microglial death, microglial repopulation and inflammation, as well as remyelination. Furthermore, initial experiments in an *ex vivo* model would allow for rapid screening of many compounds and concentrations before taking this into an *in vivo* model.

The LPC model has the advantage of being able to study remyelination without concurrent demyelination. However, one challenge is it may be difficult to detect significant improvements in remyelination in a model where this process occurs so efficiently. Therefore, a model of poor regeneration such as in spinal cord injury (*192*), or in aged mice where pro-inflammatory microglial activation

does not resolve (*193*) may be a more efficient model to look at the effects of pro-inflammatory microglial death on regeneration.

The importance of NFκB activation in the LPC model has not been investigated. A microglial-specific constitutively active NFκB transgenic mouse line could be used to investigate if altering NFκB expression in microglia alters their activation phenotype and, consequently, remyelination. This would also address the importance of NFκB activation for microglial survival; do pro-inflammatory microglia still undergo necroptosis in this model if NFκB is constitutively active? If not, then NFκB activity must be important in the survival of pro-inflammatory microglia. Furthermore, in mice with microglia-specific constitutively active NFκB, is remyelination hindered? If this is the case, then using immunomodulatory compounds that are capable of modulating NFκB activity would be interesting to use in this mouse model, with the aim of promoting pro-inflammatory microglial death and as a consequence, drive remyelination after LPC-induced demyelination of the corpus callosum, for example. Conversely, in microglial-specific NFκB-deficient mice, is there less pro-inflammatory microglial activation and does this improve remyelination?

Finally it would be important to determine the importance of microglial NFκB activation in the human context. By immunostaining of human MS tissue, it would be interesting to see if levels of NFκB activation in microglia is different in lesions with differences in remyelination potential. For example, in active lesions where efficient remyelination can take place, is there less microglial/ macrophage NFκB activity? This could potentially be measured by nuclear NFκB

staining compared to cytoplasm and comparing the ratio of nuclear: cytoplasmic NFκB localisation in microglia in different lesion types (co-staining with a microglia marker that outlines the whole cell such as IBA-1). Are there more NFκB+ microglia in lesions that fail to remyelinate (and where we know that there are less MLKL/RIPK3+ microglia and therefore potentially less death)? It may be that NFκB activity is high in all activated microglia regardless of phenotype and function, in which case we can look at different downstream NFκB-activated proteins to determine if there are differences in NFκB activity rather than just broad activation.

Chapter 6: Thesis Discussion

The aims of my PhD were to investigate the mechanisms that drive the activation of microglial phenotypes during efficient remyelination, with a particular focus in how microglia transition from an initial pro-inflammatory phenotype to a pro-regenerative phenotype at the onset of remyelination. My findings show that at the onset of demyelination, microglia rapidly activate to a pro-inflammatory phenotype, indicated by the expression of iNOS. IFN-γ/LPS treatment, used to induce a potent pro-inflammatory microglial response, is also associated with iNOS expression and production of TNF-α. Although only iNOS was used as a marker to identify pro-inflammatory microglia in my studies, iNOS expression has been associated with i) *in vitro* microglia which do not support oligodendrocyte differentiation, ii) *in vivo* microglia in focal demyelinated lesions which also express pro-inflammatory mediators TNF-α and CCL2, and iii) microglia in MS lesions which have poor remyelination potential (*8*). Indeed, persistent pro-inflammatory microglial activation is seen in models with poor regeneration such as spinal cord injury (SCI) (*192, 208, 257*) and in response to demyelination in aged mice (*147, 193*), as well as being associated with lesions with a poor remyelination potential in MS (*8, 100, 106, 240, 242*). Therefore, uncovering how microglial phenotypes are regulated during efficient remyelination could reveal promising new therapeutic avenues for remyelination in diseases like MS, of which there are no currently approved therapies. By focusing on the fate of iNOS+ microglia after demyelination, I observed that these cells underwent cell death shortly after their peak in activation in *ex vivo* and *in vivo* models of efficient remyelination. The

mechanism of cell death was identified to be necroptosis, characterised by expression of necroptosome protein RIPK3 and necroptosis initiator MLKL, and the reduction in cell death observed when necroptosis was blocked with small molecule inhibitor necrostatin-1. Although phosphorylated MLKL initiates oligomerisation with itself, leading to cell membrane pore formation and death via necroptosis (*159*), antibodies against pMLKL could not be optimised for our tissue, and this was therefore one limitation of my immunofluorescent analysis of necroptosis. Nevertheless, upregulation of RIPK3 and MLKL, reduction in pro-inflammatory microglia counts after their peak in activation, and prevention of death with necrostatin-1 provided evidence to support that pro-inflammatory microglia undergo necroptosis during efficient remyelination.

Microglial necroptosis then lead me to investigate how microglial repopulate, and leading to a subsequent peak in pro-regenerative microglial activation at the initiation of remyelination. Lineage tracing of both Nestin+ cells and Cx3cr1+ microglia showed that although the majority of repopulation appears to be via residual microglia, there are is small population of Nestin+ cells able to differentiate into microglia. With inducible Cre-based reporter systems, there is a level of spontaneous recombination that can occur, which differs with each reporter; spontaneous recombination was measured in explant cultures for both reporters prior to demyelination by fixing tissue without 4-OHT administration (and low levels of spontaneous recombination were observed in tdT(Nestin) slices, but not observed in tdT(Cx3cr1) slices (*data not shown*)). However, spontaneous recombination *in vivo*, or after demyelination was not measured, and both would have been additional controls strengthening

evidence from the lineage tracing studies. For tdT(Nestin) lineage tracing in particular, where I saw a small percentage of Nestin+ cells that expressed CD11b and CD45 during repopulation *in vivo*, it would be extremely important to analyse the levels of tdT(Nestin)+ CD11b+ $CD45^{lo}$ (used to identify microglia from peripheral macrophages in CNS tissue (CD11b+$CD45^{hi}$)) cells at the same time point post-demyelination but without prior tamoxifen administration to rule out spontaneous recombination in microglia. Particularly as I have shown that residual microglia can express Nestin during repopulation, as have others (*68, 70, 218*), it would be important to show that these tdT(Nestin)+CD11b+$CD45^{lo}$ cells are not just microglia that have undergone spontaneous recombination. If this was the case, this would support the idea that residual microglia are the only source of repopulating cells after depletion, as is shown in other studies (*68, 70*). However, this would raise the question of the source of microglia repopulation in an experimental model with 100% microglial depletion; does repopulation still take place, or is there a non-microglial source for repopulation in this case? Again this may depend on the method of depletion, and if the blood brain barrier is compromised. Furthermore, all depletion studies and my own study have neglected to investigate the role of peripheral macrophages in microglial repopulation. I have shown that *Ccr2*-RFP+ macrophages are present in the lesion site from 3 dpl and are still present, albeit in lower numbers, at 10 dpl. Although no time points past 10 dpl were investigated, it would be important to know if peripheral macrophages persist in the brain after remyelination is complete and contribute to repopulation. Indeed, recent evidence suggests that bone marrow

derived macrophages are able to populate the CNS after partial microglial depletion (25% reduction in microglia by genetic ablation), are seen to be engrafted into the brain parenchyma even 12 weeks post-depletion and maintain a unique identify compared to resident microglia (*221*).

I then aimed to determine if known immunomodulatory compounds could promote pro-inflammatory microglia to change phenotype, or if they could accelerate cell death. My findings showed that microglia loss occurred at 24 hours with IFN-γ/LPS treatment, often used to induce a pro-inflammatory phenotype in microglia *in vitro* (*8*), which was accelerated with co-treatment of 17-β Estradiol, substance P, Rho kinase inhibitor HA-1077 and PPAR-γ agonist Rosiglitazone. Although an observed loss of microglia occurred, confirmation of cell death by propidium iodide for example, would prove this loss is cell death and not a loss of adhesion. Nevertheless, this preliminary evidence suggests the possibility that some immunomodulatory compounds may act by promoting the death of pro-inflammatory microglia, a previously unappreciated mechanism for immunomodulation. By using models associated with poor regeneration and persistent pro-inflammatory microglial activation, it will be interesting to see if such compounds can promote pro-inflammatory microglial cell death and if this is sufficient to promote pro-regenerative microglial activation and remyelination. However, compounds such as 17-β Estradiol that act on ubiquitous estrogen receptors will most likely result in many off-target effects and may need to be encapsulated for specific microglia-targeted delivery.

Finally, it will be important to determine if promoting microglial necroptosis is a viable treatment option for diseases like MS. By using the LPC-mediated focal demyelinating lesion model, we are able to look at demyelination and remyelination in isolation, and therefore the timeline of microglial activation, necroptosis and repopulation are consistent. However, in models with concomitant demyelination and remyelination, and with lesions in different phases of remyelination or demyelination, it may prove difficult to determine the correct timing for treatment. Nevertheless, if microglial depletion leads to a pro-regenerative microglial repopulation (*202*), this may still be a viable approach. Therefore, investigating if microglial necroptosis promotes recovery in more complex models of inflammation, demyelination and neurodegeneration may increase the translational relevance of this work and lead to novel therapeutic approaches to support remyelination.

Chapter 7: Concluding Remarks

I have shown that pro-inflammatory microglial necroptosis is a feature of efficient remyelination which may represent a rapid approach to shut down inflammatory responses, allowing for the activation of pro-regenerative microglia that drive remyelination. After microglial necroptosis, repopulation takes place from two sources; residual microglia and Nestin+ cell differentiation. Furthermore, microglial necroptosis and repopulation are features of MS lesions with high capacity for remyelination, and blocking necroptosis experimentally leads to the inhibition of remyelination. Therefore, microglial necroptosis may be necessary for efficient remyelination to take place, and persistent pro-inflammatory microglial activation in models of poor regeneration and in human chronic inflammatory demyelinating diseases may reflect impaired microglial death. Targeting pro-inflammatory microglial necroptosis may therefore be a novel therapeutic target in promoting remyelination.

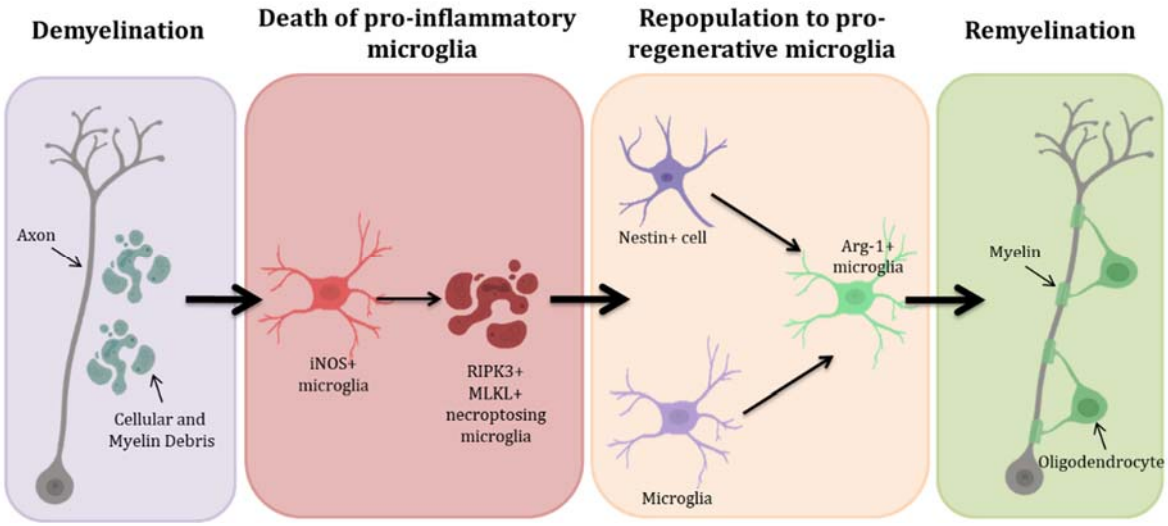

Diagram 6. Summary of microglial dynamics during efficient remyelination.

Chapter 8. Abbreviations

- 4-OHT: 4-hydroxytamoxifen
- ALS: Amyotrophic Lateral Sclerosis
- Arg-1: Arginase-1
- ATP: Adenosine Triphosphate
- BBB: Blood Brain Barrier
- CNS: Central Nervous System
- DAMPs: Damage-associated Molecular Patterns
- DCX: Doublecortin
- DT: Diphtheria toxin
- E: embryonic Day
- EAE: Experimental Autoimmune Encephalomyelitis
- EMPs: Erythroid Myeloid Progenitors
- EtOH: Ethanol
- G.W.: Gestational Week
- $GdCl_3$: Gadolinium Chloride
- GM-CSF: Granulocyte-macrophage Colony Stimulating Factor
- HSCs: Haematopoietic Stem Cells
- IDO: Indoleamine 2 3-dioxygenase
- IFN-γ: Interferon Gamma
- IGF-1: Insulin-like Growth Factor 1
- IKK: inhibitor of NFκB kinase subunit
- IL-: Interleukin

- iNOS: Inducible Nitric Oxide Synthase
- iPSCs: Inducible pluripotent stem cells
- IRF-8: Interferon regulatory factor 8
- IκBα: nuclear factor of kappa light polypeptide gene enhancer in B-cells inhibitor, alpha
- LPC: Lysophosphatidyl Choline
- LPS: Lipopolysaccharide
- MAG: Myelin Associated Glycoprotein
- MALT1: Mucosa-associated Lymphoid Tissue Lymphoma Translocation Protein 1
- MBP: Myelin Basic Protein
- M-CSF: Macrophage Colony Stimulating Factor
- MDMs: Monocyte-derived Macrophages
- MHC: Major Histocompatibility Complex
- MLKL: Mixed-lineage Kinase Domain Like Pseudokinase
- MOG: Myelin Oligodendrocyte Glycoprotein
- MRI: Magnetic Resonance Imaging
- MS: Multiple Sclerosis
- MSX3: Msh Homeobox 3
- NAWM: Normal Appearing White Matter
- NEMO: NFκB essential modulator
- NFκB: Nuclear Factor Kappa Light-chain-enhancer of Activated B Cells
- NPC: Neural Progenitor Cell

- OPC: Oligodendrocyte Progenitor Cell
- PAMPSs: Pathogen-associated Molecular Patterns
- PBMCs: Peripheral Blood Mononuclear Cells
- PLP: Proteolipid Protein
- PMD: Pelizaeus-Merzbacher Disease
- PNS: Peripheral Nervous System
- PPMS: Primary Progressive Multiple Sclerosis
- RIPK: Receptor Interacting Protein Kinase
- RRMS: Relapse-remitting Multiple Sclerosis
- SCI: Spinal Cord Injury
- SNr: Substantia Nigra Reticulata
- SPMS: Secondary Progressive Multiple Sclerosis
- TBI: Traumatic Brain Injury
- TGF-β: Transforming Growth Factor Beta
- TLR: Toll-like receptor
- TNFR1: TNF-α Receptor 1
- TNF-α: Tumour Necrosis Factor Alpha
- TUNEL: Terminal deoxynucleotidyl tranferase dUTP nick end labelling
- VTA: Ventral Tegmental Area

Chapter 9. Appendix

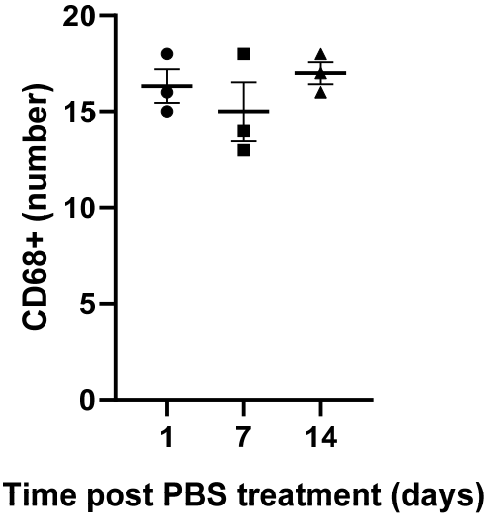

Figure 1. Mean number of CD68+ microglia from PBS treated organotypic cerebellar slice cultures at 1, 7 and 14 days post treatment ±s.e.m.. N=3 biological repeats.

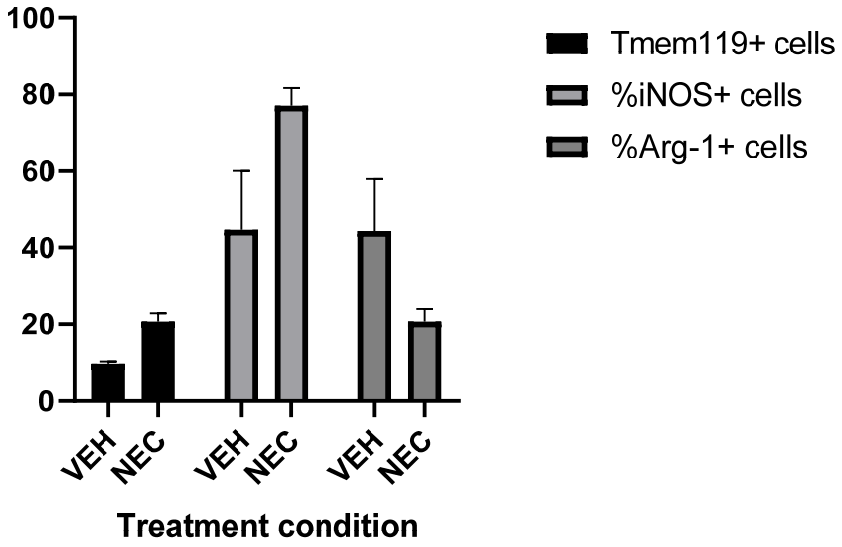

Figure 2. Raw values from mice treated with vehicle (VEH) LNCs and necrostatin-1 (NEC) LNCs immunostained for Tmem119, iNOS and Arg-1 at

10dpl. Tmem119+ cells are represented as total counts. iNOS and Arg-1 are represented as a percentage of the total number of IBA-1+ cells expressing iNOS and Arg-1.

Chapter 10. References

1. L. Lawson, V. Perry, S. Gordon, Turnover of resident microglia in the normal adult mouse brain. *Neuroscience* **48**, 405-415 (1992).
2. M. Mittelbronn, K. Dietz, H. Schluesener, R. Meyermann, Local distribution of microglia in the normal adult human central nervous system differs by up to one order of magnitude. *Acta Neuropathologica* **1**, 249-255 (2001).
3. M. Prinz, J. Priller, Microglia and brain macrophages in the molecular age: from origin to neuropsychiatric disease. *Nat Rev Neurosci* **15**, 300-312 (2014).
4. S. Haynes *et al.*, The P2Y12 receptor regulates microglial activation by extracellular nucleotides. *Nat Neurosci* **9**, 1512-1519 (2006).
5. U. Pannasch *et al.*, The potassium channels Kv1.5 and Kv1.3 modulate distinct functions of microglia. *Mol Cell Neurosci* **33**, 401-411 (2006).
6. S. Tang *et al.*, Pivotal role for neuronal Toll-like receptors in ischemic brain injury and functional deficits. *PNAS* **104**, 13798-13803 (2007).
7. M. Olah *et al.*, Identification of a microglia phenotype supportive of remyelination. *Glia* **60**, 306-321 (2012).
8. V. Miron *et al.*, M2 microglia and macrophages drive oligodendrocyte differentiation during CNS remyelination. *Nature Neuroscience* **16**, 1211-1218 (2013).
9. M. Bradl, H. Lassmann, Oligodendrocytes: biology and pathology. *Acta Neuropathologica* **119**, 37-53 (2010).
10. S. Ludwin, Remyelination in the central nervous system and the peripheral nervous system. *Adv Neurol* **47**, 215-254 (1988).
11. C. Fernandez-Valle, R. Bunge, M. Bunge, Schwann cells degrade myelin and proliferate in the absence of macrophages: evidence from in vitro studies of Wallerian degeneration. *J Neurocytol* **24**, 667-679 (1995).
12. M. Bear, B. Connors, M. Paradiso, *Neuroscience: Exploring the Brain* (Wolters Kluwer, 2015).
13. K. Nave, Myelination and the trophic support of long axons. *Nat Rev Neurosci* **11**, 275-283 (2010).
14. Y. Lee *et al.*, Oligodendroglia metabolically support axons and contribute to neurodegeneration. *Nature* **26**, 443-448 (2012).
15. S. Pfeiffer, A. Warrington, R. Bansal, The oligodendrocyte and its many cellular processes. *Trends Cell Biol* **3**, 191-197 (1993).
16. M. Craner, A. Lo, J. Black, S. Waxman, Abnormal sodium channel distribution in optic nerve axons in a model of inflammatory demyelination. *Brain* **126**, 1552-1561 (2003).
17. K. Irvine, W. Blakemore, Remyelination protects axons from demyelination-associated axon degeneration. *Brain* **131**, 1464-1477 (2008).
18. F. Mei *et al.*, Accelerated remyelination during inflammatory demyelination prevents axonal loss and improves functional recovery. *eLIFE*, (2016).
19. R. Franklin, C. Ffrench-Constant, Regenerating CNS myelin - from mechanisms to experimental medicines. *Nat Rev Neurosci* **18**, 753-769 (2017).
20. K. Smith, W. Blakemore, W. McDonald, Central remyelination restores secure conduction. *Nature* **280**, 395-396 (1979).
21. I. Duncan, A. Brower, Y. Kondo, J. Curlee, R. Schultz, Extensive remyelination of the CNS leads to functional recovery. *PNAS* **106**, 6832-6836 (2009).

22. T. Kuhlmann *et al.*, Differentiation block of oligodendroglial progenitor cells as a cause for remyelination failure in chronic multiple sclerosis. *Brain* **131**, 1749-1758 (2008).
23. C. Procaccini, V. De Rosa, V. Pucino, L. Formisano, G. Matarese, Animal models of Multiple Sclerosis. *European Journal of Pharmacology* **759**, 182-191 (2015).
24. R. J. M. Franklin, Why Does Remyelination Fail in Multiple Sclerosis? *Nature Reviews Neuroscience* **3**, 705-714 (2002).
25. M. Targett *et al.*, Failure to achieve remyelination of demyelinated rat axons following transplantation of glial cells obtained from the adult human brain. *Neuropathol Appl Neurobiol* **22**, 199-206 (1996).
26. H. Arnett *et al.*, TNF alpha promotes proliferation of oligodendrocyte progenitors and remyelination. *Nat Neurosci* **4**, 1116-1122 (2001).
27. S. Lin, L. Fan, P. Rhodes, H. Mitchell, Z. Cai, IGF-1 protects oligodendrocyte progenitor cells and improves neurological functions following cerebral hypoxia-ischemia in the neonatal rat. *Brain Res* **1063**, 15-26 (2005).
28. R. McKinnon, G. Piras, J. Ida, M. Dubois-Dalcq, A role for TGF-beta in oligodendrocyte differentiation. *J Cell Biol* **121**, 1397-1407 (1993).
29. Y. Dombrowski *et al.*, Regulatory T cells promote myelin regeneration in the central nervous system. *Nature Neuroscience* **20**, 674-680 (2017).
30. A. Hedstrom, M. Baarnheilm, T. Olsson, L. Alfredsson, Tobacco smoking, but not Swedish snuff use, increases the risk of multiple sclerosis. *Neurology* **73**, 696-671 (2009).
31. K. Munger *et al.*, Vitamin D intake and incidence of multiple sclerosis. *Neurology* **63**, 60-65 (2004).
32. J. Lunemann *et al.*, Increased frequency and broadened specificity of latent EBV nuclear antigen-1-specific T cells in multiple sclerosis. *Brain* **129**, 1493-1506 (2006).
33. I. M. S. G. Consortium. *et al.*, Risk alleles for multiple sclerosis identified by a genomewide study. *N Engl J Med* **30;357**, 851-862 (2007).
34. F. Perez-Cerda, M. Sanchez-Gomez, C. Matute, The link of inflammation and neurodegeneration in progressive multiple sclerosis. *Multiple Sclerosis and Demyelinating Disorders* **1**, 1-8 (2016).
35. A. Boyd, H. Zhang, A. Williams, Insufficient OPC migration into demyelinated lesions is a cause of poor remyelination in MS and mouse models. *Acta Neuropathologica* **125**, 841-859 (2013).
36. A. Niehaus *et al.*, Patients with active relapsing-remitting multiple sclerosis synthesize antibodies recognizing oligodendrocyte progenitor cell surface protein: implications for remyelination. *Ann Neurol* **48**, 362-371 (2000).
37. G. Wolswijk, Chronic stage multiple sclerosis lesions contain a relatively quiescent population of oligodendrocyte precursor cells. *J Neurosci* **18**, 601-609 (1998).
38. A. Chang, A. Nishiyama, J. Peterson, J. Prineas, B. Trapp, NG2-positive oligodendrocyte progenitor cells in adult human brain and multiple sclerosis lesions. *J Neurosci* **20**, 6404-6412 (2000).
39. A. Chang, W. Tourtellotte, R. Rudick, B. Trapp, Premyelinating oligodendrocytes in chronic lesions of multiple sclerosis. *N Engl J Med* **346**, 165-173 (2002).
40. K. Barron, The microglial cell. A historical review. *J Neurol Sci* **134**, 57-68 (1995).
41. W. Hickey, H. Kimura, Perivascular microglial cells of the CNS are bone marrow-derived and present antigen in vivo. *Science* **239**, 290-292 (1998).
42. F. Ginhoux *et al.*, Fate Mapping Analysis Reveals That Adult Microglia Derive from Primitive Macrophages. *Science* **330**, (2010).

43. E. Gautier *et al.*, Gene-expression profiles and transcriptional regulatory pathways that underlie the identity and diversity of mouse tissue macrophages. *Nature Immunology* **13**, 1118-1128 (2012).
44. L. Davies, S. Jenkins, J. Allen, P. Taylor, Tissue-Resident Macrophages. *Nature Immunology* **14**, 986-992 (2013).
45. A. Nimmerjahn, F. Kirchoff, F. Helmchen, Resting microglial cells are highly dynamic surveillants of brain parenchyma in vivo. *Science* **27**, 1314-1318 (2005).
46. M. Tremblay, R. Lowery, A. Majewska, Microglial Interactions with Synapses Are Modulated by Visual Experience. *Plos Biology* **8**, (2010).
47. H. Wake, A. Moorhouse, S. Jinno, S. Kohsaka, J. Nabekura, Resting microglia directly monitor the functional state of synapses in vivo and determine the fate of ischemic terminals. *J Neurosci* **29**, 3974-3980 (2009).
48. D. Schafer, B. Stevens, Microglia Function in Central Nervous System Development and Plasticity. *Cold Spring Harb Perspect Biol* **17;7**, (2015).
49. D. Low, F. Ginhoux, Recent advances in the understanding of microglial development and homeostasis. *Cellular Immunology*, (2018).
50. F. Alliot, I. Godin, B. Pessac, Microglia derive from progenitors, originating from the yolk sac, and which proliferate in the brain. *Brain Res Dev Brain Res* **117**, 145-152 (1999).
51. K. Kierdorf *et al.*, Microglia emerge from erythromyeloid precursors via Pu.1- and Irf8-dependent pathways. *Nat Neurosci* **16**, 273-280 (2013).
52. F. Ginhoux, M. Prinz, Origin of microglia: current concepts and past controversies. *Cold Spring Harb Perspect Biol* **7**, (2015).
53. A. Monier *et al.*, Entry and distribution of microglial cells in human embryonic and fetal cerebral cortex. *J Neuropathol Exp Neurol* **66**, 372-382 (2007).
54. C. Verney, A. Monier, C. Fallet-Bianco, P. Gressens, Early microglial colonization of the human forebrain and possible involvement in periventricular white-matter injury of preterm infants. *J Anat* **217**, 436-448 (2010).
55. S. Koushik *et al.*, Targeted inactivation of the sodium-calcium exchanger (Ncx1) results in the lack of a heartbeat and abnormal myofibrillar organization. *FASEB* **15**, 1209-1211 (2001).
56. E. Mass *et al.*, Specification of tissue-resident macrophages during organogenesis. *Science*, (2016).
57. O. Matcovitch-Natan *et al.*, Microglia development follows a stepwise program to regulate brain homeostasis. *Science* **353**, (2016).
58. K. Takata *et al.*, Induced-Pluripotent-Stem-Cell-Derived Primitive Macrophages Provide a Platform for Modeling Tissue Resident Macrophage Differentiation and Function. *Immunity* **47**, 183-198 (2017).
59. J. Xu *et al.*, Temporal-Spatial Resolution Fate Mapping Reveals Distinct Origins for Embryonic and Adult Microglia in Zebrafish. *Developmental Cell* **34**, 362-641 (2015).
60. J. Sheng, C. Ruedl, K. Karjalainen, Most Tissue-Resident Macrophages Except Microglia Are Derived from Fetal Hematopoietic Stem Cells. *Immunity* **43**, 382-393 (2015).
61. M. Fehrenbach, M. Tjwa, I. Bechmann, M. Krueger, Decreased microglial numbers in Vav1-Cre+:dicer knock-out mice suggest a second source of microglia beyond yolk sac macrophages. *Annals of Anatomy* **218**, 190-198 (2018).
62. A. Wlodarczyk *et al.*, A novel microglial subset plays a key role in myelinogenesis in developing brain. *The EMBO Journal* **37**, (2017).

63. D. Beers *et al.*, Wild-type microglia extend survival in PU.1 knockout mice with familial amyotrophic lateral sclerosis. *Proc Natl Acad Sci USA* **103**, 16021-16026 (2006).
64. B. Tambuyzer, P. Ponsaerts, E. Nouwen, Microglia: gatekeepers of central nervous system immunology. *J Leukoc Biol* **85**, 352-370 (2009).
65. M. Nikodemova *et al.*, Microglial numbers attain adult levels after undergoing a rapid decrease in cell number in the third postnatal week. *Journal of Neuroimmunology* **278**, 280-288 (2015).
66. K. Askew *et al.*, Coupled Proliferation and Apoptosis Maintain the Rapid Turnover of Microglia in the Adult Brain. *Cell Reports* **18**, 391-405 (2017).
67. H. Asai *et al.*, Depletion of microglia and inhibition of exosome synthesis halt tau propagation. *Nat Neurosci* **18**, 1584-1593 (2015).
68. J. Bruttger *et al.*, Genetic Cell Ablation Reveals Clusters of Local Self-Renewing Microglia in the Mammalian Central Nervous System. *Immunity* **43**, 92-106 (2015).
69. M. Elmore *et al.*, Colony-stimulating factor 1 receptor signaling is necessary for microglia viability, unmasking a microglia progenitor cell in the adult brain. *Neuron* **82**, 380-397 (2014).
70. Y. Huang *et al.*, Repopulated microglia are solely derived from the proliferation of residual microglia after acute depletion. *Nat Neurosci*, (2018).
71. K. Kigerl, J. de Rivero Vaccari, W. Dietrich, P. Popovich, R. Keane, Pattern recognition receptors and central nervous system repair. *Exp Neurol* **258**, 5-16 (2014).
72. R. Ransohoff, A polarizing question: do M1 and M2 microglia exist? *Nat Neurosci* **19**, 987-991 (2016).
73. J. Xue *et al.*, Transcriptome-based network analysis reveals a spectrum model of human macrophage activation. *Immunity* **40**, 274-288 (2014).
74. I. Chiu *et al.*, A neurodegeneration-specific gene-expression signature of acutely isolated microglia from an amyotrophic lateral sclerosis mouse model. *Cell Reports* **4**, 385-401 (2013).
75. R. Yamasaki *et al.*, Differential roles of microglia and monocytes in the inflamed central nervous system. *J Exp Med* **211**, 1533-1549 (2014).
76. J. Morganti, L. Riparip, S. Rosi, Call Off the Dog(ma): M1/M2 Polarization Is Concurrent following Traumatic Brain Injury. *PLoS One* **11**, (2016).
77. P. Murray *et al.*, Macrophage activation and polarization: nomenclature and experimental guidelines. *Immunity* **41**, 14-20 (2014).
78. J. Edwards, X. Zhang, K. Frauwirth, D. Mosser, Biochemical and functional characterization of three activated macrophage populations. *J Leukoc Biol* **80**, 1298-1307 (2006).
79. O. Butovsky *et al.*, Microglia activated by IL-4 or IFN-gamma differentially induce neurogenesis and oligodendrogenesis from adult stem/progenitor cells. *Mol Cell Neurosci* **31**, 149-160 (2006).
80. K. Kigerl *et al.*, Identification of two distinct macrophage subsets with divergent effects causing either neurotoxicity or regeneration in the injured mouse spinal cord. *J Neurosci* **29**, 13435-13444 (2009).
81. A. Fenn, J. Hall, J. Gensel, P. Popovich, J. Godbout, IL-4 signaling drives a unique arginase+/IL-1β+ microglia phenotype and recruits macrophages to the inflammatory CNS: consequences of age-related deficits in IL-4Rα after traumatic spinal cord injury. *J Neurosci* **34**, 8904-8917 (2014).

82. I. Francos-Quijorna, J. Amo-Aparicio, A. Martinez-Muriana, R. Lopez-Vales, IL-4 drives microglia and macrophages toward a phenotype conducive for tissue repair and functional recovery after spinal cord injury. *Glia* **64**, 2079-2092 (2016).
83. M. Kotter, A. Setzu, F. Sim, N. Van Rooijen, R. Franklin, Macrophage depletion impairs oligodendrocyte remyelination following lysolecithin-induced demyelination. *Glia* **35**, 204-212 (2001).
84. H. Neumann, M. Kotter, R. Franklin, Debris clearance by microglia: an essential link between degeneration and regeneration. *Brain* **132**, 288-295 (2009).
85. A. Lampron *et al.*, Inefficient clearance of myelin debris by microglia impairs remyelinating processes. *J Exp Med* **212**, 481-495 (2015).
86. M. Kotter, C. Zhao, N. Van Rooijen, R. Franklin, Macrophage-depletion induced impairment of experimental CNS remyelination is associated with a reduced oligodendrocyte progenitor cell response and altered growth factor expression. *Neurobiol Dis* **18**, 166-175 (2005).
87. K. Deonarine *et al.*, Gene expression profiling of cutaneous wound healing. *J Transl Med*, (2007).
88. D. Ruffell *et al.*, A CREB-C/EBPbeta cascade induces M2 macrophage-specific gene expression and promotes muscle injury repair. *Proc Natl Acad Sci USA* **106**, 17475-17480 (2009).
89. V. Dayan *et al.*, Mesenchymal stromal cells mediate a switch to alternatively activated monocytes/macrophages after acute myocardial infarction. *Basic Res Cardiol* **106**, 1299-1310 (2011).
90. M. Hardonk, F. Dijkhuis, C. Hulstaert, J. Koudstaal, Heterogeneity of rat liver and spleen macrophages in gadolinium chloride-induced elimination and repopulation. *J Leukoc Biol* **52**, 296-302 (1992).
91. J. Ruckh *et al.*, Rejuvenation of regeneration in the aging central nervous system. *Cell Stem Cell* **10**, 96-103 (2012).
92. M. Karamita *et al.*, Therapeutic inhibition of soluble brain TNF promotes remyelination by increasing myelin phagocytosis by microglia. *JCI Insight* **2**, (2017).
93. A. Bitsch *et al.*, Tumour necrosis factor alpha mRNA expression in early multiple sclerosis lesions: correlation with demyelinating activity and oligodendrocyte pathology. *Glia* **29**, 366-375 (2000).
94. B. Ferguson, M. Matyszak, M. Esiri, V. Perry, Axonal damage in acute multiple sclerosis lesions. *Brain* **120**, 393-399 (1997).
95. R. Patani, M. Balaratnam, A. Vora, R. Reynolds, Remyelination can be extensive in multiple sclerosis despite a long disease course. *Neuropathol Appl Neurobiol* **33**, (2007).
96. E. Benveniste, Role of macrophages/microglia in multiple sclerosis and experimental allergic encephalomyelitis. *J Mol Med* **75**, 165-173 (1997).
97. D. Ofengeim *et al.*, Activation of necroptosis in multiple sclerosis. *Cell Reports* **10**, 1836-1849 (2015).
98. M. Fischer *et al.*, NADPH oxidase expression in active multiple sclerosis lesions in relation to oxidative tissue damage and mitochondrial injury. *Brain* **135**, 886-899 (2012).
99. B. Trapp *et al.*, Axonal Transection in the Lesions of Multiple Sclerosis. *New England Journal of Medicine* **338**, 278-285 (1998).
100. J. Bogie, P. Stinissen, J. Hendriks, Macrophage subsets and microglia in multiple sclerosis. *Acta Neuropathologica* **128**, 191-213 (2014).
101. O. Butovsky *et al.*, Identification of a unique TGF-β-dependent molecular and functional signature in microglia. *Nat Neurosci* **17**, 131-143 (2014).

102. J. Satoh *et al.*, TMEM119 marks a subset of microglia in the human brain. *Neuropathology* **36**, 39-49 (2016).
103. M. Bennett *et al.*, New tools for studying microglia in the mouse and human CNS. *Proc Natl Acad Sci USA* **11**

(2016).
104. H. Xu *et al.*, Evidence of CCR2-independent transmigration of Ly6Chi monocytes into the brain after permanent cerebral ischemia in mice. *Brain Res* **1637**, 118-127 (2016).
105. M. Barnett, J. Prineas, Relapsing and remitting multiple sclerosis: pathology of the newly forming lesion. *Ann Neurol* **55**, 458-468 (2004).
106. T. Zrzavy *et al.*, Loss of 'homeostatic' microglia and patterns of their activation in active multiple sclerosis. *Brain* **140**, 1900-1913 (2017).
107. C. Marik, P. Felts, J. Bauer, H. Lassmann, K. Smith, Lesion genesis in a subset of patients with multiple sclerosis: a role for innate immunity? *Brain* **130**, 2800-2815 (2007).
108. H. Lassmann, Z. F., K. Vass, W. Hickey, Microglial cells are a component of the perivascular glia limitans. *J Neurosci Res* **28**, 236-243 (1991).
109. J. Gehrmann, R. Banati, G. Kreutzberg, Microglia in the immune surveillance of the brain: human microglia constitutively express HLA-DR molecules. *J Neuroimmunol* **48**, 189-198 (1993).
110. E. Chastain, D. Duncan, J. Rodgers, S. Miller, The Role of Antigen Presenting Cells in Multiple Sclerosis. *Biochim Biophys Acta* **1812**, 265-274 (2011).
111. Y. Wolf *et al.*, Microglial MHC class II is dispensable for experimental autoimmune encephalomyelitis and cuprizone-induced demyelination. *European Journal of Immunology* **48**, (2018).
112. F. Williams, D. Hughes, D. Middleton, A new HLA-DRB1*11 allele (DRB1*1109) differing at codons 32, 34 and 37. *Tissue Antigens* **44**, 63-64 (1994).
113. M. B. *et al.*, HLA-DRB1 polymorphism and susceptibility to multiple sclerosis in the Middle East North Africa region: A systematic review and meta-analysis. *J Neuroimmunol* **15**, 117-124 (2018).
114. A. Alcina *et al.*, Multiple Sclerosis Risk Variant HLA-DRB1*1501 Associates with High Expression of DRB1 Gene in Different Human Populations. *PLoS One* **7**, (2012).
115. F. Heppner *et al.*, Experimental autoimmune encephalomyelitis repressed by microglial paralysis. *Nat Med* **11**, 146-152 (2005).
116. E. Ponomarev, L. Shriver, K. Maresz, B. Dittel, Microglial cell activation and proliferation precedes the onset of CNS autoimmunity. *J Neurosci Res* **81**, 374-389 (2005).
117. D. Vogel *et al.*, Macrophages in inflammatory multiple sclerosis lesions have an intermediate activation status. *J Neuroinflammation* **10**, (2013).
118. E. Miller, B. Wachowicz, I. Majsterek, Advances in antioxidative therapy of multiple sclerosis. *Curr Med Chem* **20**, 4720-4730 (2013).
119. L. Haider *et al.*, Oxidative damage in multiple sclerosis lesions. *Brain* **134**, 1914-1924 (2011).
120. L. Peferoen *et al.*, Activation status of human microglia is dependent on lesion formation stage and remyelination in multiple sclerosis. *J Neuropathol Exp Neurol* **74**, 48-63 (2015).
121. J. Mikita *et al.*, Altered M1/M2 activation patterns of monocytes in severe relapsing experimental rat model of multiple sclerosis. Amelioration of clinical status by M2 activated monocyte administration. *Mult Scler* **17**, 2-15 (2011).

122. M. Ahn *et al.*, Immunohistochemical study of arginase-1 in the spinal cords of Lewis rats with experimental autoimmune encephalomyelitis. *Brain Res* **9**, 77-86 (2012).
123. V. Chhor *et al.*, Characterization of phenotype markers and neuronotoxic potential of polarised primary microglia in vitro. *Brain Behav Immun* **32**, 70-85 (2013).
124. R. Shechter, M. Schwartz, Harnessing monocyte-derived macrophages to control central nervous system pathologies: no longer 'if' but 'how'. *J Pathol* **229**, 332-346 (2013).
125. Z. Yu *et al.*, MSX3 Switches Microglia Polarization and Protects from Inflammation-Induced Demyelination. *J Neurosci* **35**, 6350-6365 (2015).
126. Y. Ohmori, T. Hamilton, Interleukin-4/STAT6 represses STAT1 and NF-kappa B-dependent transcription through distinct mechanisms. *J Biol Chem* **1;275**, 38095-38103 (2000).
127. A. Remels *et al.*, PPARgamma inhibits NF-kappaB-dependent transcriptional activation in skeletal muscle. *Am J Physiol Endocrinol Metab* **297**, E174-183 (2009).
128. O. Sharif, V. Bolshakov, S. Raines, P. Newham, N. Perkins, Transcriptional profiling of the LPS induced NF-kappaB response in macrophages. *BMC Immunol* **12**, 1 (2007).
129. H. Qin, C. Wilson, S. Lee, X. Zhao, E. Benveniste, LPS induces CD40 gene expression through the activation of NF-kappaB and STAT-1alpha in macrophages and microglia. *Blood* **1;106**, 3114-3122 (2005).
130. B. Miterski *et al.*, Inhibitors in the NFkappaB cascade comprise prime candidate genes predisposing to multiple sclerosis, especially in selected combinations. *Genes Immun* **3**, 211-219 (2002).
131. P. De Jager *et al.*, Meta-analysis of genome scans and replication identify CD6, IRF8 and TNFRSF1A as new multiple sclerosis susceptibility loci. *Nat Genet* **41**, 776-782 (2009).
132. W. Housley *et al.*, Genetic variants associated with autoimmunity drive NFκB signaling and responses to inflammatory stimuli. *Sci Transl Med* **10;7**, (2015).
133. D. Gveric, C. Kaltschmidt, M. Cuzner, J. Newcombe, Transcription Factor NF-KB and Inhibitor lκBα are Localized in Macrophages in Active Multiple Sclerosis Lesions. *Journal of Neuropathology and Experimental Neurology* **57**, 168-178 (1998).
134. A. Szanto, L. Nagy, The many faces of PPARgamma: anti-inflammatory by any means? *Immunobiology* **213**, 789-803 (2008).
135. A. Paintlia, M. Pantlia, I. Singh, A. Singh, IL-4-induced peroxisome proliferator-activated receptor gamma activation inhibits NF-kappaB trans activation in central nervous system (CNS) glial cells and protects oligodendrocyte progenitors under neuroinflammatory disease conditions: implication for CNS-demyelinating diseases. *J Immunol* **1;176**, 4385-4398 (2006).
136. D. McTigue, R. Tripathi, P. Wei, A. Lash, The PPAR gamma agonist Pioglitazone improves anatomical and locomotor recovery after rodent spinal cord injury. *Exp Neurol* **205**, 396-406 (2007).
137. P. Polak *et al.*, Protective effects of a peroxisome proliferator-activated receptor-beta/delta agonist in experimental autoimmune encephalomyelitis. *J Neuroimmunol* **168**, 65-75 (2005).
138. F. Penas *et al.*, Treatment in vitro with PPARα and PPARγ ligands drives M1-to-M2 polarization of macrophages from T. cruzi-infected mice. *Biochim Biophys Acta* **1852**, 893-904 (2015).
139. I. Marriott, K. Bost, IL-4 and IFN-gamma up-regulate substance P receptor expression in murine peritoneal macrophages. *J Immunol* **1;165**, 182-191 (2000).

140. M. Jiang *et al.*, Substance P induces M2-type macrophages after spinal cord injury. *Neuroreport* **12;23**, 786-792 (2012).
141. S. Ghisletti, C. Meda, A. Maggi, E. Vegeto, 17beta-estradiol inhibits inflammatory gene expression by controlling NF-kappaB intracellular localization. *Mol Cell Biol* **25**, 2957-2968 (2005).
142. A. Kumar, F. Piedrafita, W. Reynolds, Peroxisome proliferator-activated receptor gamma ligands regulate myeloperoxidase expression in macrophages by an estrogen-dependent mechanism involving the -463GA promoter polymorphism. *J Biol Chem* **27;279**, 8300-8315 (2004).
143. J. Feng, G. Zhang, X. Hu, C. Si Chen, X. Qin, Estrogen inhibits estrogen receptor α-mediated rho-kinase expression in experimental autoimmune encephalomyelitis rats. *Synapse* **67**, 399-406 (2013).
144. R. Deshpande, H. Khalili, R. Pergolizzi, S. Michael, M. Chang, Estradiol down-regulates LPS-induced cytokine production and NFkB activation in murine macrophages. *Am J Reprod Immunol* **38**, 46-54 (1997).
145. L. Tönges *et al.*, Rho kinase inhibition modulates microglia activation and improves survival in a model of amyotrophic lateral sclerosis. *Glia* **62**, 217-232 (2014).
146. L. Lawson, H. Perry, P. Dri, S. Gordon, HETEROGENEITY IN THE DISTRIBUTION AND MORPHOLOGY OF M~CROGLIA IN THE NORMAL ADULT MOUSE IBRAIN *Neuroscience* **39**, 151-170 (1990).
147. K. Grabert *et al.*, Microglial brain region-dependent diversity and selective regional sensitivities to aging. *Nat Neurosci* **19**, 504-516 (2016).
148. E. Bernhart *et al.*, Lysophosphatidic acid receptor activation affects the C13NJ microglia cell line proteome leading to alterations in glycolysis, motility, and cytoskeletal architecture. *Proteomics* **10**, 141-158 (2010).
149. L. De Biase *et al.*, Local Cues Establish and Maintain Region-Specific Phenotypes of Basal Ganglia Microglia. *Neuron* **19;95**, 341-356 (2017).
150. D. Gosselin *et al.*, Environment Drives Selection and Function of Enhancers Controlling Tissue-Specific Macrophage Identities. *Cell* **159**, 1327-1340 (2014).
151. L. Schnell, S. Fearn, H. Klassen, M. Schwab, H. Perry, Acute in¯ammatory responses to mechanical lesions inthe CNS: differences between brain and spinal cord. *European Journal of Neuroscience* **11**, 3648-3658 (1999).
152. V. Chhor *et al.*, Characterization of phenotype markers and neuronotoxic potential of polarised primary microglia in vitro. *Brain, Behavior and Immunity* **32**, 70-85 (2013).
153. R. Sasmono *et al.*, A macrophage colony-stimulating factor receptor-green fluorescent protein transgene is expressed throughout the mononuclear phagocyte system of the mouse. *Blood* **101**, 1155-1163 (2003).
154. J. Merrill, L. Ignarro, M. Sherman, J. Melinek, T. Lane, Microglial cell cytotoxicity of oligodendrocytes is mediated through nitric oxide. *J Immunol* **151**, 2132-2141 (1993).
155. Y. Pang *et al.*, Lipopolysaccharide-activated microglia induce death of oligodendrocyte progenitor cells and impede their development. *Neuroscience* **166**, 464-475 (2010).
156. Y. Deng, J. Lu, V. Sivakumar, E. Ling, C. Kaur, Amoeboid Microglia in the Periventricular White Matter Induce Oligodendrocyte Damage through Expression of Proinflammatory Cytokines via MAP Kinase Signaling Pathway in Hypoxic Neonatal Rats. *Brain Pathology* **18**, 387-400 (2008).

157. J. Li *et al.*, Tumor Necrosis Factor α Mediates Lipopolysaccharide-Induced Microglial Toxicity to Developing Oligodendrocytes When Astrocytes Are Present. *Journal of Neuroscience* **28**, (2008).
158. J. Li, O. Baud, T. Vartanian, J. Volpe, P. Rosenberg, Peroxynitrite generated by inducible nitric oxide synthase and NADPH oxidase mediates microglial toxicity to oligodendrocytes. *PNAS* **102**, 9936-9941 (2005).
159. P. Vandenabeele, L. Galluzzi, T. Vanden Berghe, G. Kroemer, Molecular mechanisms of necroptosis: an ordered cellular explosion. *Nature Reviews Molecular Cell Biology* **11**, 700-714 (2010).
160. A. Lurbke *et al.*, Limited TCF7L2 expression in MS lesions. *PLoS One* **20;8**, (2013).
161. A. Caccamo *et al.*, Necroptosis activation in Alzheimer's disease. *Nat Neurosci* **20**, 1236-1246 (2017).
162. J. Prineas, R. Barnard, E. Kwon, L. Sharer, E. Cho, Multiple sclerosis: remyelination of nascent lesions. *Ann Neurol* **33**, 137-151 (1993).
163. W. Bruck, T. Kuhlmann, C. Stadelmann, Remyelination in multiple sclerosis. *Journal of the neurological sciences* **206**, 181-185 (2003).
164. H. Scholz, C. Eder, Lysophosphatidylcholine activates caspase-1 in microglia via a novel pathway involving two inflammasomes. *J Neuroimmunol* **15**, 107-110 (2017).
165. J. Xu, T. Wang, Y. Wu, J. Wan, Z. Wen, Microglia Colonization of Developing Zebrafish Midbrain Is Promoted by Apoptotic Neuron and Lysophosphatidylcholine. *Developmental Cell* **38**, 214-222 (2016).
166. Y. Pan *et al.*, Caspase-1 inhibition attenuates activation of BV2 microglia induced by LPS-treated RAW264.7 macrophages. *J Biomed Res* **30**, 225-233 (2016).
167. A. Caccamo *et al.*, Necroptosis activation in Alzheimer's disease. *Nat Neurosci* **20**, 1236-1246 (2017).
168. D. Re *et al.*, Necroptosis drives motor neuron death in models of both sporadic and familial ALS. *Neuron* **5;81**, 1001-1008 (2014).
169. S. Laster, J. Wood, L. Gooding, Tumor necrosis factor can induce both apoptic and necrotic forms of cell lysis. *J Immunol* **15;141**, 2629-2634 (1988).
170. D. Rosenbaum *et al.*, Necroptosis, a novel form of caspase-independent cell death, contributes to neuronal damage in a retinal ischemia-reperfusion injury model. *J Neurosci Res* **15;88**, 1569-1576 (2010).
171. N. Robinson *et al.*, Type I interferon induces necroptosis in macrophages during infection with Salmonella enterica serovar Typhimurium. *Nat Immunol* **13**, 954-962 (2012).
172. C. Blériot *et al.*, Liver-resident macrophage necroptosis orchestrates type 1 microbicidal inflammation and type-2-mediated tissue repair during bacterial infection. *Immunity* **42**, 145-158 (2015).
173. T. Pan *et al.*, Necroptosis takes place in human immunodeficiency virus type-1 (HIV-1)-infected CD4+ T lymphocytes. *PLoS One* **8;9**, (2014).
174. M. Pasparakis, P. Vandenabeele, Necroptosis and its role in inflammation. *Nature* **15;517**, 311-320 (2015).
175. X. Wu *et al.*, Distinct roles of RIP1-RIP3 hetero- and RIP3-RIP3 homo-interaction in mediating necroptosis. *Cell Death Differ* **21**, 1709-1720 (2014).
176. X. Chen *et al.*, Translocation of mixed lineage kinase domain-like protein to plasma membrane leads to necrotic cell death. *Cell Res* **24**, 105-121 (2014).
177. Z. Cai *et al.*, Plasma membrane translocation of trimerized MLKL protein is required for TNF-induced necroptosis. *Nat Cell Biol* **16**, 55-65 (2014).
178. Y. Dondelinger *et al.*, MLKL compromises plasma membrane integrity by binding to phosphatidylinositol phosphates. *Cell Reports* **22;7**, 971-981 (2014).

179. K. Gutierrez *et al.*, MLKL Activation Triggers NLRP3-Mediated Processing and Release of IL-1β Independently of Gasdermin-D. *J Immunol* **198**, 2156-2164 (2017).
180. H. Scheiblich *et al.*, Activation of the NLRP3 inflammasome in microglia: the role of ceramide. *Journal of Neurochemistry* **143**, (2017).
181. O. Michaeu, J. Tschopp, Induction of TNF receptor I-mediated apoptosis via two sequential signaling complexes. *Cell* **25;114**, 181-190 (2003).
182. G. Quarato *et al.*, Sequential Engagement of Distinct MLKL Phosphatidylinositol-Binding Sites Executes Necroptosis. *Molecular Cell* **61**, 589-601 (2016).
183. J. Upton, W. Kaiser, E. Mocarski, DAI/ZBP1/DLM-1 complexes with RIP3 to mediate virus-induced programmed necrosis that is targeted by murine cytomegalovirus vIRA. *Cell Host Microbe* **15;11**, 290-297 (2012).
184. A. Cassamo *et al.*, Necroptosis activation in Alzheimer's Disease. *Nature Neuroscience* (2017).
185. N. Huynh, C. Passirani, P. Saulnier, J. Benoit, Lipid nanocapsules: A new platform for nanomedicine. *International Journal of Pharmaceutics* **379**, 201-209 (2009).
186. P. Vandenabeele, S. Grootjans, N. Callewaert, N. Takahashi, Necrostatin-1 blocks both RIPK1 and IDO: consequences for the study of cell death in experimental disease models. *Cell Death Differ* **20**, 185-187 (2012).
187. D. Liao *et al.*, Necrosulfonamide inhibits necroptosis by selectively targeting the mixed lineage kinase domain-like protein. *Med Chem Commun* **5**, 333-337 (2014).
188. Y. Wang *et al.*, Necrosulfonamide Attenuates Spinal Cord Injury via Necroptosis Inhibition. *World Neurosurgery*, 1186-1191 (2018).
189. N. Lewis, J. Hill, K. Juchem, D. Stefanopoulos, L. Modis, RNA sequencing of microglia and monocyte-derived macrophages from mice with experimental autoimmune encephalomyelitis illustrates a changing phenotype with disease course. *J Neuroimmunol* **277**, 26-38 (2014).
190. Z. Huang *et al.*, Necroptosis in microglia contributes to neuroinflammation and retinal degeneration through TLR4 activation. *Cell Death Differ* **25**, 180-189 (2018).
191. H. Salgado-Ceballos *et al.*, Spontaneous long-term remyelination after traumatic spinal cord injury in rats. *Brain Res* **26;782**, 126-135 (1998).
192. S. David, A. Kroner, Repertoire of microglial and macrophage responses after spinal cord injury. *Nature Reviews Neuroscience* **12**, 388-399 (2011).
193. J. Ruckh *et al.*, Rejuvenation of Regeneration in the Aging Central Nervous System. *Cell* **10**, 96-103 (2012).
194. J. Godbout *et al.*, Exaggerated neuroinflammation and sickness behavior in aged mice following activation of the peripheral innate immune system. *FASEB* **19**, (2005).
195. C. Huang *et al.*, Shikonin kills glioma cells through necroptosis mediated by RIP-1. *PLoS One* **28;8**, (2013).
196. H. Kim *et al.*, Shikonin-induced necroptosis is enhanced by the inhibition of autophagy in non-small cell lung cancer cells. *J Transl Med* **15:123**, (2017).
197. G. Gonzalez *et al.*, Tamoxifen accelerates the repair of demyelinated lesions in the central nervous system. *Scientific Reports* (2016).
198. Q. Remijsen *et al.*, Depletion of RIPK3 or MLKL blocks TNF-driven necroptosis and switches towards a delayed RIPK1 kinase-dependent apoptosis. *Cell Death and Disease*, (2014).
199. Z. Cai *et al.*, Plasma membrane translocation of trimerized MLKL protein is required for TNF-induced necroptosis. *Nat Cell Biol* **16**, 55-65 (2013).

200. N. Vanlangenakker, M. Bertrand, P. Bogaert, P. Vandenabeele, T. Berghe, TNF-induced necroptosis in L929 cells is tightly regulated by multiple TNFR1 complex I and II members. *Cell Death and Disease*, (2011).
201. S. Liu *et al.*, Necroptosis Mediates TNF-Induced Toxicity of Hippocampal Neurons. *BioMed Research International*, (2014).
202. R. Rice *et al.*, Microglial repopulation resolves inflammation and promotes brain recovery after injury. *Glia* **65**, 931-944 (2017).
203. Y. Yao *et al.*, Dynamics of spinal microglia repopulation following an acute depletion. *Sci Rep*, (2016).
204. P. Reu *et al.*, The Lifespan and Turnover of Microglia in the Human Brain. *Cell Reports* **20**, 779-784 (2017).
205. R. Busch, R. Neese, M. Awada, G. Hayes, M. Hellerstein, Measurement of cell proliferation by heavy water labeling. *Nat Protoc* **2**, 3045-3057 (2007).
206. P. Squarzoni *et al.*, Microglia modulate wiring of the embryonic forebrain. *Cell Reports* **11;8**, 1271-1279 (2014).
207. D. Sunnemark *et al.*, CX3CL1 (fractalkine) and CX3CR1 expression in myelin oligodendrocyte glycoprotein-induced experimental autoimmune encephalomyelitis: kinetics and cellular origin. *Journal of Neuroinflammation* **2**, (2005).
208. A. Abdanipour, T. Tiraihi, T. Taheri, H. Kazemi, Microglial activation in rat experimental spinal cord injury model. *Iran Biolmed J* **17**, 214-220 (2013).
209. R. Ladeby *et al.*, Proliferating resident microglia express the stem cell antigen CD34 in response to acute neural injury *Glia* **50**, (2005).
210. S. Zhang, S. Fedoroff, Expression of stem cell factor and c-kit receptor in neural cells after brain injury. *Acta Neuropathologica* **97**, 393-398 (1999).
211. C. Rolando, V. Taylor, Chapter Seven - Neural Stem Cell of the Hippocampus: Development, Physiology Regulation, and Dysfunction in Disease. *Current Topics in Developmental Biology* **107**, 183-206 (2014).
212. C. Johansson *et al.*, Identification of a Neural Stem Cell in the Adult Mammalian Central Nervous System. *Cell* **96**, 25-34 (1999).
213. U. Lendahl, L. Zimmerman, R. McKay, CNS Stem Cells Express a New Class of Intermediate Filament Protein *Cell* **60**, 585-595 (1990).
214. K. Michalczyk, M. Ziman, Nestin structure and predicted function in cellular cytoskeletal organisation. *Histology and Histopathology* **20**, 665-671 (2005).
215. J. Frisen, C. Johansson, C. Torok, M. Risling, U. Lendahl, Rapid, widespread, and longlasting induction of nestin contributes to the generation of glial scar tissue after CNS injury. *Journal of Cell Biology* **131**, (1995).
216. Y. Takamori *et al.*, Nestin-positive microglia in adult rat cerebral cortex. *Brain Res* **1270**, 10-18 (2009).
217. H. Xu, M. Chen, E. Mayer, J. Forrester, A. Dick, Turnover of resident retinal microglia in the normal adult mouse. *Glia* **55**, 1189-1198 (2007).
218. S. Wohl, C. Schmeer, T. Friese, O. Witte, S. Isenmann, In situ dividing and phagocytosing retinal microglia express nestin, vimentin, and NG2 in vivo. *PLoS One* **6**, (2011).
219. G. Brook, A. Perez-Bouza, J. Noth, W. Nacimiento, Astrocytes re-express nestin in deafferented target territories of the adult rat hippocampus. *Neuroreport* **10**, 1007-1011 (1999).
220. O. Butovsky, S. Bukshpan, G. Kunis, S. Jung, M. Schwartz, Microglia can be induced by IFN-γ or IL-4 to express neural or dendritic-like markers. *Molecular and Cellular Neuroscience* **35**, 490-500 (2007).

221. J. Cronk *et al.*, Peripherally derived macrophages can engraft the brain independent of irradiation and maintain an identity distinct from microglia. *J Exp Med* **215**, (2018).
222. J. Holley, D. Gveric, J. Newcombe, M. Cuzner, N. Gutowski, Astrocyte characterization in the multiple sclerosis glial scar. *Neuropathology and Applied Neurobiology* **29**, (2003).
223. M. Moreels, F. Vandenabeele, D. Dumont, J. Robben, I. Lambrichts, Alpha-smooth muscle actin (α-SMA) and nestin expression in reactive astrocytes in multiple sclerosis lesions: potential regulatory role of transforming growth factor-beta 1 (TGF-β1). *Neuropathol Appl Neurobiol* **34**, (2008).
224. D. Park *et al.*, Nestin Is Required for the Proper Self-Renewal of Neural Stem Cells. *Stem Cells* **28**, (2010).
225. T. Tay *et al.*, A new fate mapping system reveals context-dependent random or clonal expansion of microglia. *Nature Neuroscience*, (2017).
226. S. S. International Multiple Sclerosis Genetics Consortium; Wellcome Trust Case Control Consortium 2, Hellenthal G, Pirinen M, Spencer CC, Patsopoulos NA, Moutsianas L, Dilthey A, Su Z, Freeman C, Hunt SE, Edkins S, Gray E, Booth DR, Potter SC, Goris A, Band G, Oturai AB, Strange A, Saarela J, Bellenguez C, Fontaine B, Gillman M, Hemmer B, Gwilliam R, Zipp F, Jayakumar A, Martin R, Leslie S, Hawkins S, Giannoulatou E, D'alfonso S, Blackburn H, Martinelli Boneschi F, Liddle J, Harbo HF, Perez ML, Spurkland A, Waller MJ, Mycko MP, Ricketts M, Comabella M, Hammond N, Kockum I, McCann OT, Ban M, Whittaker P, Kemppinen A, Weston P, Hawkins C, Widaa S, Zajicek J, Dronov S, Robertson N, Bumpstead SJ, Barcellos LF, Ravindrarajah R, Abraham R, Alfredsson L, Ardlie K, Aubin C, Baker A, Baker K, Baranzini SE, Bergamaschi L, Bergamaschi R, Bernstein A, Berthele A, Boggild M, Bradfield JP, Brassat D, Broadley SA, Buck D, Butzkueven H, Capra R, Carroll WM, Cavalla P, Celius EG, Cepok S, Chiavacci R, Clerget-Darpoux F, Clysters K, Comi G, Cossburn M, Cournu-Rebeix I, Cox MB, Cozen W, Cree BA, Cross AH, Cusi D, Daly MJ, Davis E, de Bakker PI, Debouverie M, D'hooghe MB, Dixon K, Dobosi R, Dubois B, Ellinghaus D, Elovaara I, Esposito F, Fontenille C, Foote S, Franke A, Galimberti D, Ghezzi A, Glessner J, Gomez R, Gout O, Graham C, Grant SF, Guerini FR, Hakonarson H, Hall P, Hamsten A, Hartung HP, Heard RN, Heath S, Hobart J, Hoshi M, Infante-Duarte C, Ingram G, Ingram W, Islam T, Jagodic M, Kabesch M, Kermode AG, Kilpatrick TJ, Kim C, Klopp N, Koivisto K, Larsson M, Lathrop M, Lechner-Scott JS, Leone MA, Leppä V, Liljedahl U, Bomfim IL, Lincoln RR, Link J, Liu J, Lorentzen AR, Lupoli S, Macciardi F, Mack T, Marriott M, Martinelli V, Mason D, McCauley JL, Mentch F, Mero IL, Mihalova T, Montalban X, Mottershead J, Myhr KM, Naldi P, Ollier W, Page A, Palotie A, Pelletier J, Piccio L, Pickersgill T, Piehl F, Pobywajlo S, Quach HL, Ramsay PP, Reunanen M, Reynolds R, Rioux JD, Rodegher M, Roesner S, Rubio JP, Rückert IM, Salvetti M, Salvi E, Santaniello A, Schaefer CA, Schreiber S, Schulze C, Scott RJ, Sellebjerg F, Selmaj KW, Sexton D, Shen L, Simms-Acuna B, Skidmore S, Sleiman PM, Smestad C, Sørensen PS, Søndergaard HB, Stankovich J, Strange RC, Sulonen AM, Sundqvist E, Syvänen AC, Taddeo F, Taylor B, Blackwell JM, Tienari P, Bramon E, Tourbah A, Brown MA, Tronczynska E, Casas JP, Tubridy N, Corvin A, Vickery J, Jankowski J, Villoslada P, Markus HS, Wang K, Mathew CG, Wason J, Palmer CN, Wichmann HE, Plomin R, Willoughby E, Rautanen A, Winkelmann J, Wittig M, Trembath RC, Yaouanq J, Viswanathan AC, Zhang H, Wood NW, Zuvich R, Deloukas P, Langford C, Duncanson A, Oksenberg JR, Pericak-Vance MA, Haines JL, Olsson T, Hillert J, Ivinson AJ, De Jager PL, Peltonen L, Stewart GJ, Hafler DA, Hauser SL, McVean G, Donnelly P, Compston A., Genetic risk and a

primary role for cell-mediated immune mechanisms in multiple sclerosis. *Nature* **476**, 214-219 (2011).
227. P. Drew, J. Xu, M. Racke, PPAR-gamma: Therapeutic Potential for Multiple Sclerosis. *PPAR Res*, (2008).
228. S. Shimizu *et al.*, Involvement of nuclear factor-kB activation through RhoA/Rho-kinase pathway in LPS-induced IL-8 production in human cervical stromal cells. *Mol Hum Reprod* **13**, 181-187 (2007).
229. J. Sun, R. Ramnath, L. Zhi, R. Tamizhselvi, M. Bhatia, Substance P enhances NF-kappaB transactivation and chemokine response in murine macrophages via ERK1/2 and p38 MAPK signaling pathways. *Am J Physiol Cell Physiol* **294**, 1586-1596 (2008).
230. R. Scirpo *et al.*, Stimulation of nuclear receptor PPAR-γ limits NF-kB-dependent inflammation in mouse cystic fibrosis biliary epithelium. *Hepatology* **62**, 1551-1562 (2015).
231. K. De Bosscher, W. Vanden Berghe, G. Haegeman, Cross-talk between nuclear receptors and nuclear factor kappaB. *Oncogene* **25**, 6868-6886 (2006).
232. Y. Hou, F. Moreau, K. Chadee, PPARγ is an E3 ligase that induces the degradation of NFκB/p65. *Nat Commun* **3**, (2012).
233. L. Seethalakshmi *et al.*, 156. *5* **1838-1842**, (1996).
234. S. Kovats, Estrogen receptors regulate innate immune cells and signalling pathways. *Cellular Immunology* **294**, 63-69 (2015).
235. T. Lawrence, The Nuclear Factor NF-κB Pathway in Inflammation. *Cold Spring Harb Perspect Biol* **10**, (2009).
236. , (!!! INVALID CITATION !!!).
237. R. Kuno *et al.*, Autocrine activation of microglia by tumor necrosis factor-alpha. *J Neuroimmunol* **162**, 89-96 (2005).
238. N. Lukacs, R. Strieter, S. Chensue, M. Widmer, S. Kunkel, TNF-alpha mediates recruitment of neutrophils and eosinophils during airway inflammation. *J Immunol* **154**, 5411-5417 (1995).
239. E. Cacci, J. Claasen, Z. Kokaia, Microglia-derived tumor necrosis factor-alpha exaggerates death of newborn hippocampal progenitor cells in vitro. *J Neurosci Res* **80**, 789-797 (2005).
240. Y. Yiangou *et al.*, COX-2, CB2 and P2X7-immunoreactivities are increased in activated microglial cells/macrophages of multiple sclerosis and amyotrophic lateral sclerosis spinal cord. *BMC Neurology* **6**, (2006).
241. O. Howell *et al.*, Activated Microglia Mediate Axoglial Disruption That Contributes to Axonal Injury in Multiple Sclerosis. *Journal of Neuropathology and Experimental Neurology* **69**, 1077-1033 (2010).
242. L. Airas, E. Rissanen, J. Tuisku, M. Gardberg, J. Rinne, Microglial activation correlates with disease progression in multiple sclerosis. *Journal of the neurological sciences* **357**, e17-e18 (2015).
243. P. Popovich, P. Wei, B. Stokes, Cellular inflammatory response after spinal cord injury in sprague-dawley and lewis rats. *Journal of Comparative Neurology* **377**, 443-464 (1998).
244. B. Hains, S. Waxman, Activated Microglia Contribute to the Maintenance of Chronic Pain after Spinal Cord Injury. *Journal of Neuroscience* **26**, (2006).
245. A. Frakes *et al.*, Microglia induce motor neuron death via the classical NF-κB pathway in amyotrophic lateral sclerosis. *Neuron* **81**, 1009-1023 (2014).

246. L. Pagliari, H. Perlman, H. Liu, R. Pope, Macrophages require constitutive NF-kappaB activation to maintain A1 expression and mitochondrial homeostasis. *Mol Cell Biol* **20**, 8855-8865 (2000).
247. K. Pahan, M. Schmid, Activation of nuclear factor-kB in the spinal cord of experimental allergic encephalomyelitis. *Neuroscience Letters* **287**, 17-20 (2000).
248. G. van Loo *et al.*, Inhibition of transcription factor NF-kappaB in the central nervous system ameliorates autoimmune encephalomyelitis in mice. *Nat Immunol* **7**, 954-961 (2006).
249. A. Gregory *et al.*, TNF receptor 1 genetic risk mirrors outcome of anti-TNF therapy in multiple sclerosis. *Nature* **488**, 508-511 (2012).
250. E. Serfling *et al.*, Ubiquitous and lymphocyte-specific factors are involved in the induction of the mouse interleukin 2 gene in T lymphocytes. *EMBO J* **8**, 465-473 (1989).
251. K. Lai *et al.*, A kinase-deficient splice variant of the human JAK3 is expressed in hematopoietic and epithelial cancer cells. *J Biol Chem* **270**, 25028-25036 (1995).
252. T. Libermann, D. Baltimore, Activation of interleukin-6 gene expression through the NF-kappa B transcription factor. *Mol Cell Biol* **10**, 2327-2334 (1990).
253. Y. Shimizu, G. van Seventer, K. Horgan, S. Shaw, Costimulation of proliferative responses of resting CD4+ T cells by the interaction of VLA-4 and VLA-5 with fibronectin or VLA-6 with laminin. *J Immunol* **145**, 59-67 (1990).
254. A. Shakhov, D. Kuprash, M. Azizov, C. Jongeneel, S. Nedospasov, Gene. *95* **2**, (Structural analysis of the rabbit TNF locus, containing the genes encoding TNF-beta (lymphotoxin) and TNF-alpha (tumor necrosis factor)).
255. M. Collart, P. Baeuerle, P. Vassalli, Regulation of tumor necrosis factor alpha transcription in macrophages: involvement of four kappa B-like motifs and of constitutive and inducible forms of NF-kappa B. *Mol Cell Biol* **10**, 1498-1506 (1990).
256. Y. Wu *et al.*, zVAD-induced necroptosis in L929 cells depends on autocrine production of TNFα mediated by the PKC–MAPKs–AP-1 pathway. *Cell Death and Differentiation* **18**, 26-37 (2010).
257. K. Satake *et al.*, Nitric oxide via macrophage iNOS induces apoptosis following traumatic spinal cord injury. *Molecular Brain Research* **85**, 114-122 (2000).